Supporting Information

Polysubstitution of dipyrrolonaphthyridinediones as a potent strategy towards strongly emitting fluorophores

Kamil Skonieczny,[a] Łukasz Kielesiński,[a] Marek Grzybowski*[a] and Daniel T. Gryko*[a]*

[a] *Institute of Organic Chemistry of Polish Academy of Sciences, Kasprzaka 44/52, 01-224 Warsaw, Poland*

SUMMARY

1. General methods

All chemicals were used as received unless otherwise noted. All reported ^{1}H NMR and ^{13}C NMR spectra were recorded on 500 or 600 MHz spectrometer. Chemical shifts (δ ppm) were determined with TMS as the internal reference; *J* values are given in Hz. Mass spectra were obtained via APCI MS. For HRMS measurements both quadruple and TOF mass analyzer types were used. Chromatography was performed on silica (Kieselgel 60, 200–400 mesh). Absorption and emission spectra were recorded in dichloromethane. DPND **1** and **3** were prepared according to the literature procedures.[1]

[1] M. Grzybowski, I. Deperasińska, M. Chotkowski, M. Banasiewicz, A. Makarewicz, B. Kozankiewicz, D. T. Gryko, *Chem. Commun.*, 2016, **52**, 5108−5111

2. Experimental Part

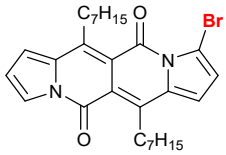

3-Bromo-6,12-diheptyl-5*H*,11*H*-dipyrrolo[1,2-*b*:1',2'-*g*][2,6]naphthyridine-5,11-dione (2)

To the ice-bath-cooled solution of DPND **1** (299 mg, 0.69 mmol) in 40 mL of dry chloroform, freshly recrystallized *N*-bromosuccinimide (123 mg, 0.69 mmol) was added. The reaction mixture was gradually warmed to room temperature and stirred overnight. The mixture was transferred to the separatory funnel and the organic layer was washed with degassed water (3 × 25 mL) and brine. The organic layer was then dried over $MgSO_4$ and the solvent was evaporated with Celite. The target product was purified by silica gel chromatography using hexanes / toluene (5/1) solution as eluent and recrystallized by addition of methanol to a solution of the dye in a small amount of toluene. Yield: 106 mg (30%). Dark red powder; ^{1}H NMR (500 MHz, $CDCl_3$) δ 7.82 (d, J = 1.8 Hz, 1H), 6.86 (d, J = 2.5 Hz, 1H), 6.80 (d, J = 4.0 Hz, 1H), 6.58 (d, J = 4.0 Hz, 1H), 6.53 (t, J = 3.4 Hz, 1H), 3.26 – 3.17 (m, 4H), 1.73 – 1.60 (m, 4H), 1.56 – 1.46 (m, 4H), 1.42 – 1.27 (m, 12H), 0.89 (t, J = 6.4 Hz, 6H); ^{13}C NMR (125 MHz, $CDCl_3$) δ 159.0, 158.1, 144.9, 143.8, 134.9, 133.2, 122.2, 120.5, 116.4, 115.9, 115.4, 114.9, 114.7, 106.8, 31.9, 31.8, 31.0, 30.4, 30.3, 30.24, 30.19, 29.2, 22.69, 22.66, 14.13, 14.12; HRMS (APCI): calcd for $C_{28}H_{36}BrN_2O_2$ $[M+H]^+$ 511.1960, found 511.1963.

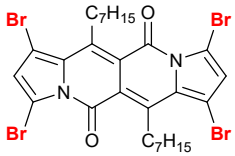

1,3,7,9-Tetrabromo-6,12-diheptyl-5*H*,11*H*-dipyrrolo[1,2-*b*:1',2'-*g*][2,6]naphthyridine-5,11-dione (4)

To the solution of DPND **1** (217 mg, 0.50 mmol) and freshly recrystallized *N*-bromosuccinimide (402 mg, 2.25 mmol) in 60 mL of dry chloroform, BBr_3 (50 µL, 0.05 mmol) was added dropwise. The reaction mixture was stirred at room temperature for 36h. The mixture was transferred to the separatory funnel and the organic layer was washed with degassed water (3 × 25 mL) and brine. The organic layer was then dried over $MgSO_4$ and the solvent was evaporated with Celite. The target product was purified by silica gel chromatography using hexanes / toluene (10/1) solution as eluent and recrystallized by addition of methanol to a solution of the dye in a small amount of toluene. Yield: 190 mg (51%). Dark red powder; ^{1}H NMR (500 MHz, $CDCl_3$) δ 6.66 (s, 2H), 3.53 – 3.35 (m, 4H), 1.66 (s, 4H), 1.54 – 1.50 (m, 4H), 1.42 – 1.35 (m, 4H), 1.35 – 1.28 (m, 8H), 0.89 (t, J = 6.6 Hz, 6H); ^{13}C NMR (125 MHz, $CDCl_3$) δ 158.2, 143.1, 129.8, 125.4, 116.2, 106.5, 105.6, 31.8, 30.0, 29.8, 29.7, 29.1, 28.5, 22.7, 14.1; HRMS (APCI): calcd for $C_{28}H_{33}Br_4N_2O_2$ $[M+H]^+$ 744.9275, found 744.9278.

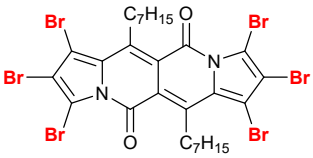

1,2,3,7,8,9-Hexabromo-6,12-diheptyl-5*H*,11*H*-dipyrrolo[1,2-*b*:1',2'-*g*][2,6]naphthyridine-5,11-dione (5)

To the solution of DPND **1** (100 mg, 0.23 mmol) in 40 mL of dry 1,2-dichloroethane, freshly recrystallized *N*-bromosuccinimide (411 mg, 2.31 mmol) was added. The reaction mixture was stirred at 70 ºC for 60h. The mixture was transferred to the separatory funnel and the organic layer was washed with degassed water (3 × 25 mL) and brine. The organic layer was then dried over $MgSO_4$ and the solvent was evaporated with Celite. The target product was purified by silica gel chromatography using hexanes / toluene (10/1) solution as eluent and recrystallized by addition of methanol to a solution of the dye in a small amount of toluene. Yield: 37 mg (18%). Dark red powder; ^{1}H NMR (600 MHz, $CDCl_3$) δ 3.51 – 3.38 (m, 4H), 1.69 – 1.61 (m, 4H), 1.56 – 1.50 (m, 4H), 1.41 – 1.36 (m, 4H), 1.35 – 1.29 (m, 8H), 0.90 (t, J = 6.9 Hz, 6H); ^{13}C NMR (150 MHz, $CDCl_3$) δ 157.2, 142.8, 130.1, 117.2, 116.3, 108.3, 108.2, 31.8, 29.9, 29.8, 29.1, 28.6, 22.7, 14.1; HRMS (APCI): calcd for $C_{28}H_{31}Br_6N_2O_2$ $[M+H]^+$ 900.7486, found 900.7490.

To the solution of DPND **1** (568 mg, 1.31 mmol) in 180 mL of chloroform, freshly recrystallized *N*-bromosuccinimide (479 mg, 2.69 mmol) was added. The reaction mixture was then cooled to 0 ºC in an ice bath and 1M BBr_3 (0.13 mmol, 131 µL) was added dropwise. The mixture was gradually warmed to room temperature and stirred for 3 days. The mixture was transferred to the separatory funnel and the organic layer was washed with degassed water (3 × 25 mL) and brine. The organic layer was then dried over $MgSO_4$ and the solvent was evaporated with Celite. The two products, **9** and **10**, were separated by silica gel chromatography using a hexanes / toluene (9/1) mixture as the eluent. The purified compounds were then recrystallized by adding methanol to a solution of the dye in a small amount of toluene.

1-Bromo-6,12-diheptyl-5*H*,11*H*-dipyrrolo[1,2-*b*:1',2'-*g*][2,6]naphthyridine-5,11-dione (9)

Yield: 260 mg (39%). Red powder; ^{1}H NMR (600 MHz, $CDCl_3$) δ 7.85 (dd, J = 3.1, 1.3 Hz, 1H), 7.81 (d, J = 3.3 Hz, 1H), 6.88 (dd, J = 3.7, 1.3 Hz, 1H), 6.57 (d, J = 3.3 Hz, 1H), 6.54 – 6.52 (m, 1H), 3.87 – 3.75 (m, 1H), 3.51 – 3.40 (m, 1H), 3.34 – 3.13 (m, 2H), 1.77 – 1.61 (m, 4H), 1.58 – 1.48 (m, 4H), 1.44 – 1.35 (m, 4H), 1.35 – 1.28 (m, 8H), 0.92 – 0.86 (m, 6H); ^{13}C NMR (150 MHz, $CDCl_3$) δ 158.4, 157.3, 145.9, 145.8, 133.0, 127.6, 123.0, 121.2, 120.6, 117.0, 115.6, 115.5, 113.5, 106.1, 31.94, 31.87, 31.2, 30.4, 30.3, 30.1, 29.7, 29.2, 29.1, 29.0, 22.70, 22.67, 14.2, 14.1; HRMS (APCI): calcd for $C_{28}H_{36}BrN_2O_2$ $[M+H]^+$ 511.1960, found 511.1964.

1,7-Dibromo-6,12-diheptyl-5*H*,11*H*-dipyrrolo[1,2-*b*:1',2'-*g*][2,6]naphthyridine-5,11-dione (10)
Yield: 146 mg (19%). Red powder; ^{1}H NMR (600 MHz, $CDCl_3$) δ 7.85 (d, *J* = 3.3 Hz, 2H), 6.59 (d, *J* = 3.3 Hz, 2H), 3.83 – 3.60 (m, 2H), 3.55 – 3.40 (m, 2H), 1.74 – 1.63 (m, 4H), 1.60 – 1.55 (m, 4H), 1.44 – 1.37 (m, 4H), 1.35 – 1.29 (m, 8H), 0.89 (t, *J* = 6.9 Hz, 6H); ^{13}C NMR (150 MHz, $CDCl_3$) δ 157.4, 146.2, 127.5, 121.7, 120.7, 114.7, 106.6, 31.9, 30.1, 29.7, 29.2, 29.1, 22.7, 14.2; HRMS (APCI): calcd for $C_{28}H_{35}Br_2N_2O_2$ $[M+H]^+$ 589.1065, found 589.1068.

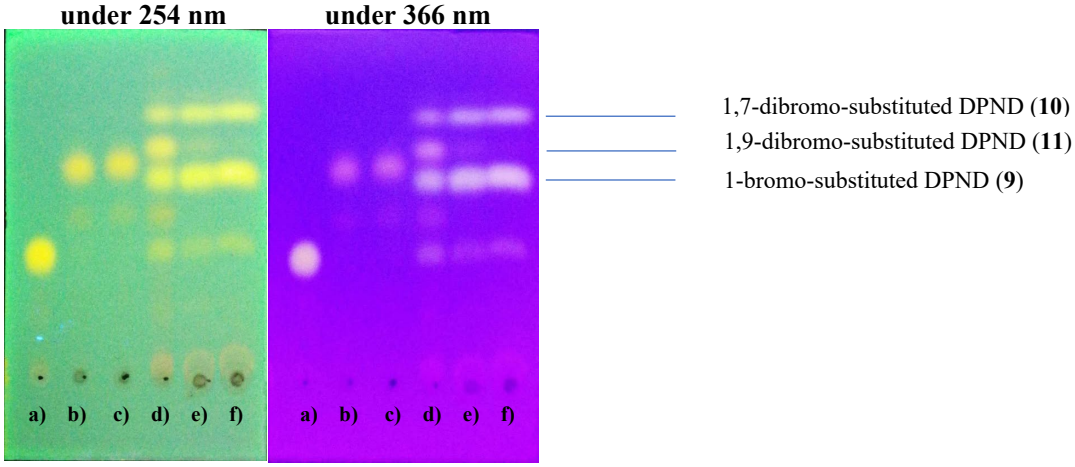

Figure S1. TLC plate showing the isomerization process of compound **3** to **9** and **10**. It was prepared using a double elution with a hexane/toluene (3:1) mixture; a) DPND **1**; b) solution after NBS addition; c) solution after BBr_3 addition; d) solution after 1 day; e) solution after 2 days; f) solution after 3 days

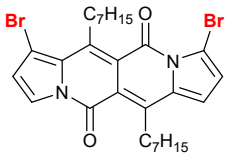

To the solution of DPND **9** (170 mg, 0.33 mmol) in 30 mL of dry chloroform, freshly recrystallized *N*-bromosuccinimide (60 mg, 0.34 mmol) was added. The reaction mixture was stirred at 50 ºC for 24h. The mixture was transferred to the separatory funnel and the organic layer was washed with degassed water (3 × 25 mL) and brine. The organic layer was then dried over $MgSO_4$ and the solvent was evaporated with Celite. The target product was purified by silica gel chromatography using hexanes / toluene (9/1) solution as eluent and recrystallized by addition of methanol to a solution of the dye in a small amount of toluene.
1,9-Dibromo-6,12-diheptyl-5*H*,11*H*-dipyrrolo[1,2-*b*:1',2'-*g*][2,6]naphthyridine-5,11-dione (11)
Yield: 158 mg (68%). Red powder; ^{1}H NMR (600 MHz, $CDCl_3$) δ 7.80 (d, *J* = 3.3 Hz, 1H), 6.82 (d, *J* = 4.0 Hz, 1H), 6.58 (d, *J* = 4.0 Hz, 1H), 6.57 (d, *J* = 3.3 Hz, 1H), 3.60 – 3.43 (m, 2H), 3.27 – 3.13 (m, 2H), 1.75 – 1.66 (m, 2H), 1.66 – 1.57 (m, 4H), 1.53 – 1.46 (m, 2H), 1.41 – 1.28 (m, 12H), 0.91 – 0.88 (m, 6H); ^{13}C NMR (125 MHz, $CDCl_3$) δ 159.2, 157.0, 144.8, 144.1, 134.8, 127.5, 121.0, 120.7, 120.6, 116.3, 116.2, 113.8, 107.5, 105.9, 31.88, 31.86, 30.4, 30.34, 30.31, 29.9, 29.8, 29.2, 29.1, 28.9, 22.73, 22.66, 14.2, 14.1; HRMS (APCI): calcd for $C_{28}H_{35}Br_2N_2O_2$ $[M+H]^+$ 589.1065, found 589.1069.

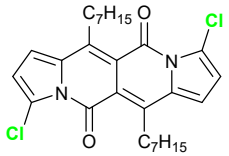

3,9-Dichloro-6,12-diheptyl-5*H*,11*H*-dipyrrolo[1,2-*b*:1',2'-*g*][2,6]naphthyridine-5,11-dione (6)

To the solution of DPND **1** (620 mg, 1.43 mmol) in 50 mL of dry 1,2-dichloroethane, *N*-chlorosuccinimide (402 mg, 3.01 mmol) and hexafluoro-2-propanol (1.00 mL, 9.53 mmol) were added. The reaction mixture was stirred at 75 ºC overnight. After completion, the mixture was transferred to a separatory funnel, and the organic layer was washed with degassed water (3 × 25 mL) and brine. The organic layer was then dried over $MgSO_4$, and the solvent was evaporated with Celite. The target product was purified by silica gel chromatography using a hexanes / toluene (5/1) mixture as the eluent and recrystallized by adding methanol to a solution of the dye in a small amount of toluene. Yield: 446 mg (62%). Red powder; ^{1}H NMR (500 MHz, $CDCl_3$) δ 6.79 (d, J = 4.0 Hz, 2H), 6.45 (d, J = 4.0 Hz, 2H), 3.18 – 3.13 (m, 4H), 1.66 (dt, J = 15.5, 7.6 Hz, 4H), 1.55 – 1.46 (m, 4H), 1.40 – 1.27 (m, 12H), 0.89 (t, J = 6.9 Hz, 6H); ^{13}C NMR (125 MHz, $CDCl_3$) δ 158.8, 143.5, 133.4, 123.1, 116.2, 115.3, 114.7, 31.8, 30.3, 30.22, 30.20, 29.2, 22.7, 14.1; HRMS (APCI): calcd for $C_{28}H_{35}Cl_2N_2O_2$ $[M+H]^+$ 501.2076, found 501.2077.

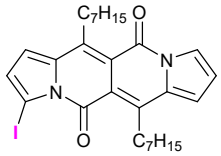

6,12-Diheptyl-3-iodo-5*H*,11*H*-dipyrrolo[1,2-*b*:1',2'-*g*][2,6]naphthyridine-5,11-dione (7)

To the ice-bath-cooled solution of DPND **1** (610 mg, 1.41 mmol) and freshly recrystallized *N*-iodosuccinimide (333 mg, 1.48 mmol) in 70 mL of dry chloroform, hexafluoro-2-propanol (1.48 mL, 14.1 mmol) was added dropwise. The reaction mixture was stirred overnight. The mixture was transferred to the separatory funnel and the organic layer was washed with degassed water (3 × 25 mL) and brine. The organic layer was then dried over $MgSO_4$ and the solvent was evaporated with Celite. The target product was purified by silica gel chromatography using hexanes / ethyl acetate (10/1) solution as eluent. Yield: 302 mg (31%). Dark red powder; ^{1}H NMR (600 MHz, $CDCl_3$) δ 7.83 (dd, *J* = 2.9, 1.0 Hz, 1H), 6.89 – 6.86 (m, 1H), 6.81 (s, 2H), 6.54 (t, *J* = 3.4 Hz, 1H), 3.26 – 3.21 (m, 4H), 1.72 – 1.62 (m, 4H), 1.56 – 1.47 (m, 4H), 1.41 – 1.34 (m, 4H), 1.34 – 1.29 (m, 8H), 0.91 – 0.87 (m, 6H); ^{13}C NMR (150 MHz, $CDCl_3$) δ 159.1, 158.2, 145.2, 143.3, 136.8, 133.2, 128.4, 122.3, 117.7, 116.5, 115.4, 114.9, 114.7, 69.4, 31.9, 31.8, 30.9, 30.5, 30.4, 30.3, 30.2, 29.7, 29.2, 29.1, 22.70, 2.67, 14.2, 14.1; HRMS (APCI): calcd for $C_{28}H_{36}IN_2O_2$ $[M+H]^+$ 559.1821, found 559.1825.

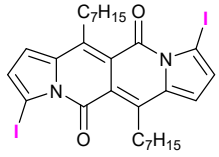

6,12-Diheptyl-3,9-diiodo-5*H*,11*H*-dipyrrolo[1,2-*b*:1',2'-*g*][2,6]naphthyridine-5,11-dione (8)

To the solution of DPND **1** (200 mg, 0.46 mmol) and freshly recrystallized *N*-iodosuccinimide (250 mg, 1.11 mmol) in 20 mL of dry chloroform, hexafluoro-2-propanol (485 µL, 4.62 mmol) was added dropwise. The reaction mixture was stirred overnight. After completion, the mixture was filtered through a short silica layer and washed with chloroform. The filtrate was concentrated to 5 mL and then treated with 100 mL of methanol. The resulting precipitate was filtered off and washed with cold methanol.

Yield: 300 mg (95%). Dark wine crystals; ^{1}H NMR (500 MHz, $CDCl_3$) δ 6.80 (s, 4H), 3.22 – 3.14 (m, 4H), 1.66 (dt, J = 15.4, 7.6 Hz, 4H), 1.54 – 1.47 (m, 4H), 1.37 (dt, J = 14.0, 6.9 Hz, 4H), 1.34 – 1.27 (m, 8H), 0.90 (t, J = 6.9 Hz, 6H); ^{13}C NMR (125 MHz, $CDCl_3$) δ 158.9, 143.0, 136.7, 128.4, 117.6, 115.2, 69.1, 31.8, 30.3, 30.2, 30.1, 29.1, 22.7, 14.2; ^{1}H NMR (500 MHz, THF-d8) δ 6.95 (d, *J* = 3.9 Hz, 2H), 6.84 (d, *J* = 3.9 Hz, 2H), 3.26 – 3.18 (m, 4H), 1.71 – 1.64 (m, 4H), 1.58 – 1.50 (m, 4H), 1.46 – 1.39 (m, 4H), 1.37 – 1.32 (m, 8H), 0.91 (t, *J* = 6.9 Hz, 6H); HRMS (APCI): calcd for $C_{28}H_{35}I_2N_2O_2$ $[M+H]^+$ 685.0788, found 685.0791.

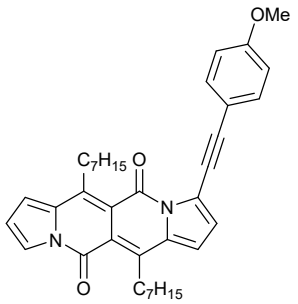

6,12-Diheptyl-3-((4-methoxyphenyl)ethynyl)-5*H*,11*H*-dipyrrolo[1,2-*b*:1',2'-*g*][2,6]naphthyridine-5,11-dione (12a)

In a Schlenck flask containing a magnetic stirring bar were placed: **2** (60 mg, 0.12 mmol), CuI (4 mg, 0.02 mmol), $Pd(PPh_3)_4$ (13 mg, 0.01 mmol), and 4-ethynylanisole (23 mg, 0.18 mmol). The vessel was evacuated and backfilled with argon (3 times) and anhydrous, degassed toluene was added (8 mL) followed by dry triethylamine (2 mL). The content of the flask was stirred for 20 h at 80 °C. The mixture was transferred to the separatory funnel and the organic layer was washed with degassed water (3 × 25 mL) and brine. The organic layer was then dried over $MgSO_4$ and the solvent was evaporated with Celite. The target product was purified by silica gel chromatography using hexanes / toluene (3/2) solution as eluent and recrystallized by slow addition of methanol to a solution of the dye in a small amount of toluene. Yield: 64 mg (91%). Dark violet powder; ^{1}H NMR (500 MHz, $CDCl_3$) δ 7.82 (d, *J* = 1.9 Hz, 1H), 7.56 (d, *J* = 8.7 Hz, 2H), 6.90 (d, *J* = 8.7 Hz, 2H), 6.85 (dd, *J* = 3.0, 2.0 Hz, 1H), 6.84 (d, *J* = 4.1 Hz, 1H), 6.76 (d, *J* = 4.0 Hz, 1H), 6.53 (t, *J* = 3.3 Hz, 1H), 3.85 (s, 3H), 3.31 – 3.23 (m, 4H), 1.78 – 1.62 (m, 4H), 1.61 – 1.47 (m, 4H), 1.47 – 1.27 (m, 12H), 0.94 – 0.86 (m, 6H); ^{13}C NMR (125 MHz, $CDCl_3$) δ 160.0, 158.6, 158.2, 144.8, 143.8, 134.1, 133.3, 133.1, 122.10, 122.08, 119.9, 116.2, 116.1, 115.3, 115.2, 115.1, 114.0, 98.3, 81.8, 55.3, 32.0, 31.9, 31.0, 30.8, 30.4, 30.3, 30.2, 29.7, 29.2, 29.0, 22.69, 22.67, 14.2, 14.1; HRMS (APCI): calcd for $C_{37}H_{43}N_2O_3$ $[M+H]^+$ 563.3274, found 563.3276.

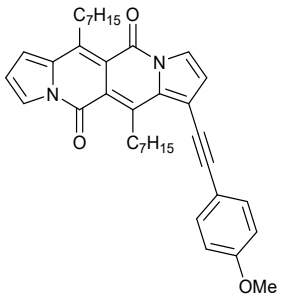

6,12-Diheptyl-1-((4-methoxyphenyl)ethynyl)-5*H*,11*H*-dipyrrolo[1,2-*b*:1',2'-*g*][2,6]naphthyridine-5,11-dione (12b)

In a Schlenck flask containing a magnetic stirring bar were placed: **9** (103 mg, 0.20 mmol), CuI (4 mg, 0.02 mmol), $Pd(PPh_3)_4$ (12 mg, 0.01 mmol), and 4-ethynylanisole (40 mg, 0.30 mmol). The vessel was evacuated and backfilled with argon (3 times) and anhydrous, degassed toluene was added (15 mL) followed by dry triethylamine (5 mL). The content of the flask was stirred for 20 h at 80 °C. The mixture was transferred to the separatory funnel and the organic layer was washed with degassed water (3 × 25 mL) and brine. The organic layer was then dried over $MgSO_4$ and the solvent was evaporated with Celite. The target product was purified by silica gel chromatography using toluene / hexanes (1/1) solution as eluent and recrystallized by slow addition of methanol to a solution of the dye in a small amount of toluene. Yield: 87 mg (90%). Dark red powder; ^{1}H NMR (500 MHz, $CDCl_3$) δ 7.85 (d, *J* = 1.9 Hz, 1H), 7.82 (d, *J* = 3.2 Hz, 1H), 7.46 (d, *J* = 8.8 Hz, 2H), 6.89 (d, *J* = 8.8 Hz, 2H), 6.87 (d, *J* = 3.6 Hz, 1H), 6.63 (d, *J* = 3.2 Hz, 1H), 6.53 (t, *J* = 3.4 Hz, 1H), 3.84 (s, 3H), 3.84 – 3.63 (m, 2H), 3.34 – 3.19 (m, 2H), 1.81 – 1.71 (m, 2H), 1.71 – 1.62 (m, 2H), 1.57 – 1.48 (m, 4H), 1.43 – 1.27 (m, 8H), 1.24 – 1.16 (m, 4H), 0.90 (t, *J* = 6.8 Hz, 3H), 0.82 (t, *J* = 6.8 Hz, 3H); ^{13}C NMR (125 MHz, $CDCl_3$) δ 160.0, 158.4, 157.9, 146.0, 145.3, 133.2, 132.9, 132.1, 122.7, 121.7, 120.0, 116.7, 115.4, 115.2, 115.1, 114.13, 114.09, 113.5, 97.5, 83.7, 55.3, 31.92, 31.89, 31.2, 30.44, 30.40, 30.3, 30.1, 29.9, 29.7, 29.5, 29.2, 22.7, 22.6, 14.1; HRMS (APCI): calcd for $C_{37}H_{43}N_2O_3$ $[M+H]^+$ 563.3274, found 563.3276.

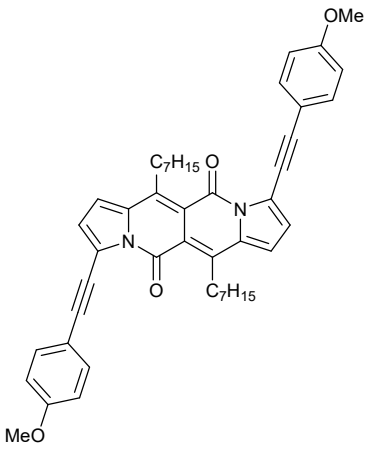

6,12-Diheptyl-3,9-bis((4-methoxyphenyl)ethynyl)-5*H*,11*H*-dipyrrolo[1,2-*b*:1',2'-*g*][2,6]naphthyridine-5,11-dione (12c)

In a Schlenck flask containing a magnetic stirring bar were placed: **2** (63 mg, 0.11 mmol), CuI (4 mg, 0.02 mmol), $Pd(PPh_3)_4$ (25 mg, 0.02 mmol), and 4-ethynylanisole (35 mg, 0.27 mmol). The vessel was evacuated and backfilled with argon (3 times) and anhydrous, degassed toluene was added (20 mL) followed by dry triethylamine (8 mL). The content of the flask was stirred for 20 h at 90 °C.

The mixture was transferred to the separatory funnel and the organic layer was washed with degassed water (3 × 25 mL) and brine. The organic layer was then dried over $MgSO_4$ and the solvent was evaporated with Celite. The target product was purified by silica gel chromatography using hexanes / toluene (3/2) solution as eluent and recrystallized by slow addition of methanol to a solution of the dye in a small amount of toluene. Yield: 60 mg (81%). Dark violet powder; ^{1}H NMR (500 MHz, $CDCl_3$) δ 7.56 (d, *J* = 8.8 Hz, 4H), 6.90 (d, *J* = 8.8 Hz, 4H), 6.83 (t, *J* = 6.2 Hz, 2H), 6.77 (d, *J* = 4.0 Hz, 2H), 3.85 (s, 6H), 3.31 – 3.24 (m, 4H), 1.72 (dt, *J* = 15.1, 7.5 Hz, 4H), 1.60 – 1.51 (m, 4H), 1.48 – 1.40 (m, 4H), 1.37 – 1.32 (m, 8H), 0.90 (t, *J* = 6.7 Hz, 6H); ^{13}C NMR (125 MHz, CDCl3) δ 160.0,

158.5, 143.2, 134.3, 133.1, 122.1, 119.6, 116.0, 115.8, 115.4, 114.0, 98.2, 81.9, 55.3, 32.0, 30.7, 30.3, 29.0, 22.7, 14.2. The NMR spectra are consistent with data previously published in the literature.[1]

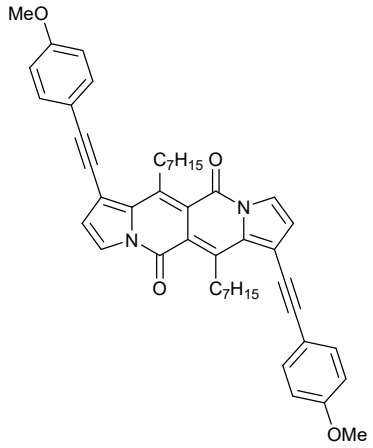

6,12-Diheptyl-1,7-bis((4-methoxyphenyl)ethynyl)-5*H*,11*H*-dipyrrolo[1,2-*b*:1',2'-*g*][2,6]naphthyridine-5,11-dione (12d)

In a Schlenck flask containing a magnetic stirring bar were placed: **10** (66 mg, 0.11 mmol), CuI (4 mg, 0.02 mmol), $Pd(PPh_3)_4$ (13 mg, 0.01 mmol), and 4-ethynylanisole (34 mg, 0.26 mmol). The vessel was evacuated and backfilled with argon (3 times) and anhydrous, degassed toluene was added (15 mL) followed by dry triethylamine (5 mL). The content of the flask was stirred for 48 h at 80 °C. The mixture was transferred to the separatory funnel and the organic layer was washed with degassed water (3 × 25 mL) and brine. The organic layer was then dried over $MgSO_4$ and the solvent was evaporated with Celite. The target product was purified by silica gel chromatography using hexanes / toluene (3/2) solution as eluent and recrystallized by slow addition of methanol to a solution of the dye in a small amount of toluene. Yield: 47 mg (61%). Dark violet powder; ^{1}H NMR (500 MHz, $CDCl_3$) δ 7.85 (d, J = 3.2 Hz, 2H), 7.47 (d, J = 8.7 Hz, 4H), 6.90 (d, J = 8.7 Hz, 4H), 6.65 (d, J = 3.2 Hz, 2H), 3.85 (s, 6H), 3.83 – 3.65 (m, 4H), 1.82 – 1.69 (m, 4H), 1.60 – 1.53 (m, 4H), 1.40 – 1.28 (m, 4H), 1.24 – 1.16 (m, 8H), 0.82 (t, J = 6.7 Hz, 6H); ^{13}C NMR (125 MHz, $CDCl_3$) δ 160.2, 160.0, 158.0, 145.8, 134.0, 133.0, 132.2, 122.0, 120.1, 115.2, 114.9, 114.1, 113.9, 113.7, 97.8, 83.8, 81.2, 72.9, 55.3, 31.9, 30.4, 30.2, 30.0, 29.5, 22.6, 14.1; HRMS (APCI): calcd for $C_{46}H_{49}N_2O_4$ $[M+H]^+$ 693.3692, found 693.3695.

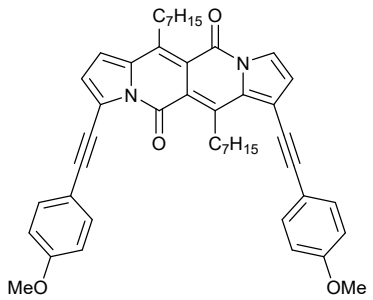

6,12-Diheptyl-1,9-bis((4-methoxyphenyl)ethynyl)-5*H*,11*H*-dipyrrolo[1,2-*b*:1',2'-*g*][2,6]naphthyridine-5,11-dione (12e)

In a Schlenck flask containing a magnetic stirring bar were placed: **11** (57 mg, 0.10 mmol), CuI (4 mg, 0.02 mmol), $Pd(PPh_3)_4$ (11 mg, 0.01 mmol), and 4-ethynylanisole (38 mg, 0.30 mmol). The vessel was evacuated and backfilled with argon (3 times) and anhydrous, degassed toluene was added

(20 mL) followed by dry triethylamine (5 mL). The content of the flask was stirred for 36 h at 80 °C. The mixture was transferred to the separatory funnel and the organic layer was washed with degassed water (3 × 25 mL) and brine. The organic layer was then dried over $MgSO_4$ and the solvent was evaporated with Celite. The target product was purified by silica gel chromatography using hexanes / toluene (3/2) solution as eluent and recrystallized by slow addition of methanol to a solution of the dye in a small amount of toluene. Yield: 54 mg (81%). Dark violet powder; ^{1}H NMR (500 MHz, $CDCl_3$) δ 7.80 (d, *J* = 3.2 Hz, 1H), 7.55 (d, *J* = 8.8 Hz, 2H), 7.46 (d, *J* = 8.8 Hz, 2H), 6.89 (d, *J* = 8.4 Hz, 4H), 6.84 (d, *J* = 4.0 Hz, 1H), 6.75 (d, *J* = 4.0 Hz, 1H), 6.62 (d, *J* = 3.2 Hz, 1H), 3.84 (s, 3H), 3.84 (s, 3H), 3.81 – 3.68 (m, 2H), 3.31 – 3.19 (m, 2H), 1.85 – 1.77 (m, 2H), 1.71 – 1.63 (m, 2H), 1.61 – 1.55 (m, 2H), 1.54 – 1.47 (m, 2H), 1.46 – 1.35 (m, 4H), 1.34 – 1.28 (m, 4H), 1.27 – 1.22 (m, 4H), 0.90 (t, *J* = 6.8 Hz, 3H), 0.83 (t, *J* = 6.8 Hz, 3H); ^{13}C NMR (125 MHz, $CDCl_3$) δ 160.0, 159.9, 158.7, 157.8, 145.2, 143.6, 134.1, 133.1, 132.9, 132.3, 122.0, 121.4, 120.1, 119.9, 116.3, 116.0, 115.4, 115.3, 114.9, 114.1, 114.0, 112.9, 98.7, 97.3, 83.9, 82.0, 55.32, 55.29, 32.1, 31.9, 30.9, 30.5, 30.4, 29.9, 29.8, 29.22, 29.18, 22.7, 22.6, 14.2, 14.1; HRMS (APCI): calcd for $C_{46}H_{49}N_2O_4$ $[M+H]^+$ 693.3692, found 693.3693.

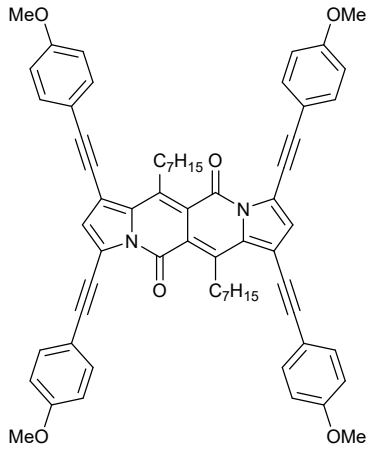

6,12-Diheptyl-1,3,7,9-tetrakis((4-methoxyphenyl)ethynyl)-5*H*,11*H*-dipyrrolo[1,2-*b*:1',2'-*g*][2,6]naphthyridine-5,11-dione (12f)

In a Schlenck flask containing a magnetic stirring bar were placed: **4** (36 mg, 0.05 mmol), CuI (4 mg, 0.02 mmol), $Pd(PPh_3)_4$ (22 mg, 0.02 mmol), and 4-ethynylanisole (38 mg, 0.29 mmol). The vessel was evacuated and backfilled with argon (3 times) and anhydrous, degassed toluene was added (40 mL) followed by dry triethylamine (10 mL). The content of the flask was stirred for 36 h at 90 °C. The mixture was transferred to the separatory funnel and the organic layer was washed with degassed water (3 × 40 mL) and brine. The organic layer was then dried over $MgSO_4$ and the solvent was evaporated with Celite. The target product was purified by silica gel chromatography using toluene / hexanes (5/1) solution as eluent and recrystallized by slow addition of methanol to a solution of the dye in a small amount of toluene. Yield: 34 mg (74%). Dark blue solid; ^{1}H NMR (500 MHz, $CDCl_3$) δ 7.56 (d, *J* = 8.7 Hz, 4H), 7.47 (d, *J* = 8.7 Hz, 4H), 6.91 (d, *J* = 2.5 Hz, 4H), 6.89 (d, *J* = 2.5 Hz, 4H), 6.88 (s, 2H), 3.85 (s, 6H), 3.85 (s, 6H), 3.82 – 3.73 (m, 4H), 1.85 – 1.78 (m, 4H), 1.62 – 1.56 (m, 4H), 1.44 – 1.35 (m, 4H), 1.29 – 1.19 (m, 8H), 0.83 (t, *J* = 6.8 Hz, 6H); ^{13}C NMR (125 MHz, $CDCl_3$) δ 160.1, 160.0, 158.3, 143.5, 133.2, 133.0, 126.2, 119.1, 116.6, 115.3, 115.2, 114.1, 114.0, 112.7, 98.7, 97.4, 83.4, 81.3, 55.4, 55.3, 32.1, 30.3, 30.2, 29.6, 29.2, 22.6, 14.2; HRMS (APCI): calcd for $C_{64}H_{61}N_2O_6$ $[M+H]^+$ 953.4530, found 953.4534.

3. X-ray structures

Table S1. Crystallographic data for compound **8**.

Chemical formula	$C_{28}H_{34}N_2O_2I_2$	
Formula weight	684.37 g/mol	
Temperature	100 K	
Wavelength	0.71073 Å	
Crystal size	0.23 x 0.04 x 0.02 mm	
Crystal habit	violet needle	
Crystal system	monoclinic	
Space group	C2/a	
Unit cell dimensions	a = 31.5672(7) Å	α = 90°
	b = 4.64730(10) Å	β = 101.217(2)°
	c = 18.6492(4) Å	γ = 90°
Volume	2683.62(10) Å^3	
Z	4	
Density	1.694 g/cm^3	
Absorption coefficient	2.371 mm^{-1}	
F(000)	1352	
Index ranges	$-53 \leq h \leq 54$, $-7 \leq k \leq 6$, $-31 \leq l \leq 31$	
Diffractometer	Rigaku XtaLAB Synergy, Dualflex, HyPix-Arc 150	
Radiation source	MoK_α	
Reflections collected	40165	
Independent reflections	6814 [R(int) = 0.0491]	
Tmin, Tmax	0.953, 1.000	
Absorption correction	multi-scan	
Refinement method	Full-matrix least-squares on F^2	
Restraints / parameters	0 / 155	
Goodness-of-fit on F^2	0.893	
Final R indices	$[F^2 > 2\sigma(F^2)]$	R1 = 0.0395, wR2 = 0.1191
	all data	R1 = 0.0662, wR2 = 0.1341

Single violet needle-shaped crystals of compound **8** were obtained by vapour diffusion from DCE/MeOH. A suitable crystal 0.23×0.04×0.02 mm^3 was selected and loop on an XtaLAB Synergy, Dualflex, HyPix-Arc 150 diffractometer. The crystal was kept at a steady T = 100.01(10) K during data collection. The structure was solved with the ShelXT 2018/2 (Sheldrick, 2018) structure solution program using the Intrinsic Phasing solution method and by using **Olex2** (Dolomanov et al., 2009) as the graphical interface. The model was refined with version 2018/3 of ShelXL 2018/3 (Sheldrick, 2015) using Least Squares minimisation.

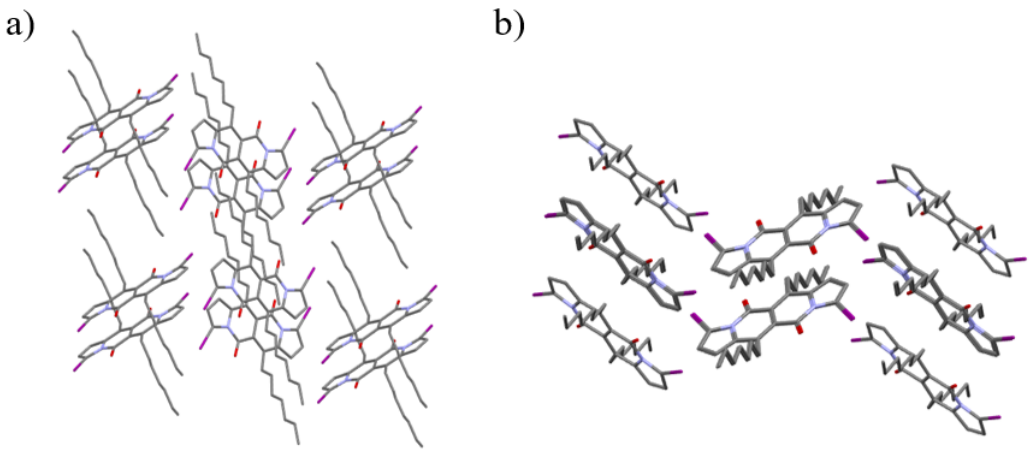

Figure S2. Packing diagram of crystal in elementary cell of compound **8** a) front view, b) side view.

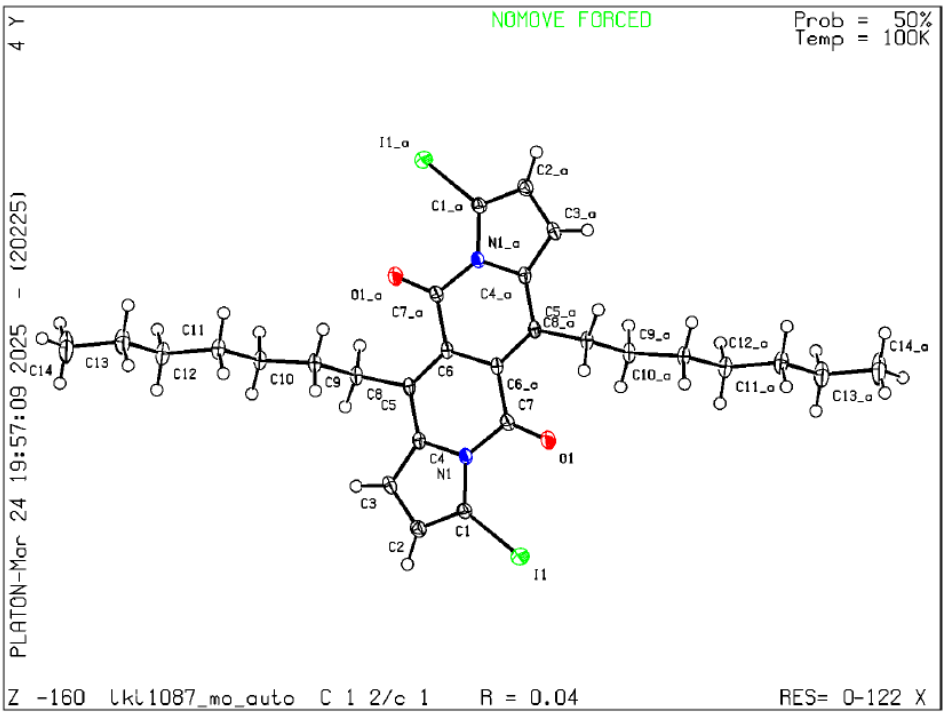

Figure S3. Thermal ellipsoid plot for compound **8** with 50% probability level of ellipsoids contour.

Crystallographic data have been deposited at the Cambridge Crystallographic Data Centre with the deposition number CCDC 2434014.

Table S2. Crystallographic data for compound **10**.

Chemical formula	$C_{28}H_{34}Br_2N_2O_2$	
Formula weight	590.39 g/mol	
Temperature	100 K	
Wavelength	1.54184 Å	
Crystal size	0.17 x 0.03 x 0.03 mm	
Crystal habit	red needle	
Crystal system	triclinic	
Space group	P-1	
Unit cell dimensions	a = 4.5767(4) Å	α = 74.174(13)°
	b = 9.1416(19) Å	β = 89.890(8)°
	c = 16.1020(16) Å	γ = 76.786(12)°
Volume	629.67(16) Å^3	
Z	1	
Density	1.557 g/cm^3	
Absorption coefficient	4.303 mm^{-1}	
F(000)	302	
Index ranges	$-5 \leq h \leq 5$, $-8 \leq k \leq 4$, $-19 \leq l \leq 19$	
Diffractometer	Rigaku XtaLAB Synergy, Dualflex, HyPix-Arc 150	
Radiation source	CuK_α	
Reflections collected	2173	
Independent reflections	1681 [R(int) = 0.0570]	
Tmin, Tmax	0.563, 1.000	
Absorption correction	multi-scan	
Refinement method	Full-matrix least-squares on F^2	
Restraints / parameters	0 / 156	
Goodness-of-fit on F^2	1.151	
Final R indices	[$F^2 > 2\sigma(F^2)$]	R1 = 0.0999, wR2 = 0.2790
	all data	R1 = 0.1062, wR2 = 0.2828

Single red needle-shaped crystals of compound **10** were obtained by vapour diffusion from DCM/MeOH. A suitable crystal 0.17×0.03×0.03 mm^3 was selected and mounted on a suitable support on an XtaLAB Synergy, Dualflex, HyPix-Arc 150 diffractometer. The crystal was kept at a steady T = 100.0(5) K during data collection. The structure was solved with the ShelXT 2018/2 (Sheldrick, 2018) structure solution program using the Intrinsic Phasing solution method and by using **Olex2** (Dolomanov et al., 2009) as the graphical interface. The model was refined with version 2018/3 of ShelXL 2018/3 (Sheldrick, 2015) using Least Squares minimisation.

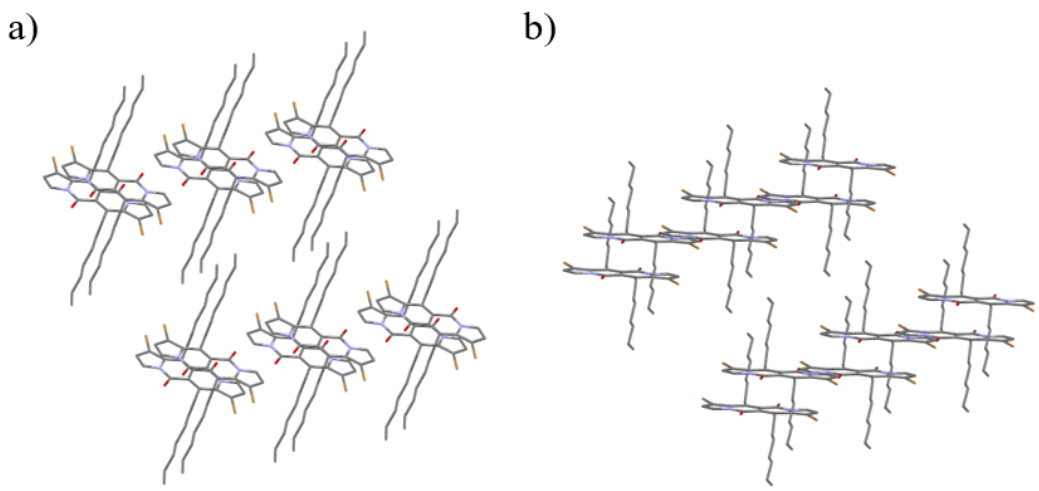

Figure S4. Packing diagram of crystal in elementary cell of compound **10** a) front view, b) side view.

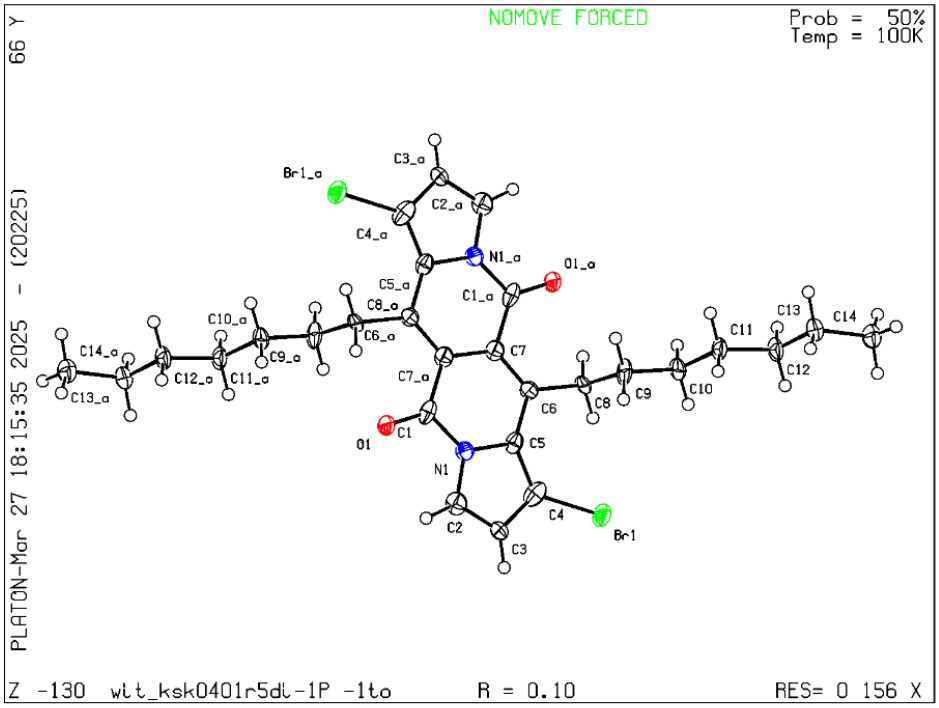

Figure S5. Thermal ellipsoid plot for compound **10** with 50% probability level of ellipsoids contour.

Crystallographic data have been deposited at the Cambridge Crystallographic Data Centre with the deposition number CCDC 2434047.

4. Spectral Data

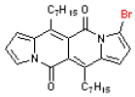

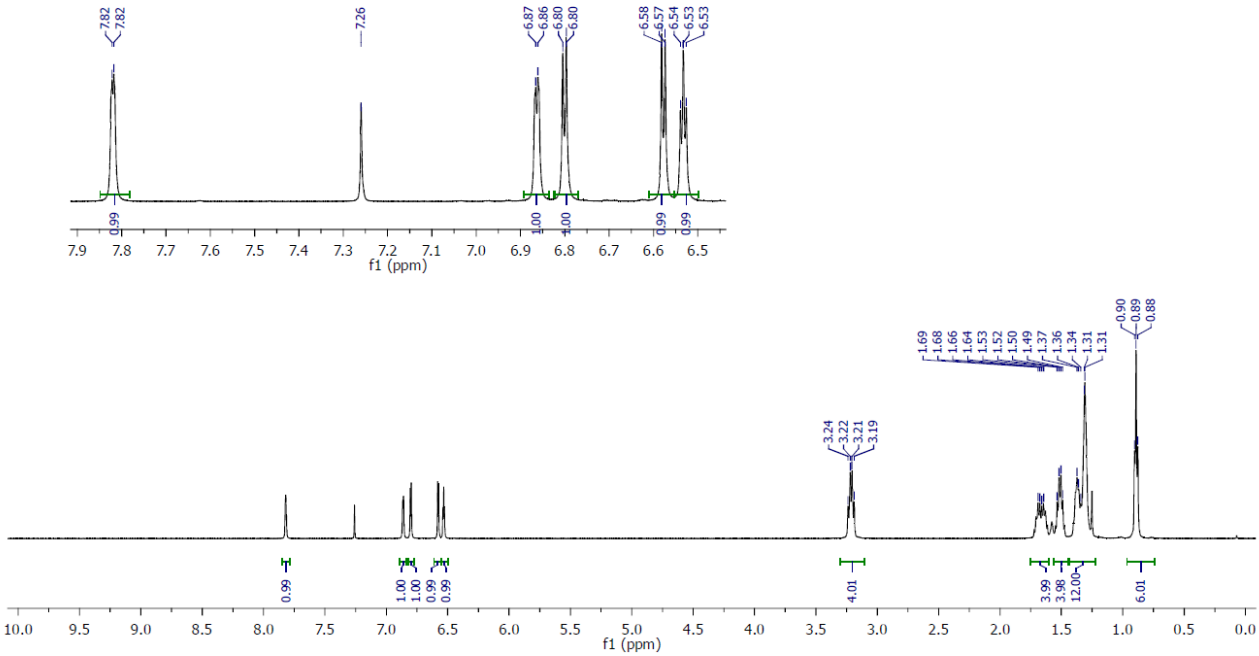

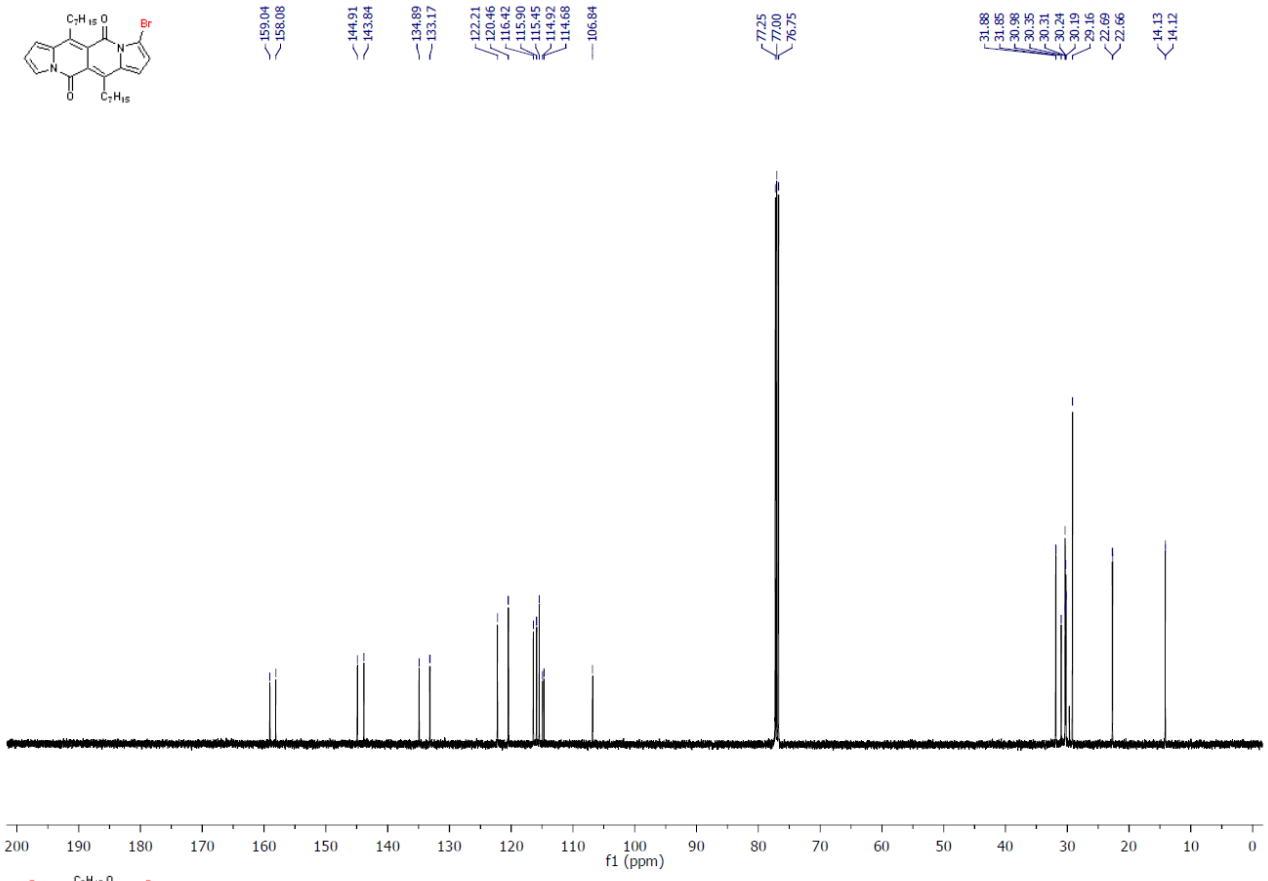
159.04
158.08
144.91
143.84
134.89
133.17
122.21
120.46
116.42
115.90
115.45
114.92
114.68
106.84
77.25
77.00
76.75
31.88
31.85
30.98
30.35
30.31
30.24
30.19
29.16
22.69
22.66
14.13
14.12
f1 (ppm)

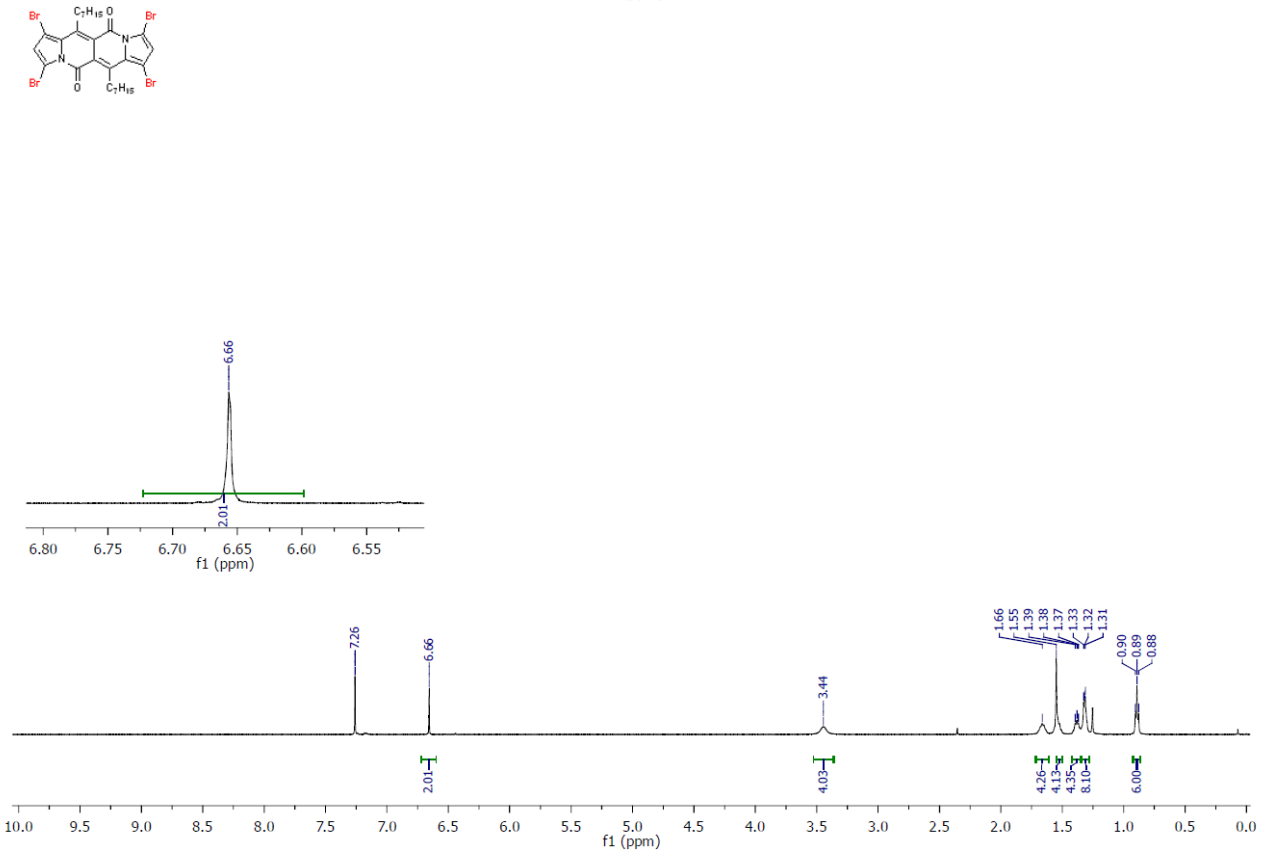
6.66
2.01
f1 (ppm)
7.26
6.66
3.44
1.66
1.55
1.39
1.38
1.37
1.33
1.32
1.31
0.90
0.89
0.88
2.01
4.03
4.26
4.13
4.35
8.10
6.00
f1 (ppm)

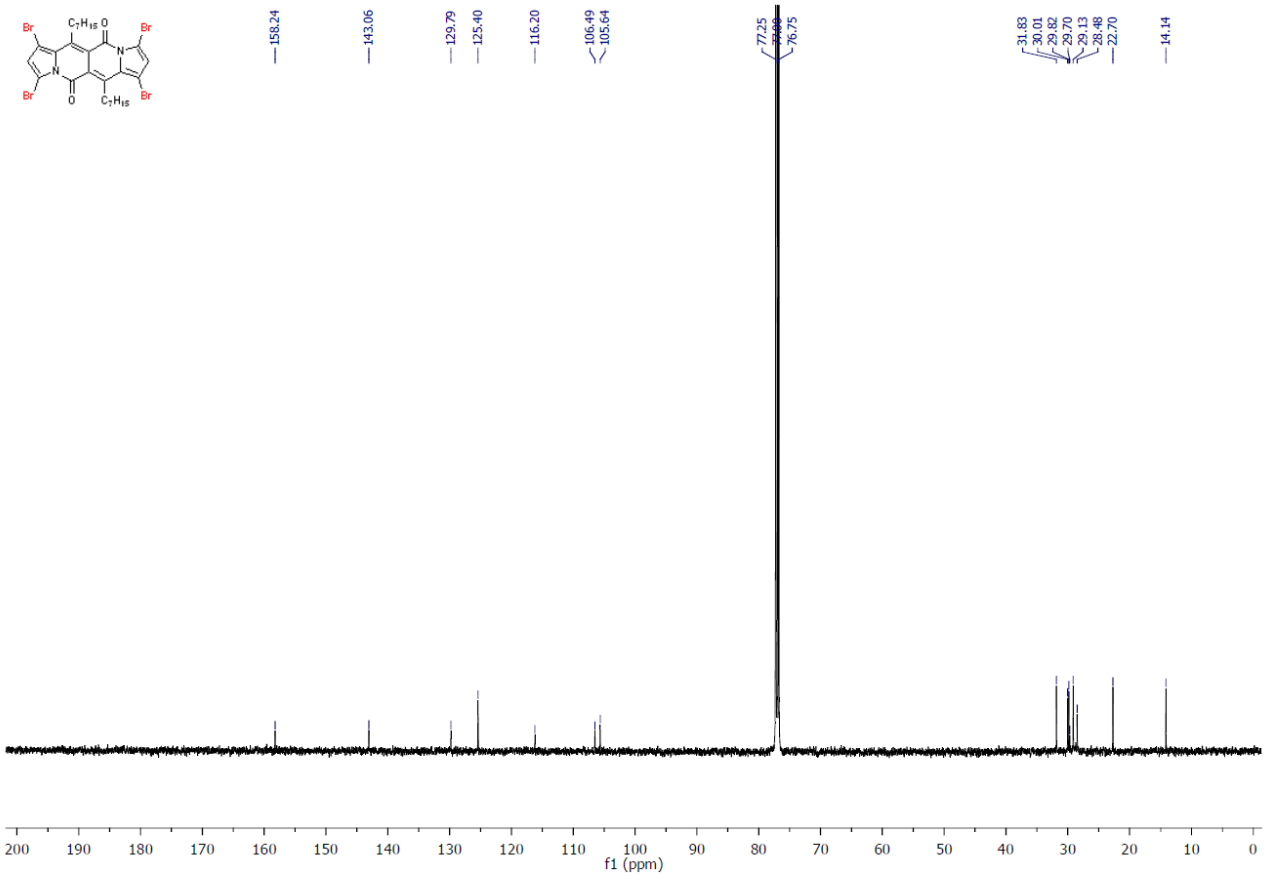
158.24
143.06
129.79
125.40
116.20
106.49
105.64
77.25
76.75
31.83
30.01
29.82
29.70
29.13
28.48
22.70
14.14
f1 (ppm)

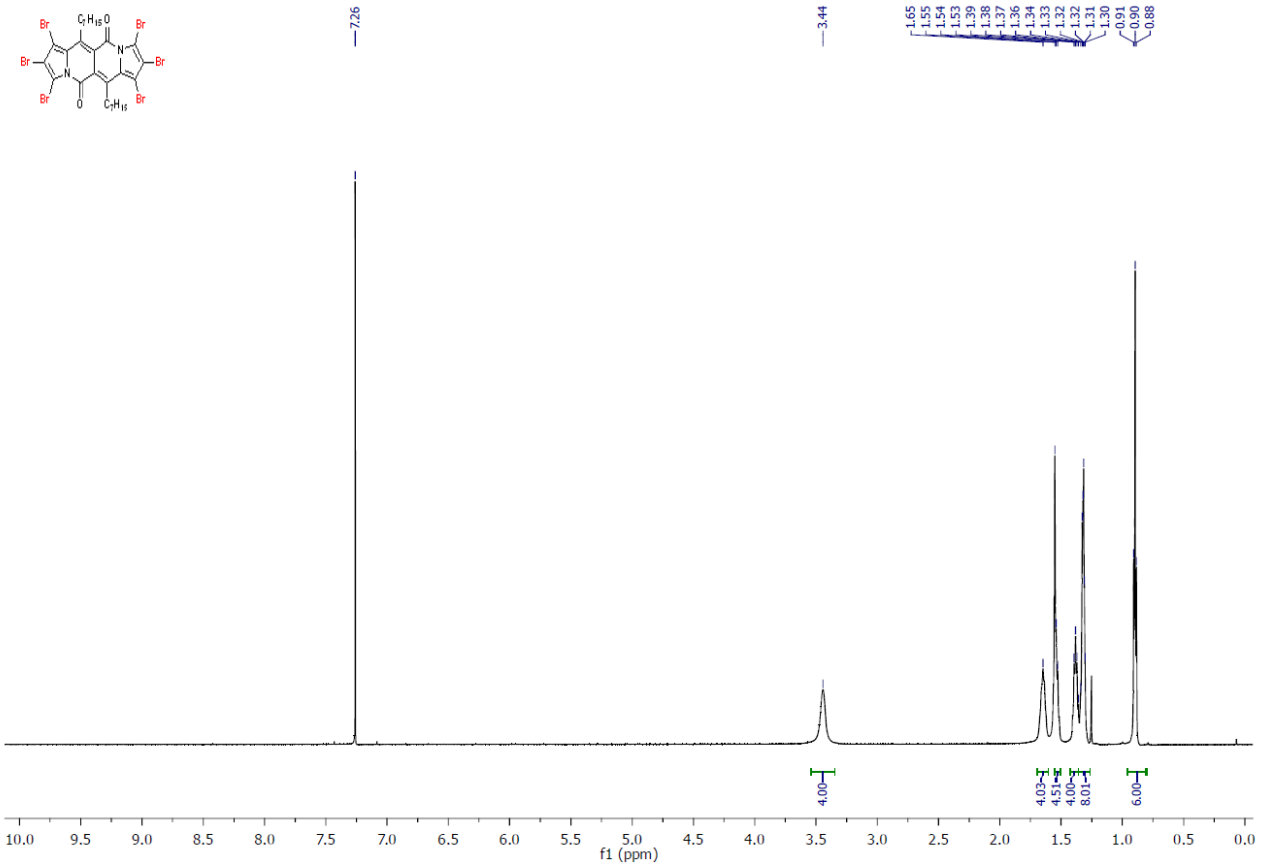
7.26
3.44
1.65
1.55
1.54
1.53
1.39
1.38
1.37
1.36
1.34
1.33
1.32
1.32
1.31
1.30
0.91
0.90
0.88
4.00
4.03
4.51
4.00
8.01
6.00
f1 (ppm)

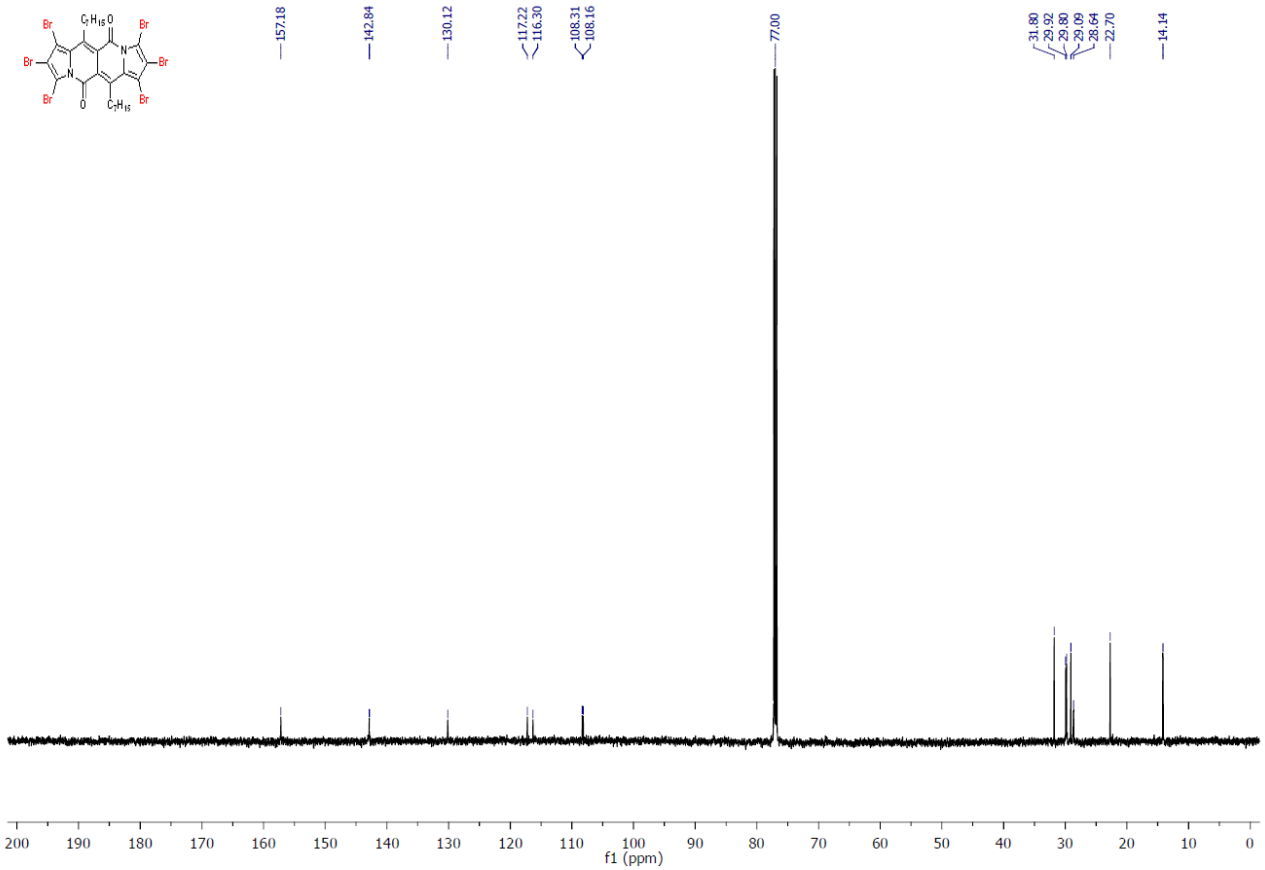
157.18
142.84
130.12
117.22
116.30
108.31
108.16
77.00
31.80
29.92
29.80
29.09
28.64
22.70
14.14
f1 (ppm)

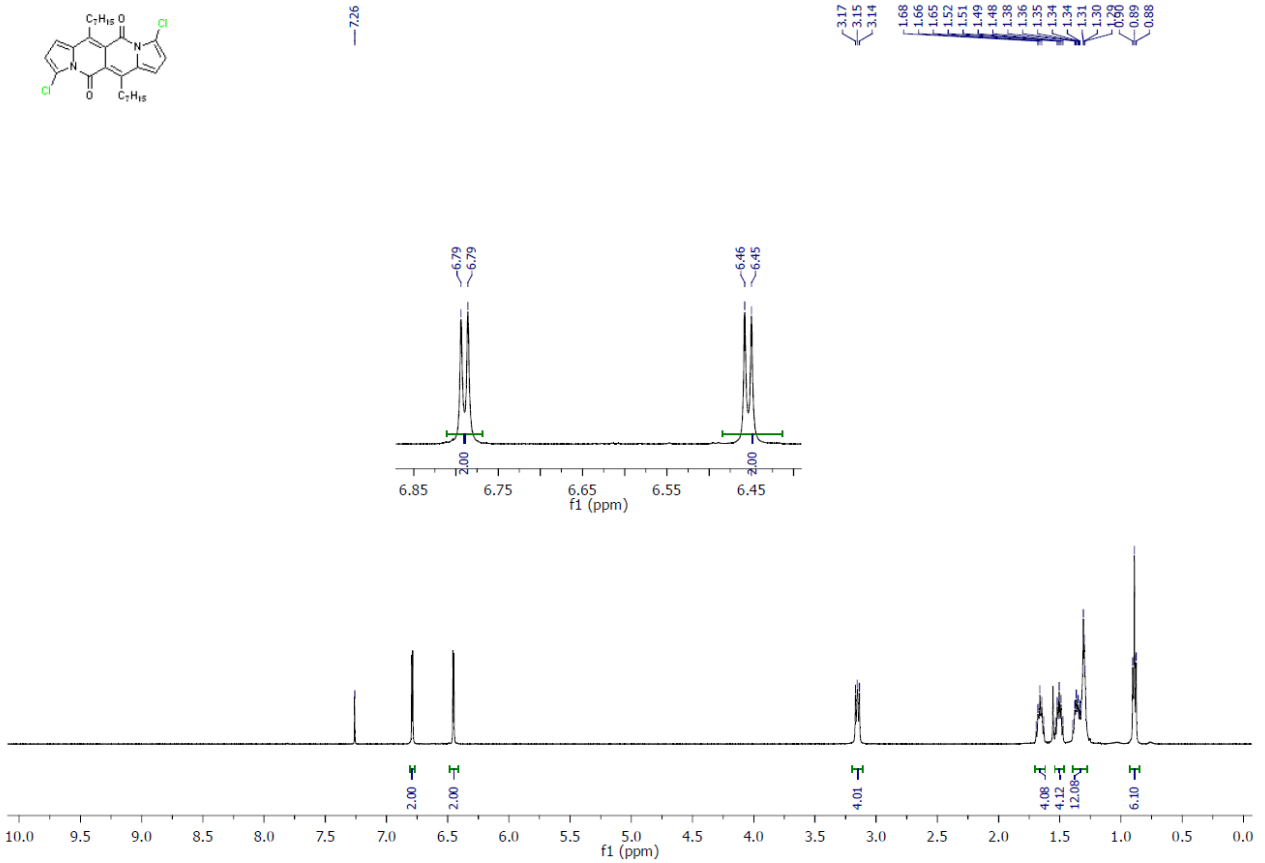
7.26
3.17
3.15
3.14
1.68
1.66
1.65
1.52
1.51
1.49
1.48
1.38
1.36
1.35
1.34
1.34
1.31
1.30
0.90
0.89
0.88
6.79
6.79
6.46
6.45
2.00
2.00
f1 (ppm)
2.00
2.00
4.01
4.08
4.12
12.08
6.10
f1 (ppm)

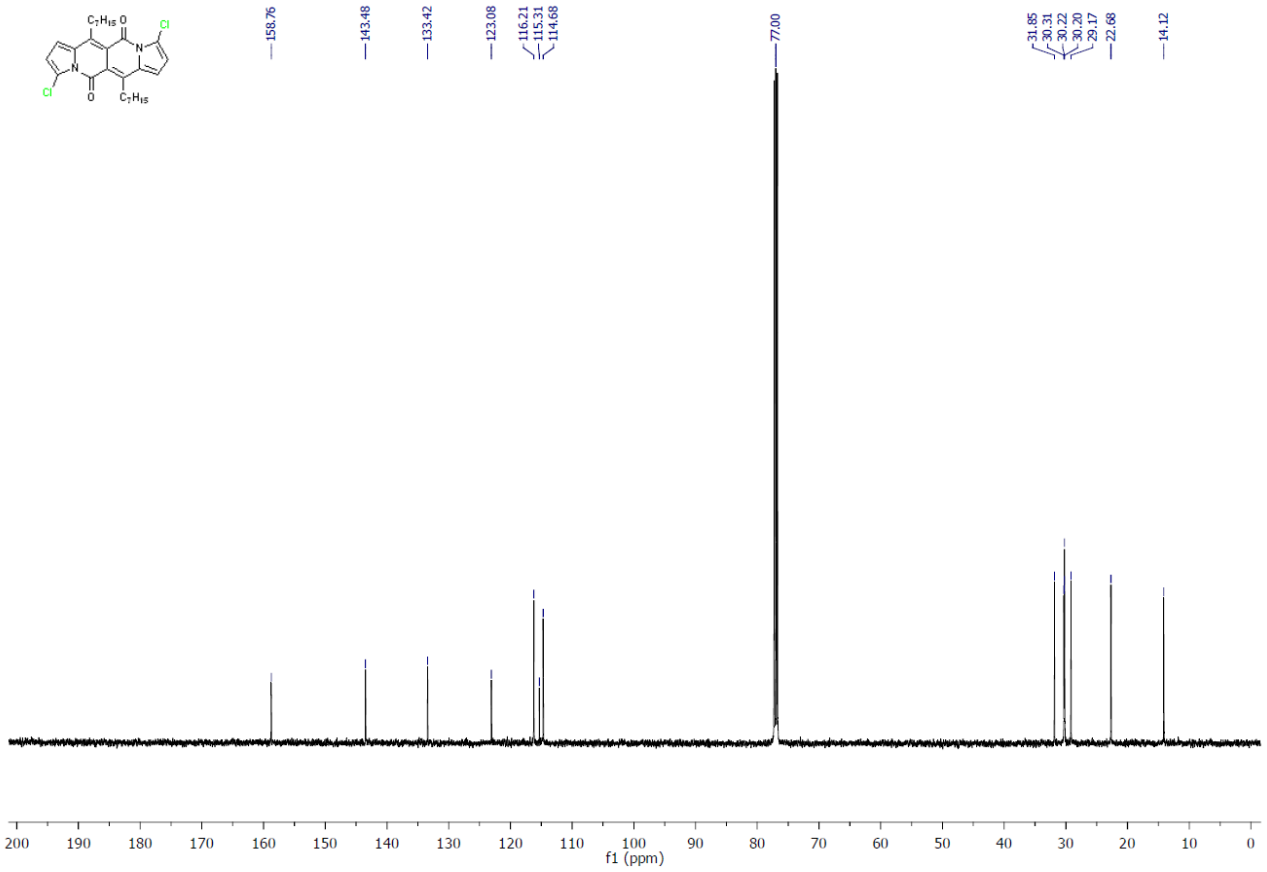
158.76
143.48
133.42
123.08
116.21
115.31
114.68
77.00
31.85
30.31
30.22
30.20
29.17
22.68
14.12
f1 (ppm)

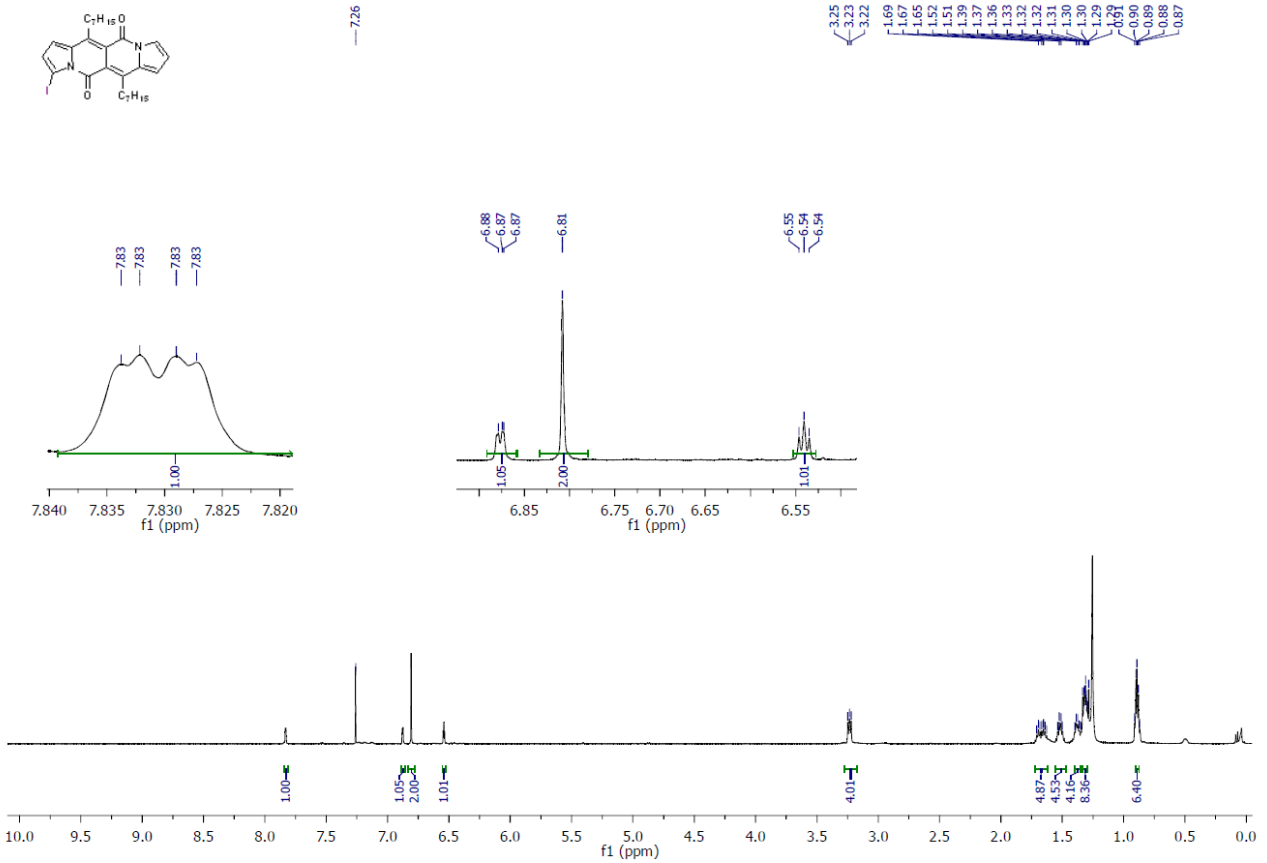
7.26
3.25
3.23
3.22
1.69
1.67
1.65
1.52
1.51
1.39
1.37
1.36
1.33
1.32
1.32
1.31
1.30
1.30
1.29
0.91
0.90
0.89
0.88
0.87
7.83
7.83
7.83
7.83
6.88
6.87
6.87
6.81
6.55
6.54
6.54
1.00
1.05
2.00
1.01
4.01
4.87
4.53
4.16
8.36
6.40
f1 (ppm)

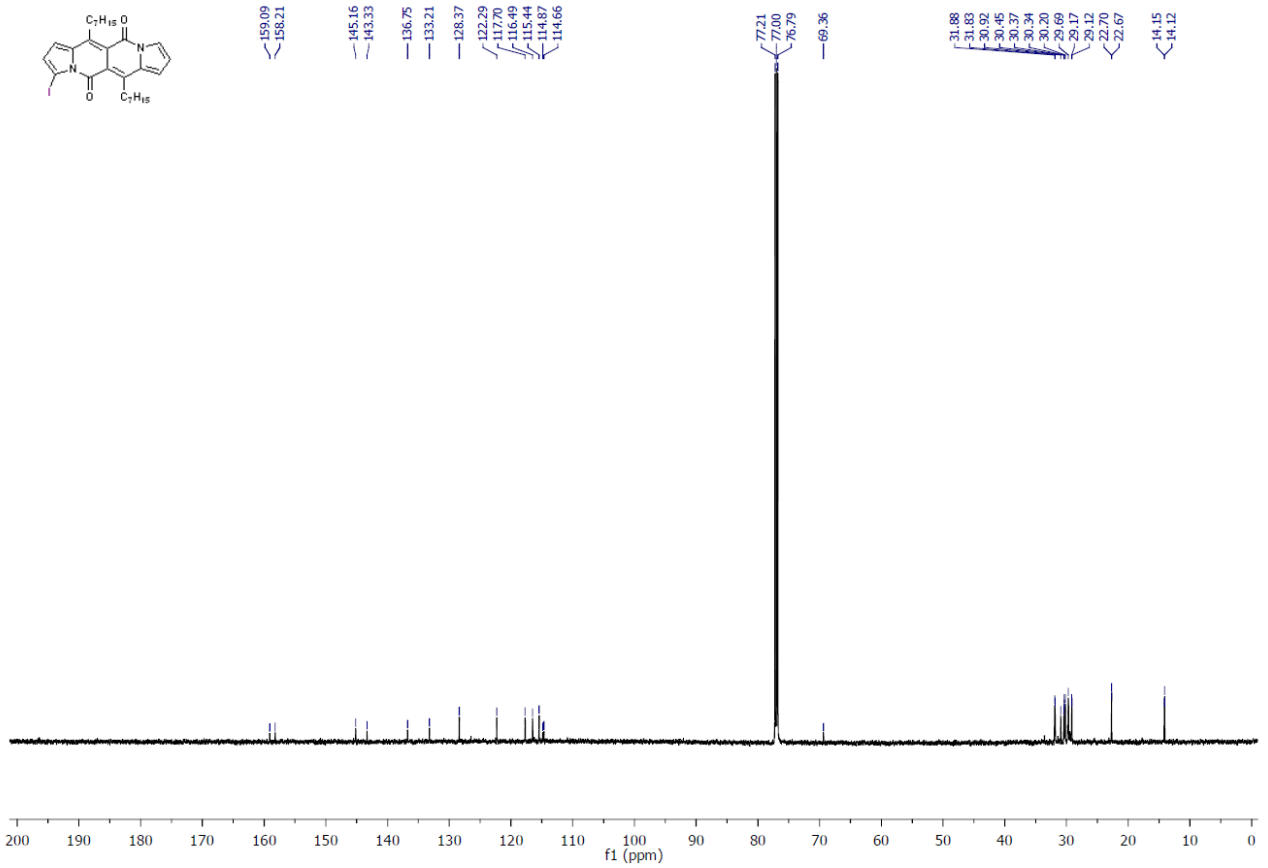
159.09
158.21
145.16
143.33
136.75
133.21
128.37
122.29
117.70
116.49
115.44
114.87
114.66
77.21
77.00
76.79
69.36
31.88
31.83
30.92
30.45
30.37
30.34
30.20
29.69
29.17
29.12
22.70
22.67
14.15
14.12
f1 (ppm)

$CDCl_3$

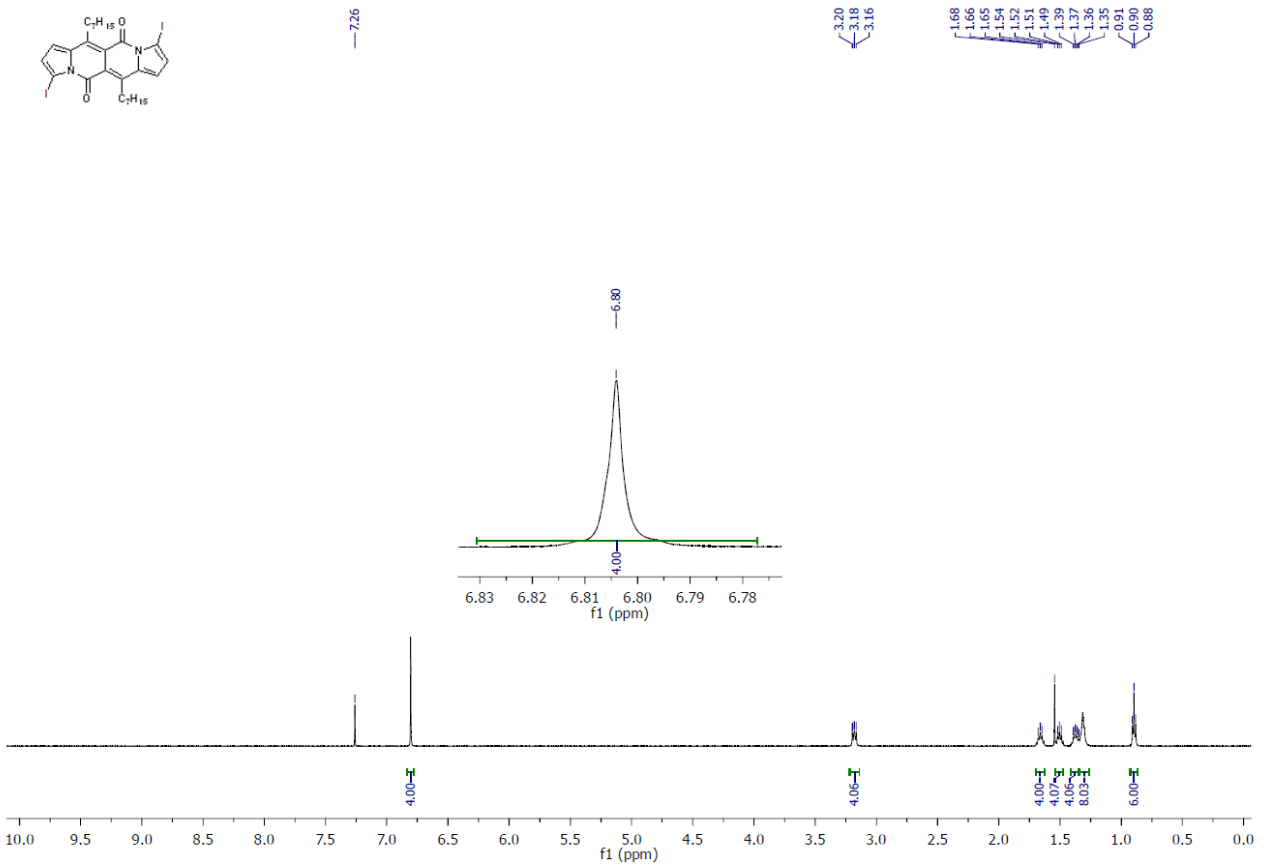
7.26
3.20
3.18
3.16
1.68
1.66
1.65
1.54
1.52
1.51
1.49
1.39
1.37
1.36
1.35
0.91
0.90
0.88
6.80
4.00
f1 (ppm)
4.00
4.06
4.00
4.07
4.06
8.03
6.00
f1 (ppm)

THF-D8

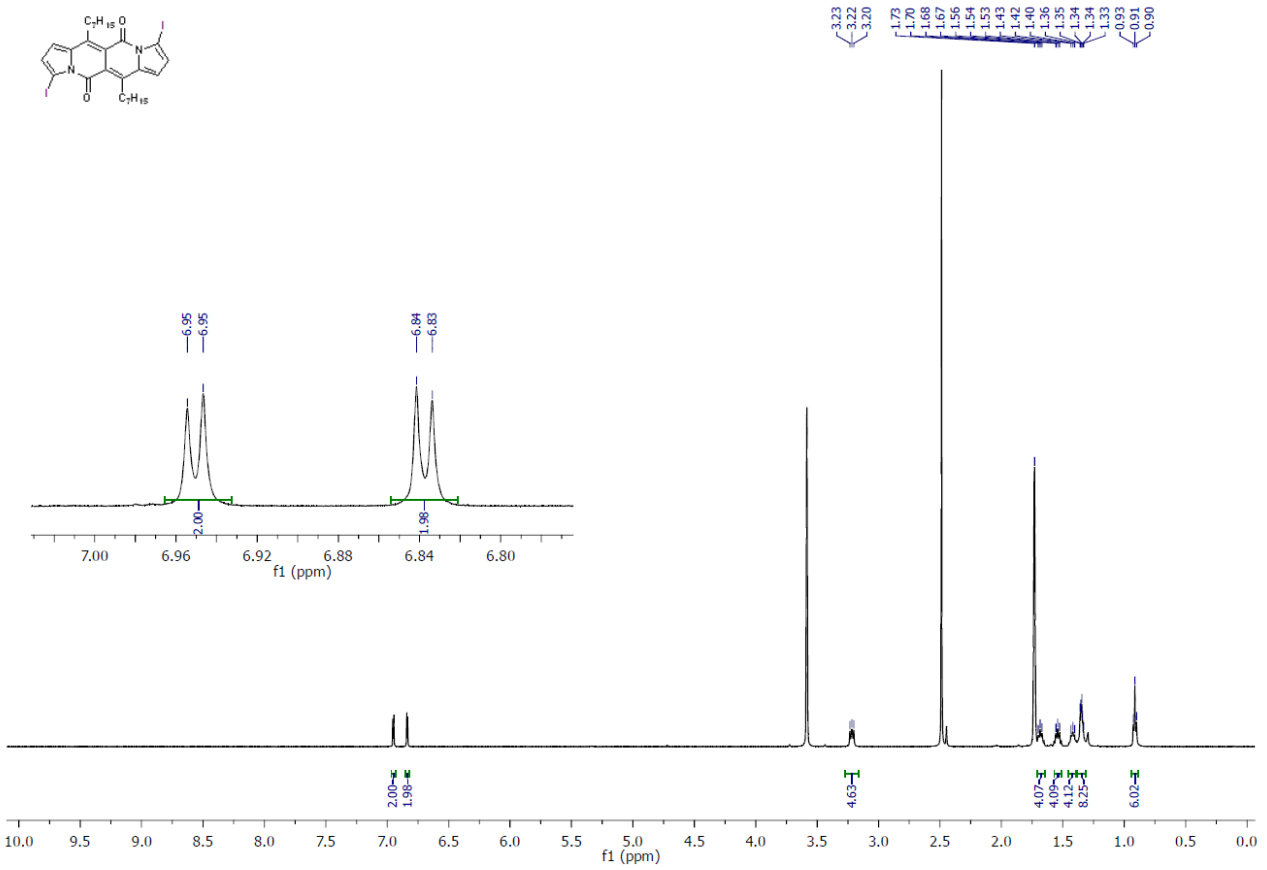
3.23
3.22
3.20
1.73
1.70
1.68
1.67
1.56
1.54
1.53
1.43
1.42
1.40
1.36
1.35
1.34
1.34
1.33
0.93
0.91
0.90
6.95
6.95
6.84
6.83
2.00
1.98
7.00
6.96
6.92
6.88
6.84
6.80
f1 (ppm)
2.00
1.98
4.63
4.07
4.09
4.12
8.25
6.02
10.0
9.5
9.0
8.5
8.0
7.5
7.0
6.5
6.0
5.5
5.0
4.5
4.0
3.5
3.0
2.5
2.0
1.5
1.0
0.5
0.0
f1 (ppm)

$CDCl_3$

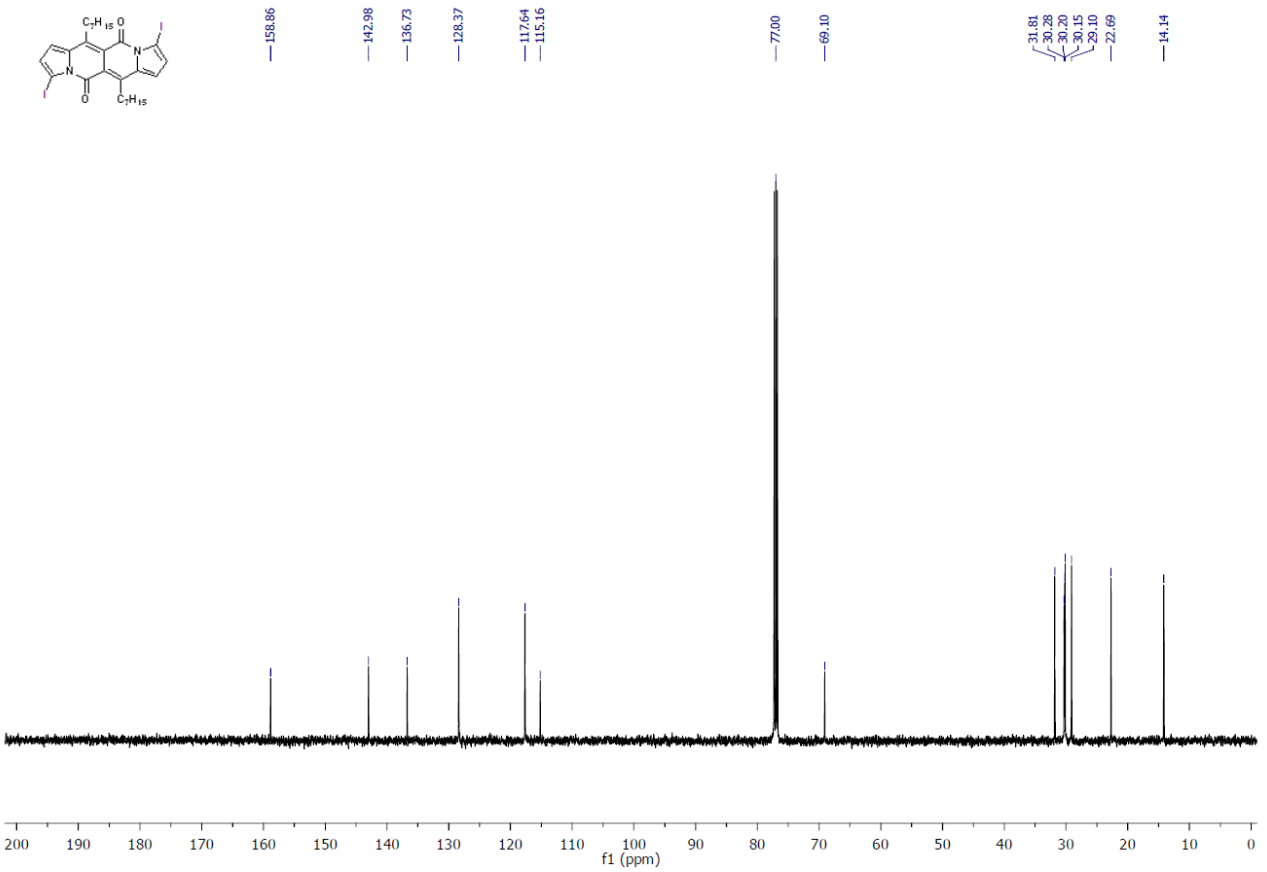
158.86
142.98
136.73
128.37
117.64
115.16
77.00
69.10
31.81
30.28
30.20
30.15
29.10
22.69
14.14
200
190
180
170
160
150
140
130
120
110
100
90
80
70
60
50
40
30
20
10
0
f1 (ppm)

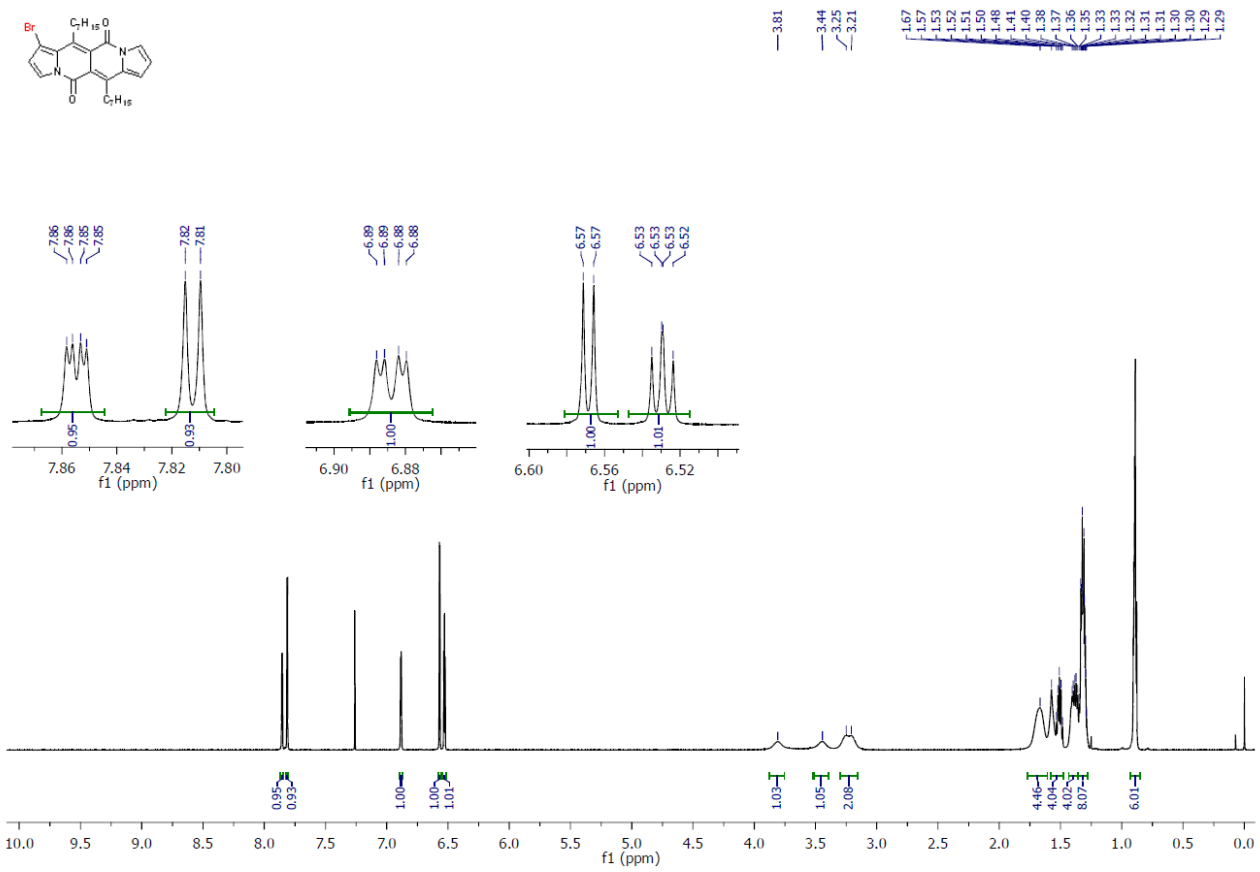
Br
C7H15
O
N
O
C7H15
3.81
3.44
3.25
3.21
1.67
1.57
1.53
1.52
1.51
1.50
1.48
1.41
1.40
1.38
1.37
1.36
1.35
1.33
1.33
1.32
1.31
1.31
1.30
1.30
1.29
1.29
7.86
7.86
7.85
7.85
7.82
7.81
6.89
6.89
6.88
6.88
6.57
6.57
6.53
6.53
6.53
6.52
0.95
0.93
1.00
1.00
1.01
7.86
7.84
7.82
7.80
6.90
6.88
6.60
6.56
6.52
f1 (ppm)
0.95
0.93
1.00
1.00
1.01
1.03
1.05
2.08
4.46
4.04
4.02
8.07
6.01
10.0
9.5
9.0
8.5
8.0
7.5
7.0
6.5
6.0
5.5
5.0
4.5
4.0
3.5
3.0
2.5
2.0
1.5
1.0
0.5
0.0
f1 (ppm)

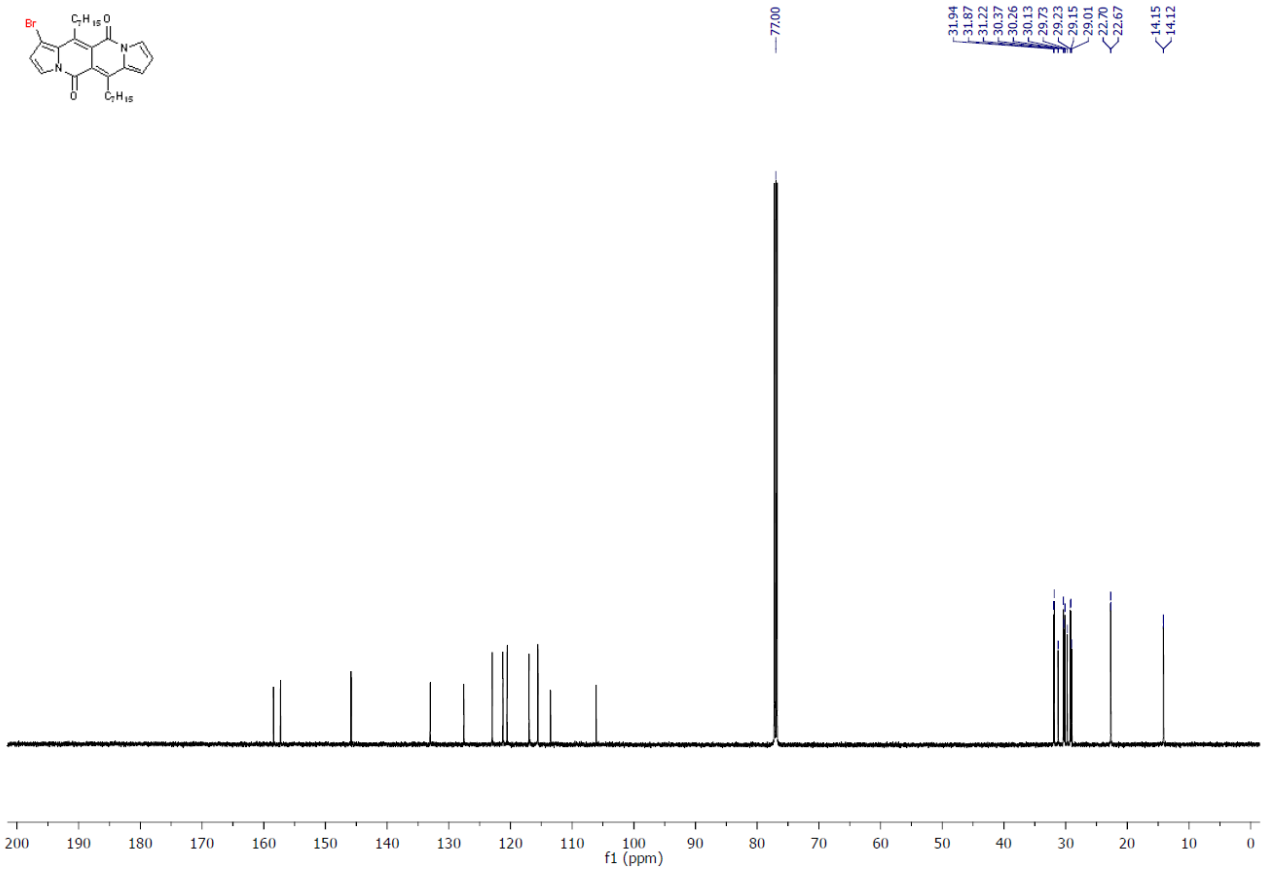
Br
C7H15
O
N
O
C7H15
77.00
31.94
31.87
31.22
30.37
30.26
30.13
29.73
29.23
29.15
29.01
22.70
22.67
14.15
14.12
200 190 180 170 160 150 140 130 120 110 100 90 80 70 60 50 40 30 20 10 0
f1 (ppm)

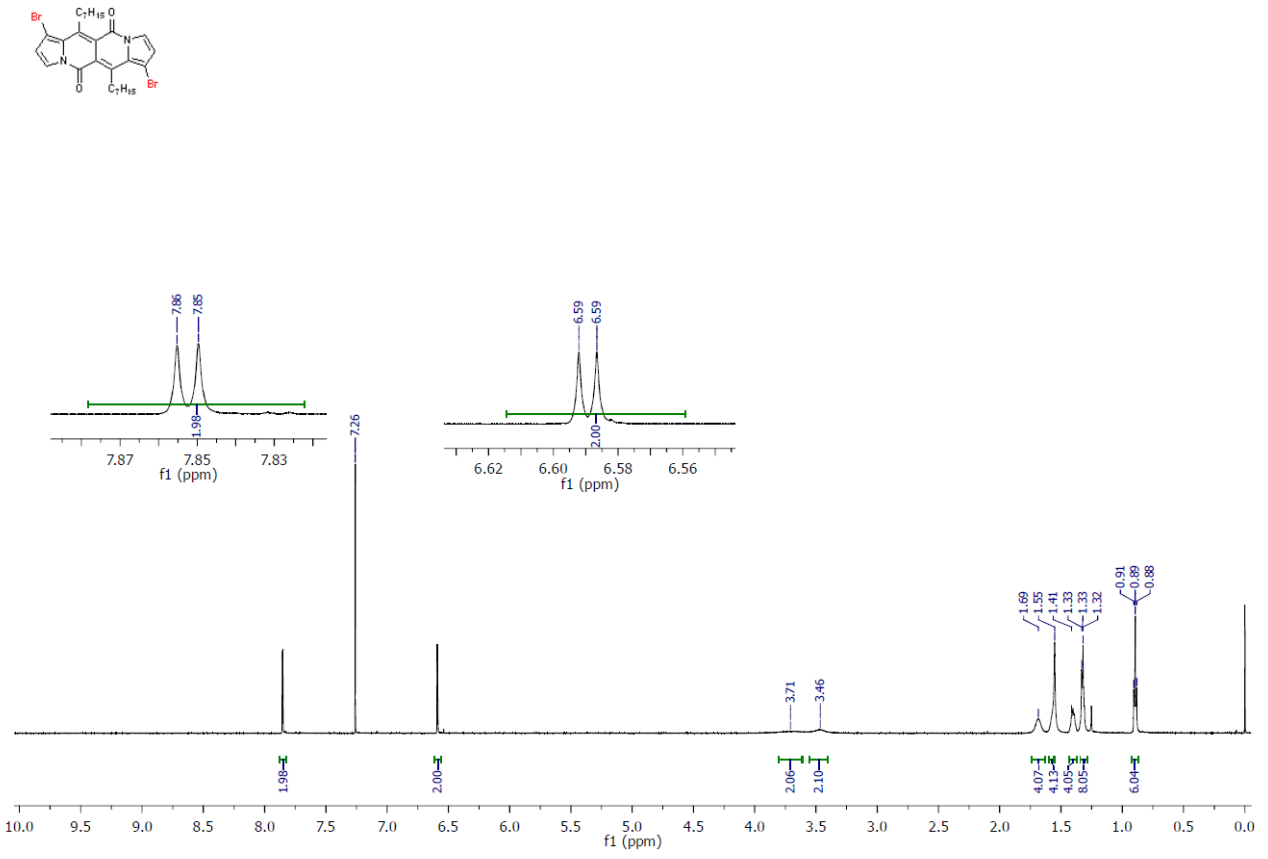
Br
C7H15
O
N
O
C7H15
Br
7.86
7.85
1.98
7.87
7.85
7.83
f1 (ppm)
6.59
6.59
2.00
6.62
6.60
6.58
6.56
f1 (ppm)
7.26
3.71
3.46
1.69
1.55
1.41
1.33
1.33
1.32
0.91
0.89
0.88
1.98
2.00
2.06
2.10
4.07
4.13
4.05
8.05
6.04
10.0 9.5 9.0 8.5 8.0 7.5 7.0 6.5 6.0 5.5 5.0 4.5 4.0 3.5 3.0 2.5 2.0 1.5 1.0 0.5 0.0
f1 (ppm)

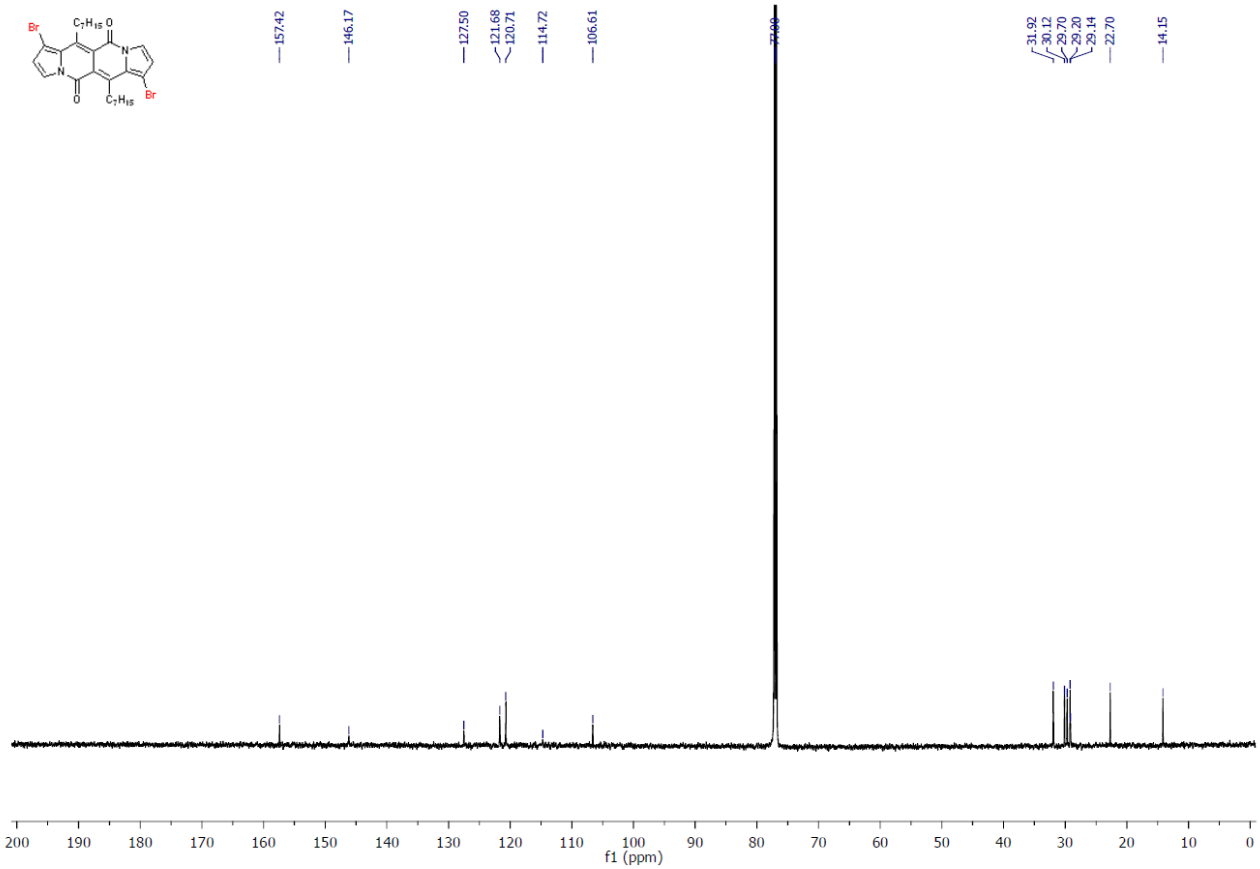
157.42
146.17
127.50
121.68
120.71
114.72
106.61
77.00
31.92
30.12
29.70
29.20
29.14
22.70
14.15
f1 (ppm)

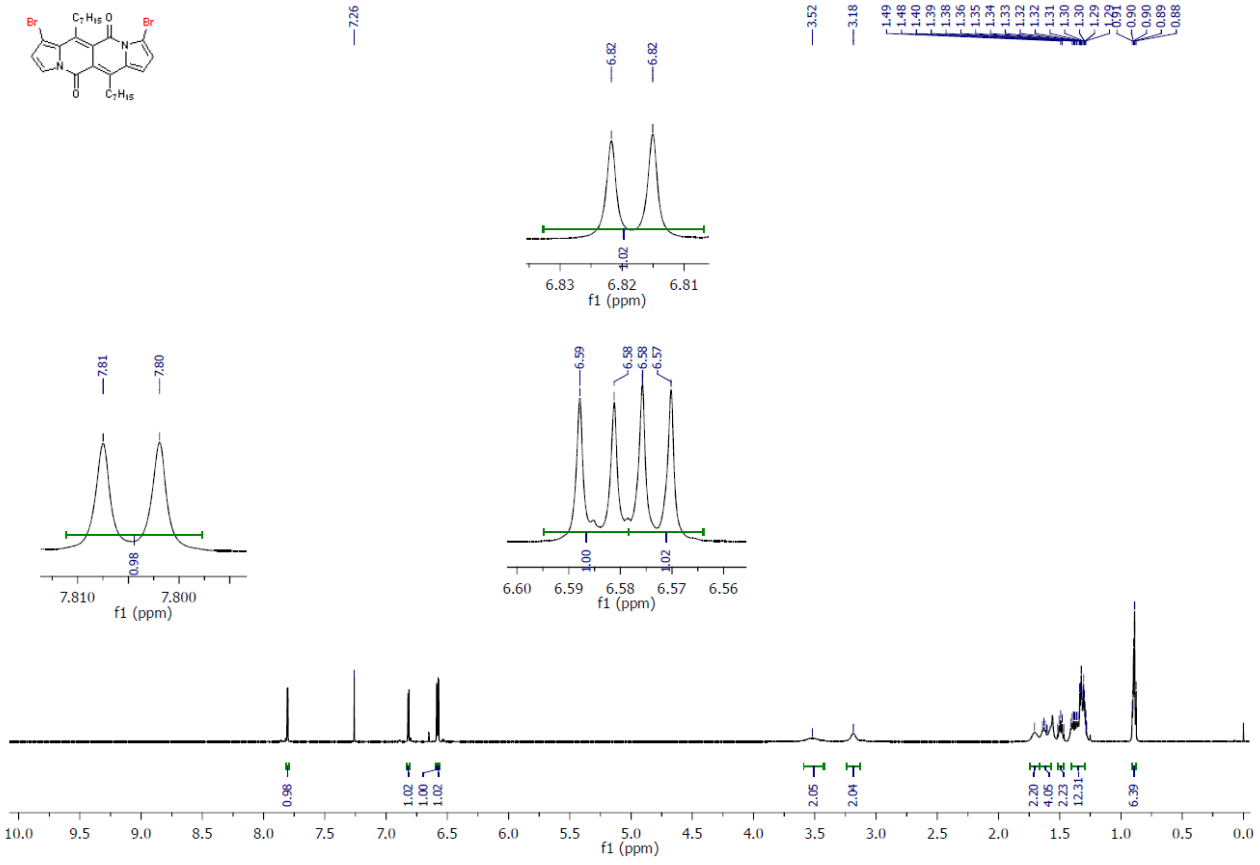
7.26
6.82
6.82
3.52
3.18
1.02
6.83
6.82
6.81
7.81
7.80
0.98
7.810
7.800
6.59
6.58
6.58
6.57
1.00
1.02
6.60
6.59
6.58
6.57
6.56
f1 (ppm)

0.98
1.02
1.00
1.02
2.05
2.04
2.20
4.05
2.23
12.31
6.39
f1 (ppm)

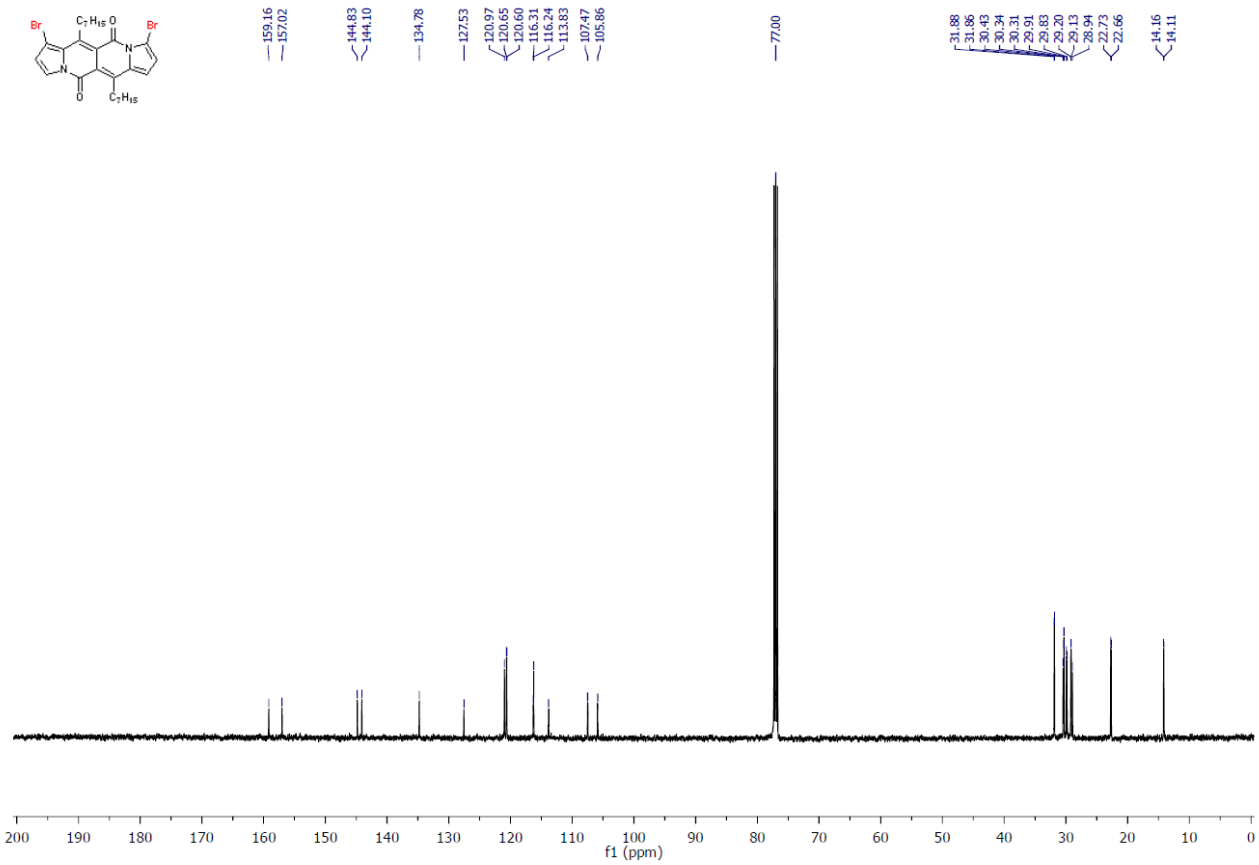
Br
Br
159.16
157.02
144.83
144.10
134.78
127.53
120.97
120.65
120.60
116.31
116.24
113.83
107.47
105.86
77.00
31.88
31.86
30.43
30.34
30.31
29.91
29.83
29.20
29.13
28.94
22.73
22.66
14.16
14.11
f1 (ppm)

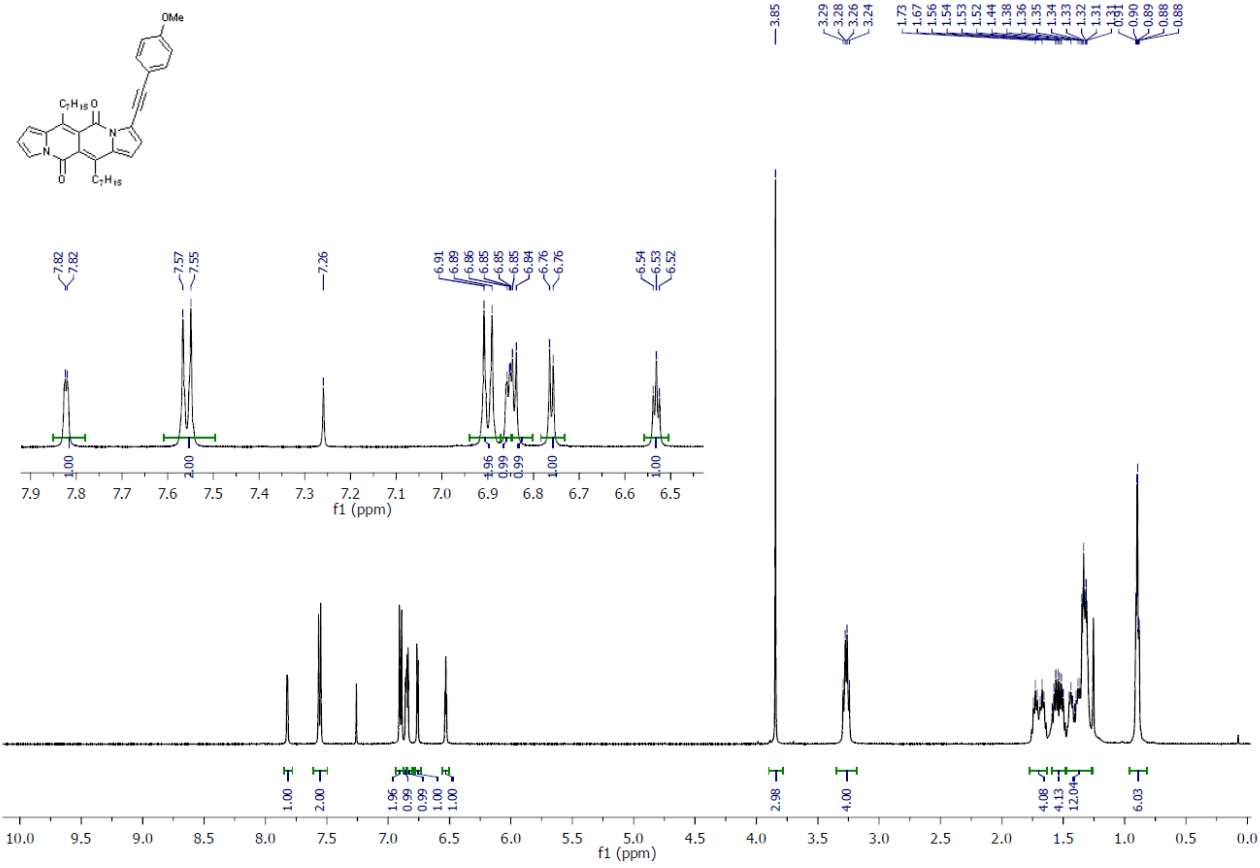
OMe
3.85
3.29
3.28
3.26
3.24
1.73
1.67
1.56
1.54
1.53
1.52
1.44
1.38
1.36
1.35
1.34
1.33
1.32
1.31
0.91
0.90
0.89
0.88
0.88
7.82
7.82
7.57
7.55
7.26
6.91
6.89
6.86
6.85
6.85
6.85
6.84
6.76
6.76
6.54
6.53
6.52
1.00
2.00
1.96
0.99
0.99
1.00
1.00
2.98
4.00
4.08
4.13
12.04
6.03
f1 (ppm)

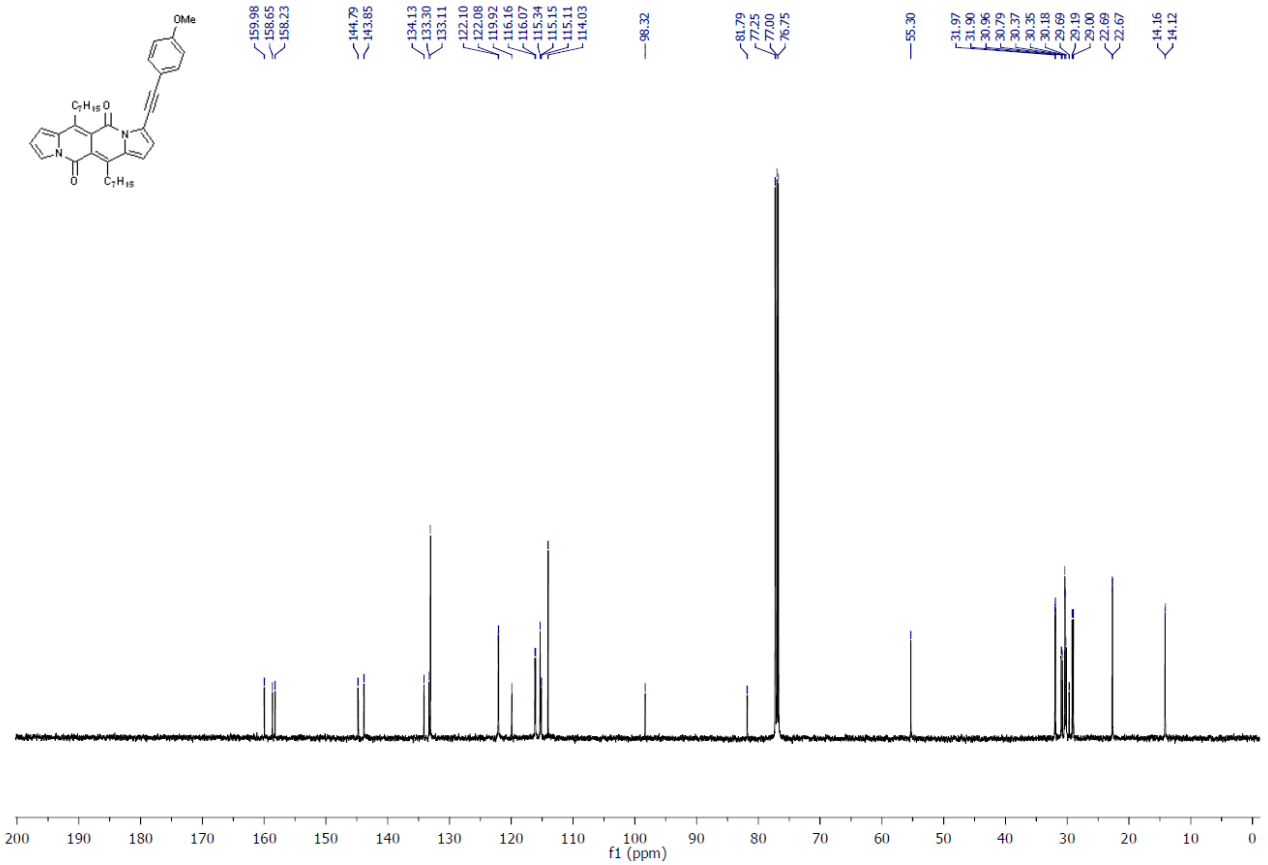
159.98
158.65
158.23
144.79
143.85
134.13
133.30
133.11
122.10
122.08
119.92
116.16
116.07
115.34
115.15
115.11
114.03
98.32
81.79
77.25
77.00
76.75
55.30
31.97
31.90
30.96
30.79
30.37
30.35
30.18
29.69
29.19
29.00
22.69
22.67
14.16
14.12
OMe
f1 (ppm)

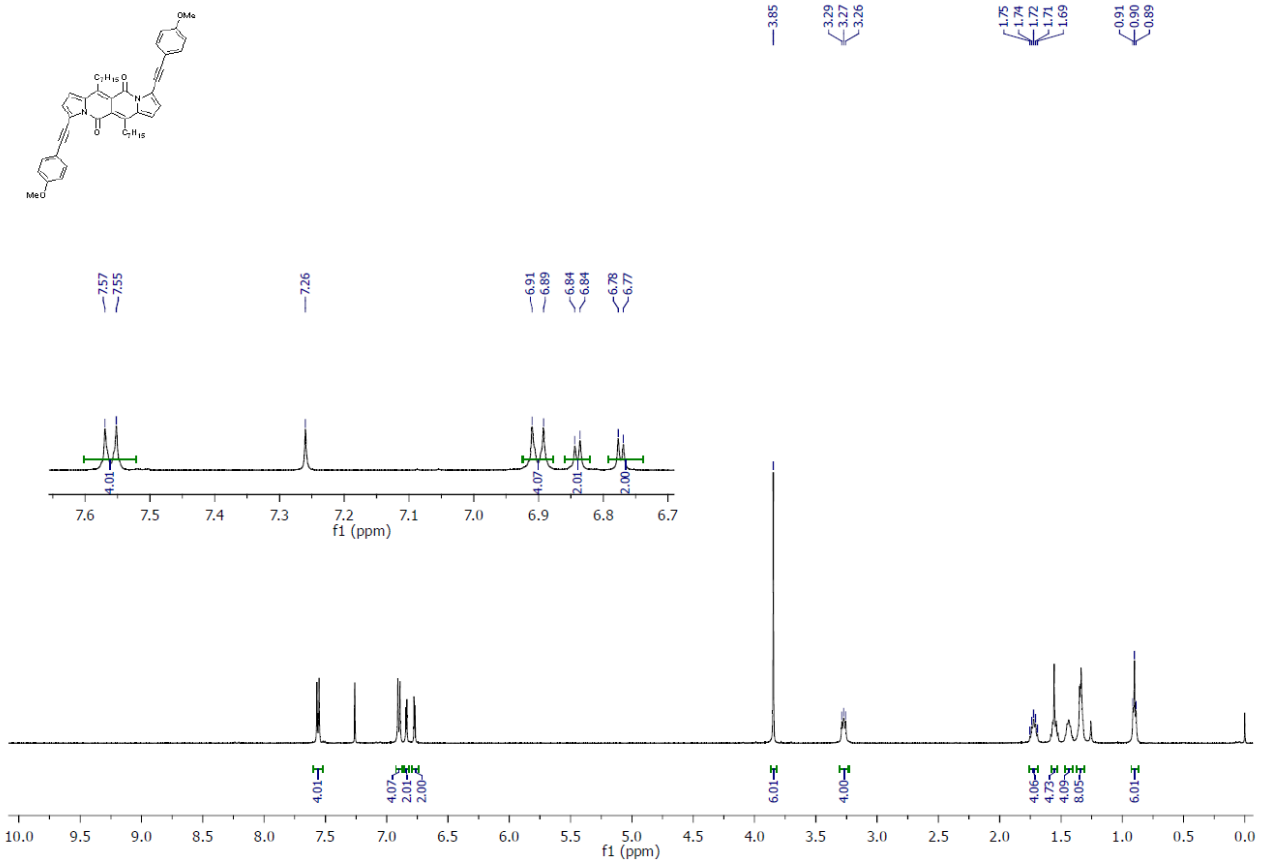
3.85
3.29
3.27
3.26
1.75
1.74
1.72
1.71
1.69
0.91
0.90
0.89
7.57
7.55
7.26
6.91
6.89
6.84
6.84
6.78
6.77
4.01
4.07
2.01
2.00
6.01
4.00
4.06
4.73
4.09
8.05
6.01
OMe
MeO
f1 (ppm)

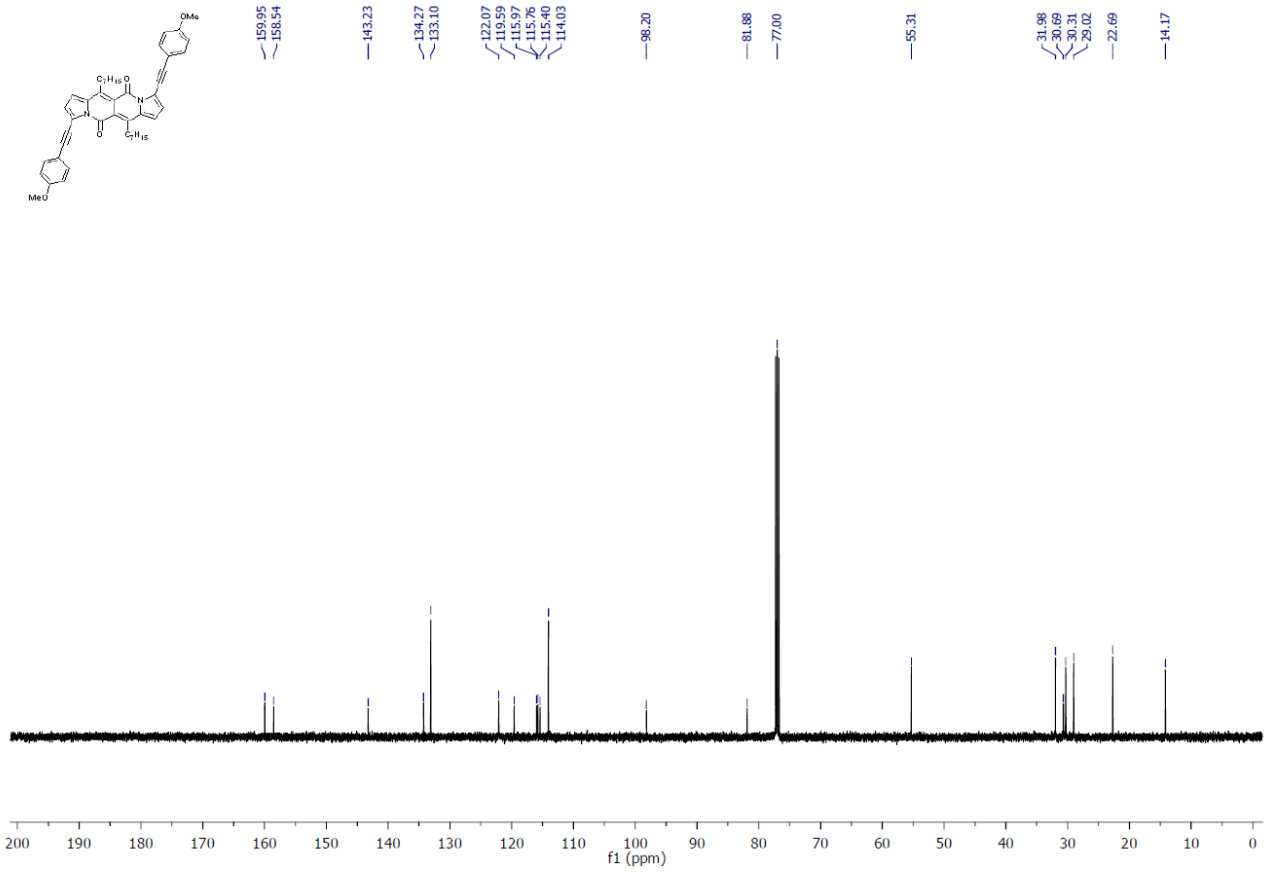
159.95
158.54
143.23
134.27
133.10
122.07
119.59
115.97
115.76
115.40
114.03
98.20
81.88
77.00
55.31
31.98
30.69
30.31
29.02
22.69
14.17
f1 (ppm)

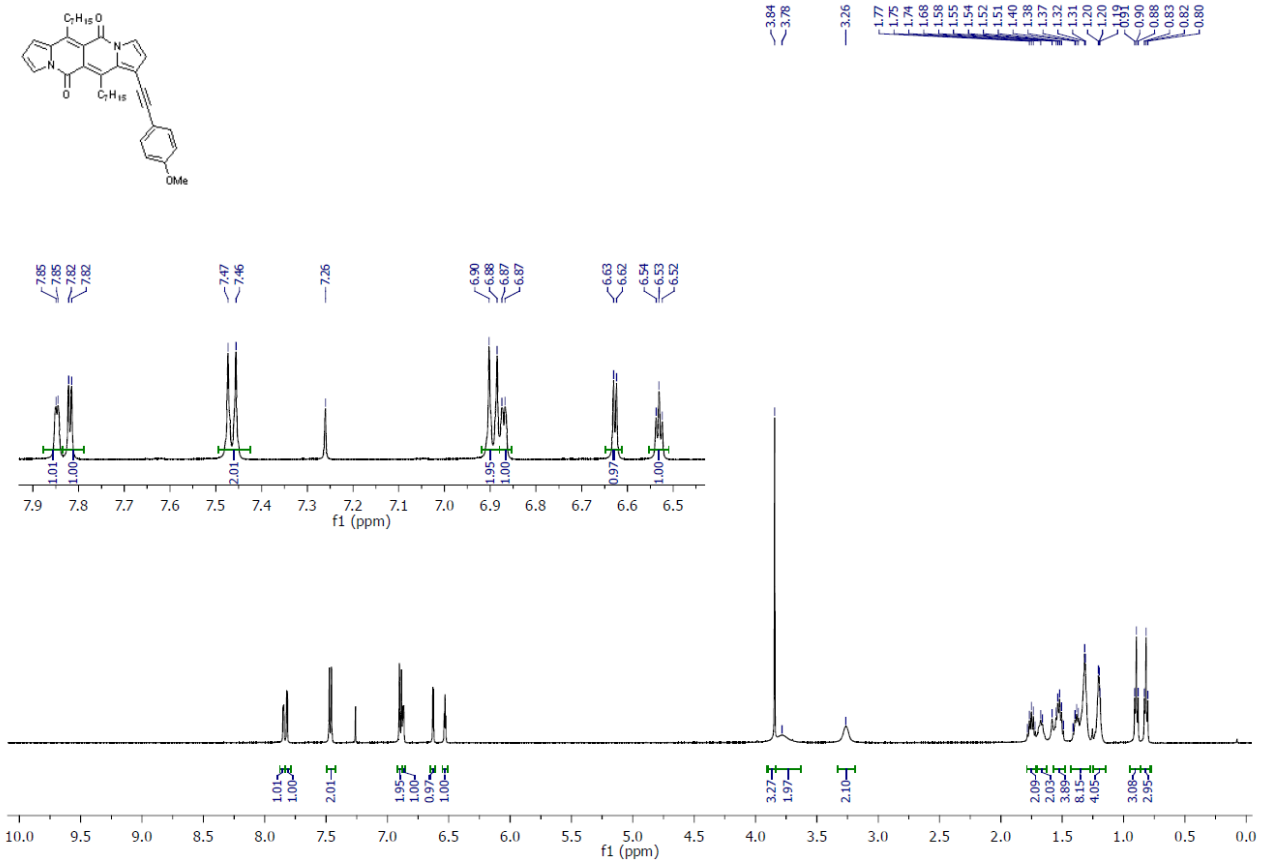
3.84
3.78
3.26
7.85
7.85
7.82
7.82
7.47
7.46
7.26
6.90
6.88
6.87
6.87
6.63
6.62
6.54
6.53
6.52
f1 (ppm)

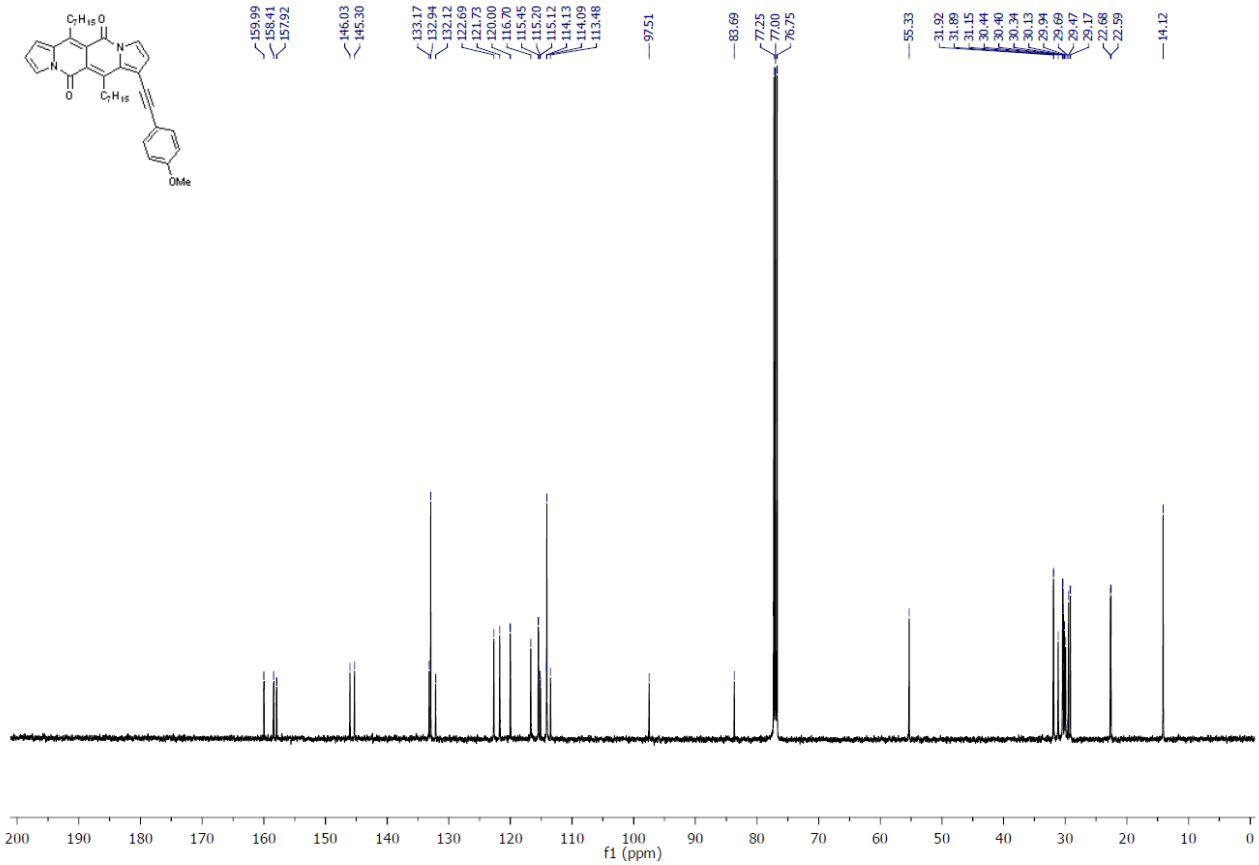
159.99
158.41
157.92
146.03
145.30
133.17
132.94
132.12
122.69
121.73
120.00
116.70
115.45
115.20
115.12
114.13
114.09
113.48
97.51
83.69
77.25
77.00
76.75
55.33
31.92
31.89
31.15
30.44
30.40
30.34
30.13
29.94
29.69
29.47
29.17
22.68
22.59
14.12
f1 (ppm)

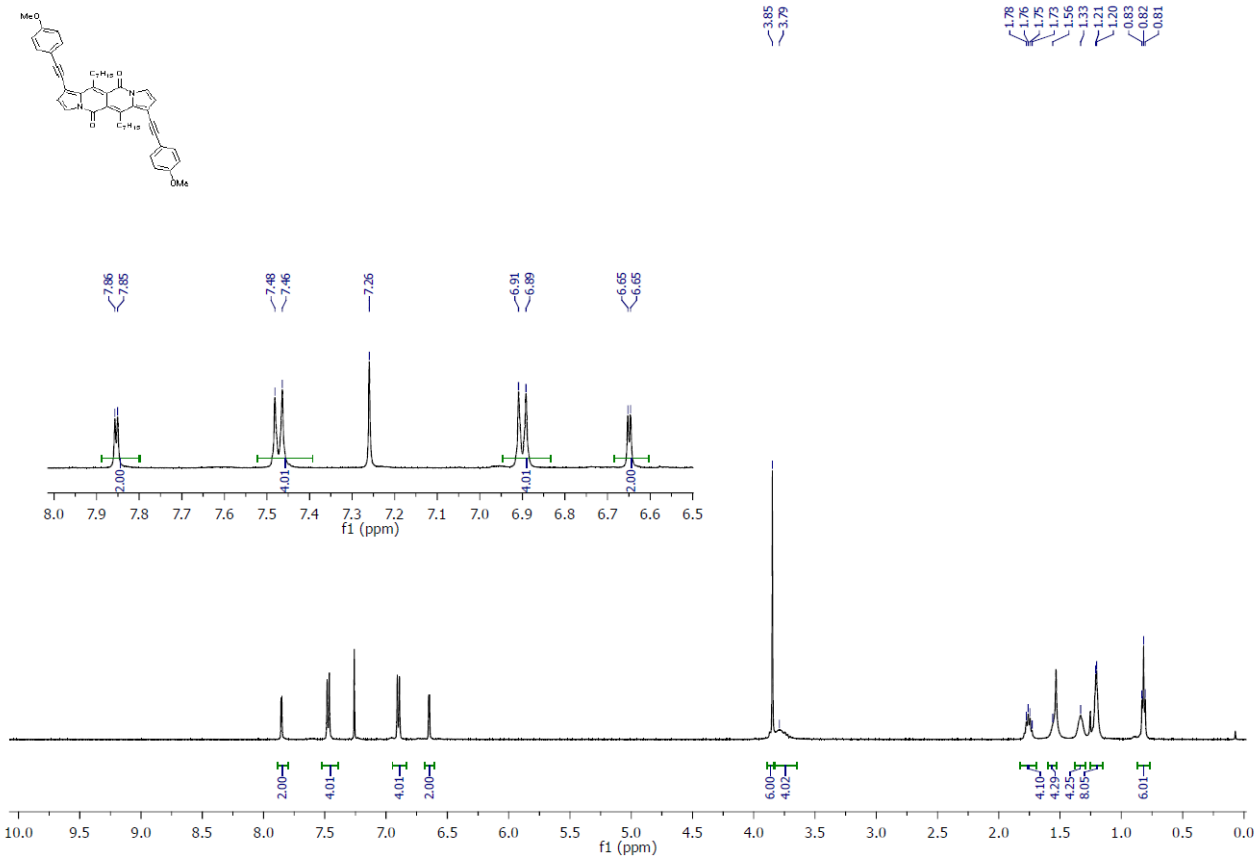
3.85
3.79
1.78
1.76
1.75
1.73
1.56
1.33
1.21
1.20
0.83
0.82
0.81
7.86
7.85
7.48
7.46
7.26
6.91
6.89
6.65
6.65
2.00
4.01
4.01
2.00
6.00
4.02
4.10
4.29
4.25
8.05
6.01
f1 (ppm)

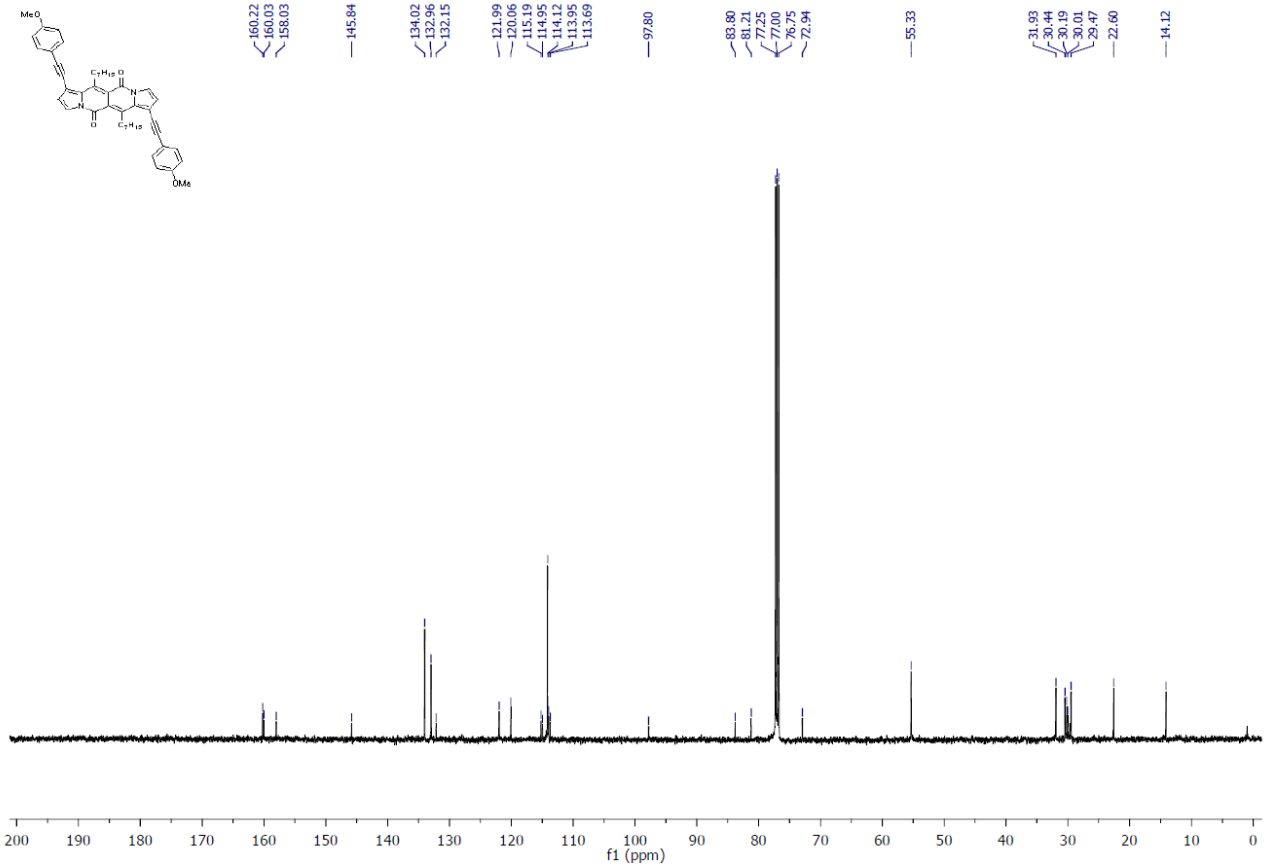
160.22
160.03
158.03
145.84
134.02
132.96
132.15
121.99
120.06
115.19
114.95
114.12
113.95
113.69
97.80
83.80
81.21
77.25
77.00
76.75
72.94
55.33
31.93
30.44
30.19
30.01
29.47
22.60
14.12
f1 (ppm)

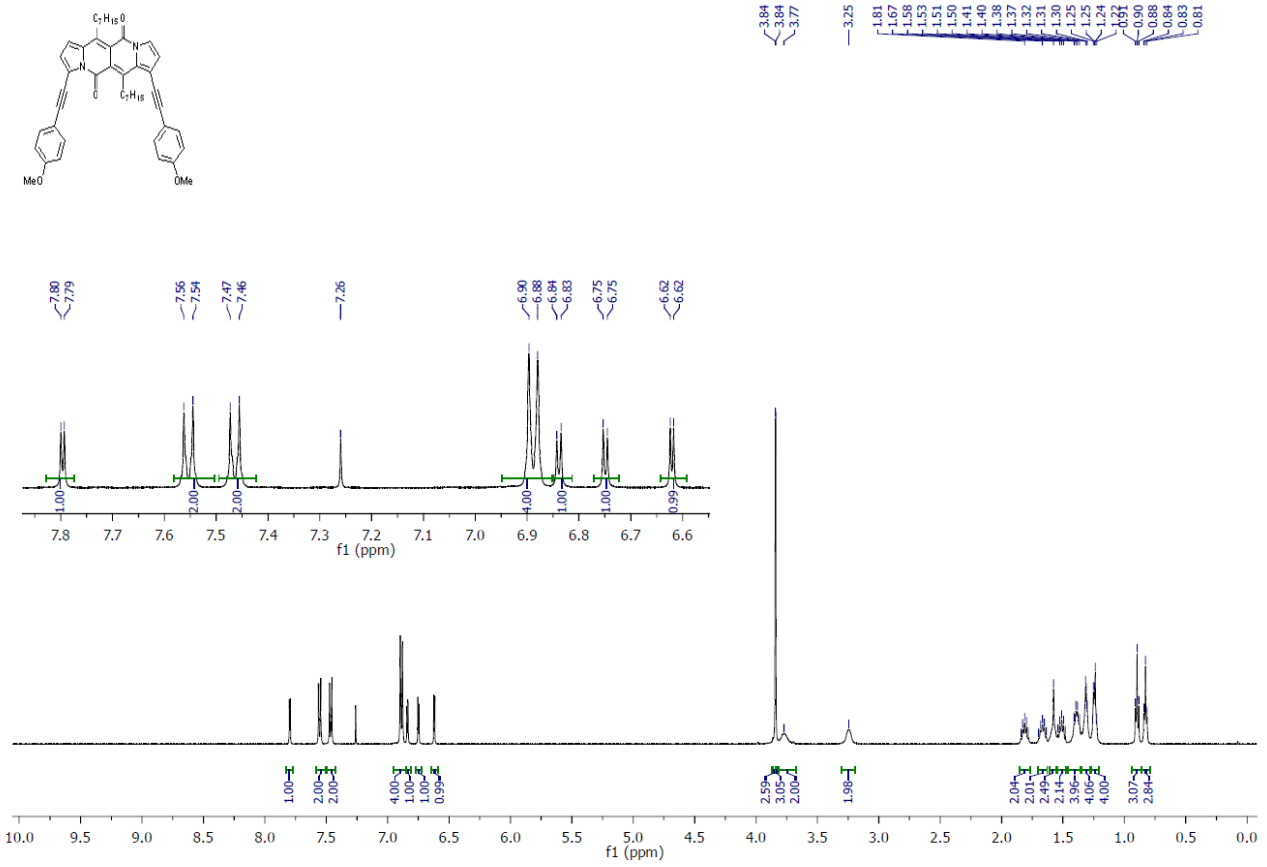
3.84
3.84
3.77
3.25
1.81
1.67
1.58
1.53
1.51
1.50
1.41
1.40
1.38
1.37
1.32
1.31
1.30
1.25
1.25
1.24
0.90
0.88
0.84
0.83
0.81
7.80
7.79
7.56
7.54
7.47
7.46
7.26
6.90
6.88
6.84
6.83
6.75
6.75
6.62
6.62
f1 (ppm)

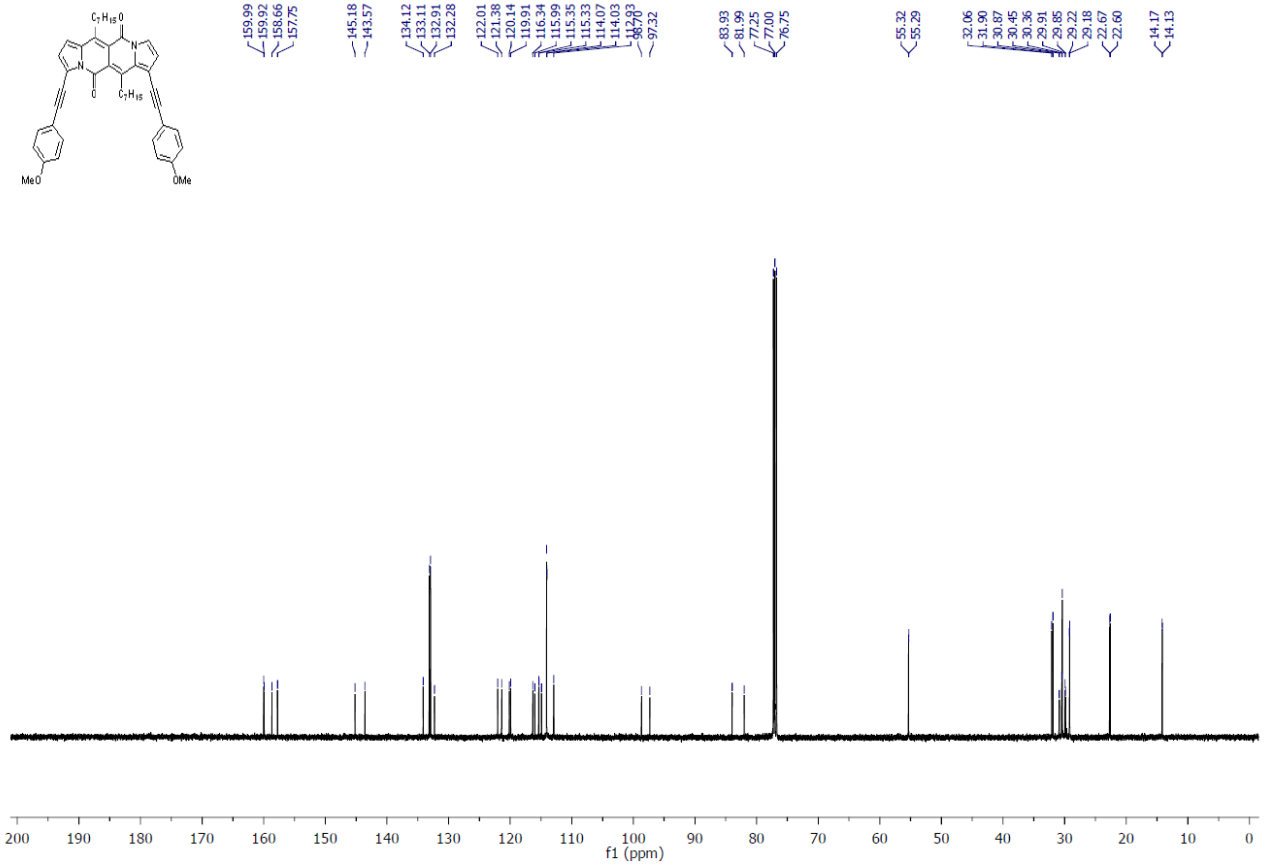
159.99
159.92
158.66
157.75
145.18
143.57
134.12
133.11
132.91
132.28
122.01
121.38
120.14
119.91
116.34
115.99
115.35
115.33
114.07
114.03
97.32
83.93
81.99
77.25
77.00
76.75
55.32
55.29
32.06
31.90
30.87
30.45
30.36
29.91
29.85
29.22
29.18
22.67
22.60
14.17
14.13
f1 (ppm)

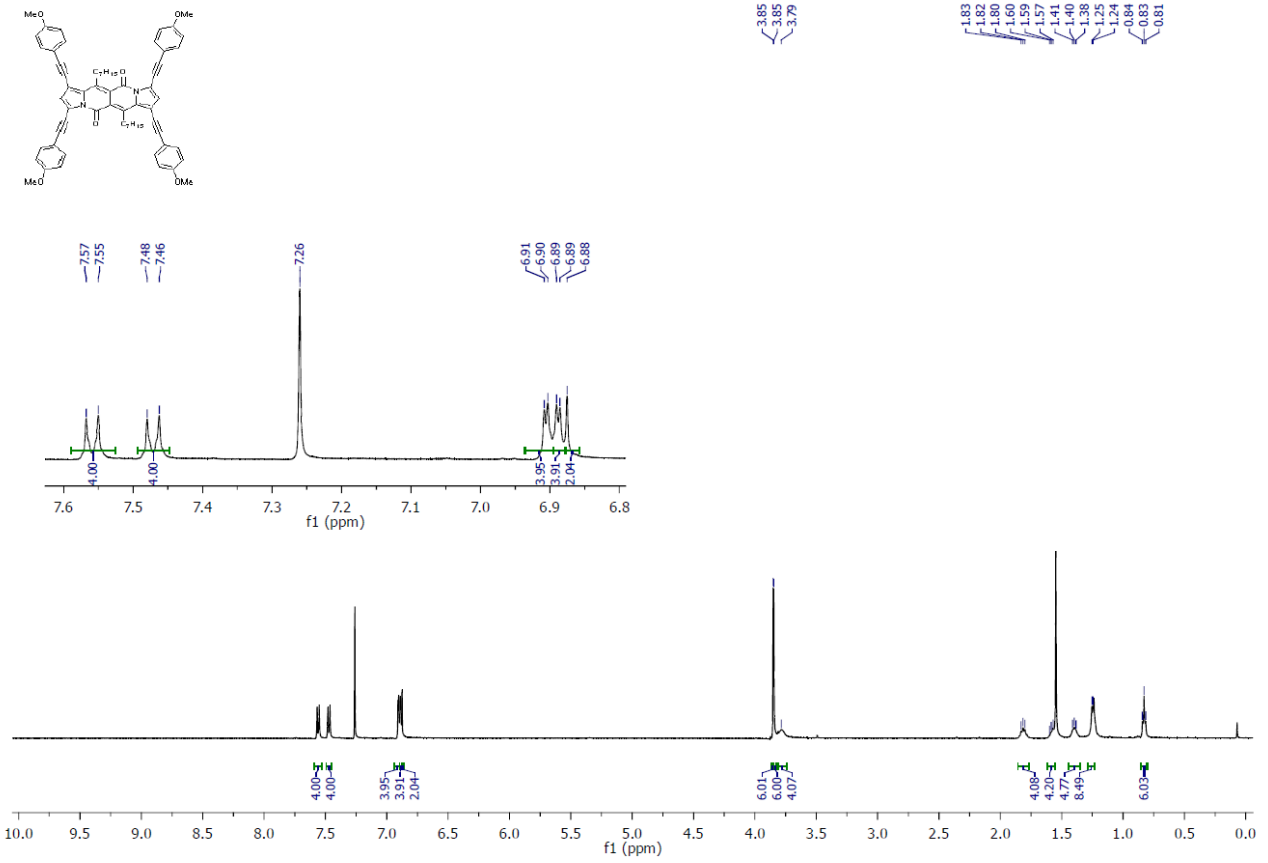
3.85
3.85
3.79
1.83
1.82
1.80
1.60
1.59
1.57
1.41
1.40
1.38
1.25
1.24
0.84
0.83
0.81
7.57
7.55
7.48
7.46
7.26
6.91
6.90
6.89
6.89
6.88
4.00
4.00
3.95
3.91
2.04
f1 (ppm)
4.00
4.00
3.95
3.91
2.04
6.01
6.00
4.07
4.08
4.20
4.77
8.49
6.03
f1 (ppm)

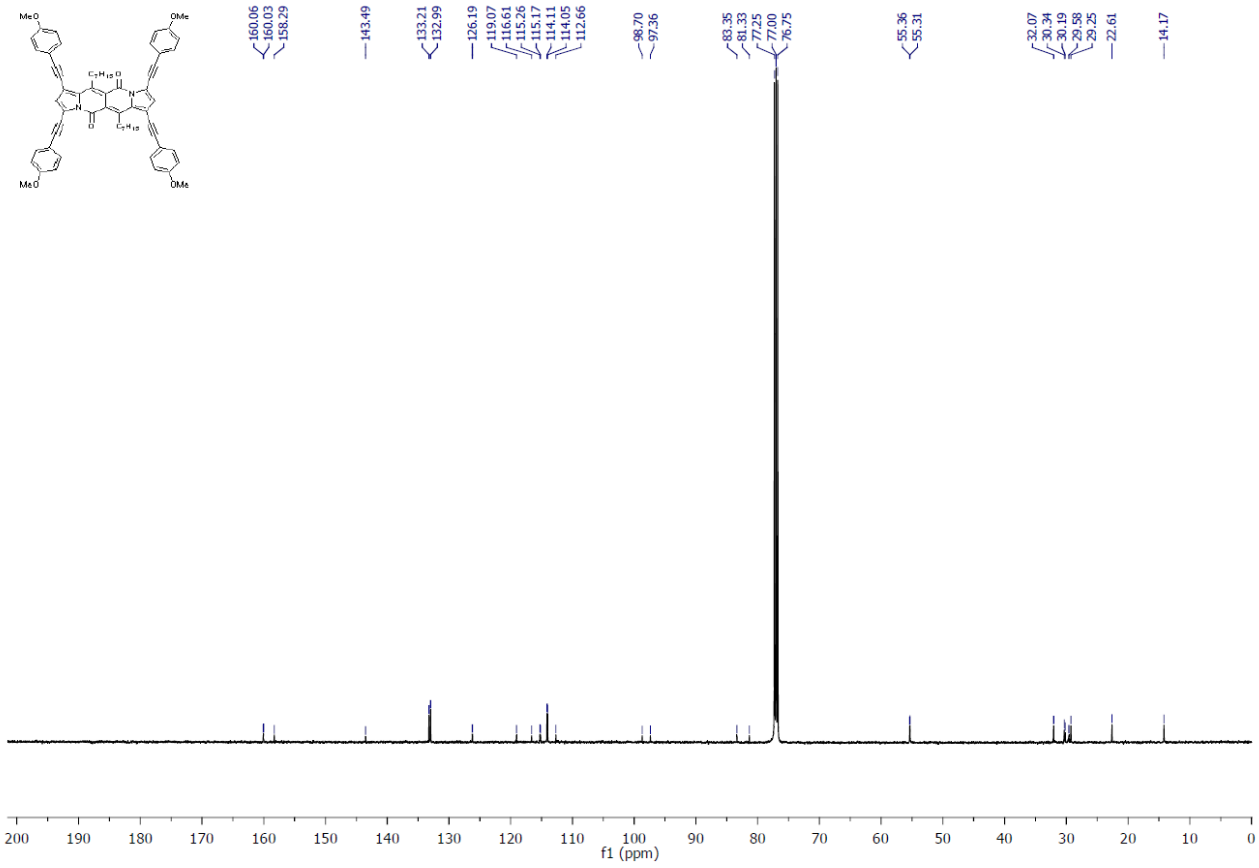
MeO
OMe
MeO
OMe
160.06
160.03
158.29
143.49
133.21
132.99
126.19
119.07
116.61
115.26
115.17
114.11
114.05
112.66
98.70
97.36
83.35
81.33
77.25
77.00
76.75
55.36
55.31
32.07
30.34
30.19
29.58
29.25
22.61
14.17
200
190
180
170
160
150
140
130
120
110
100
90
80
70
60
50
40
30
20
10
0
f1 (ppm)

5. Photophysical Data

Absorption and Emission Spectra

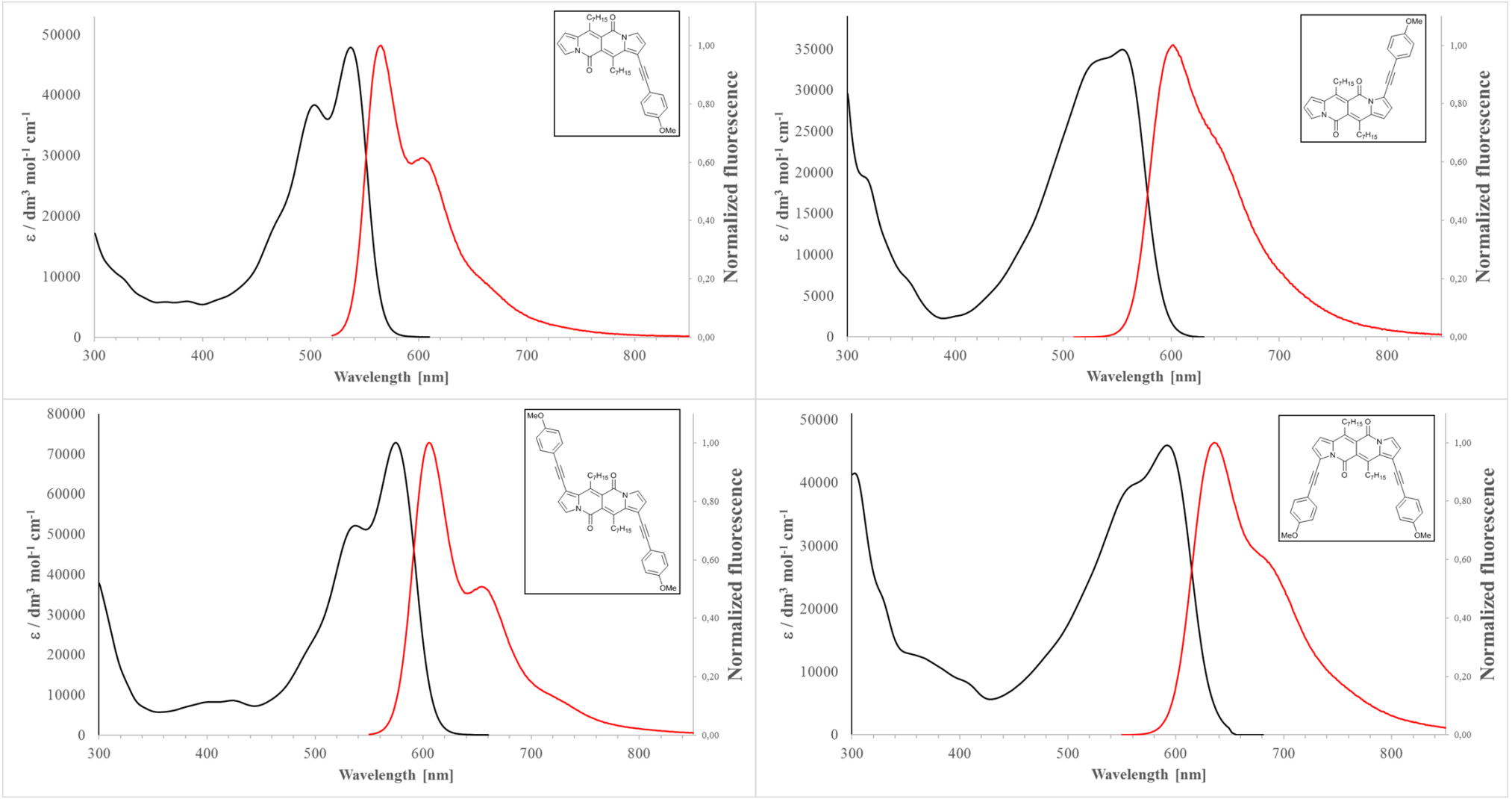

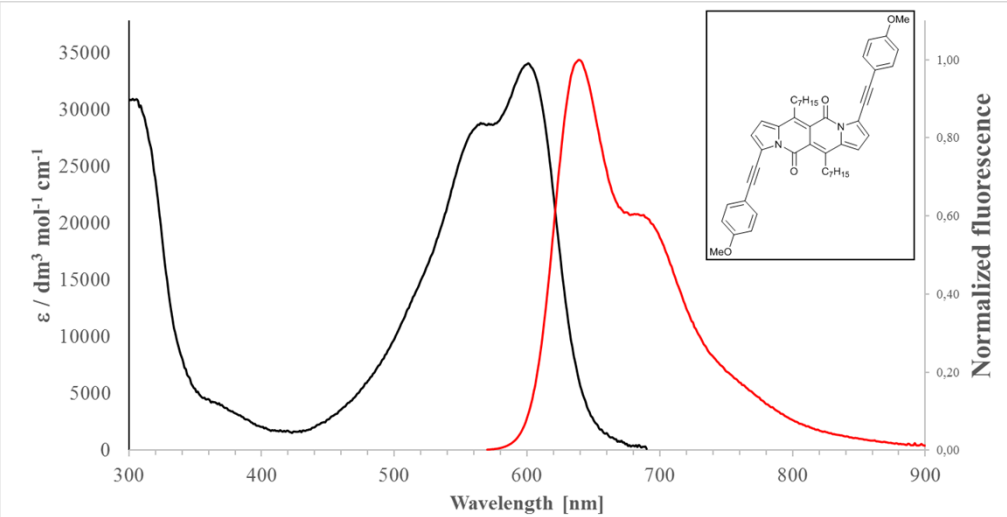
ε / dm³ mol⁻¹ cm⁻¹
Normalized fluorescence
Wavelength [nm]
OMe
MeO

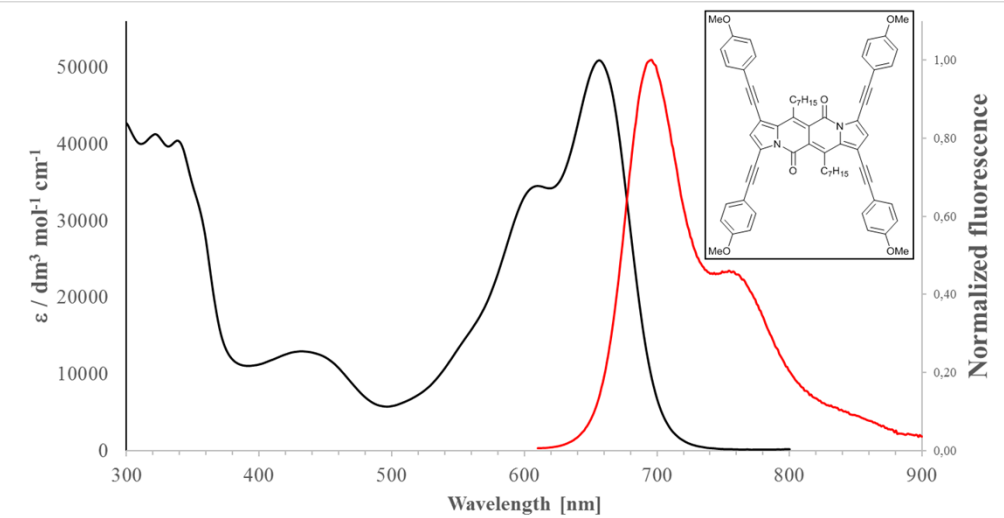
ε / dm³ mol⁻¹ cm⁻¹
Normalized fluorescence
Wavelength [nm]
MeO
OMe

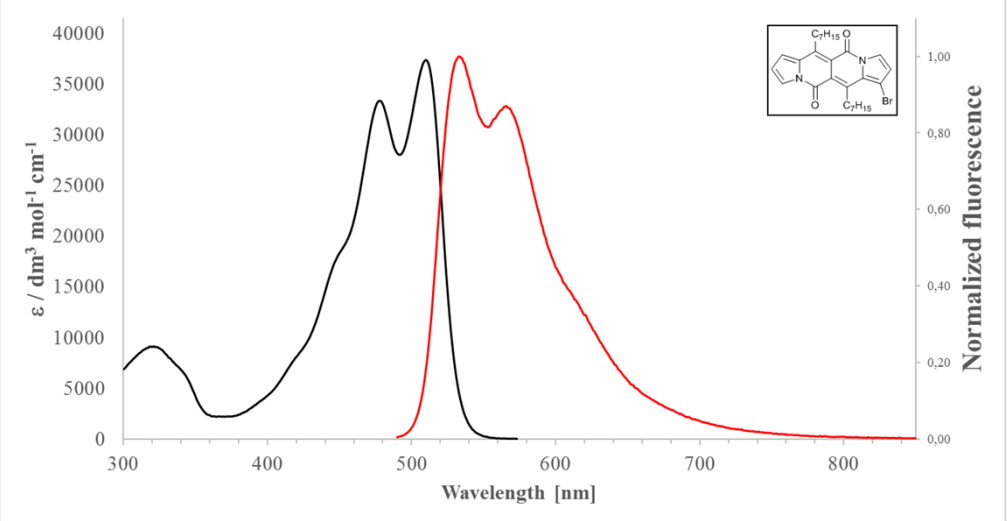
ε / dm³ mol⁻¹ cm⁻¹
Normalized fluorescence
Wavelength [nm]
Br

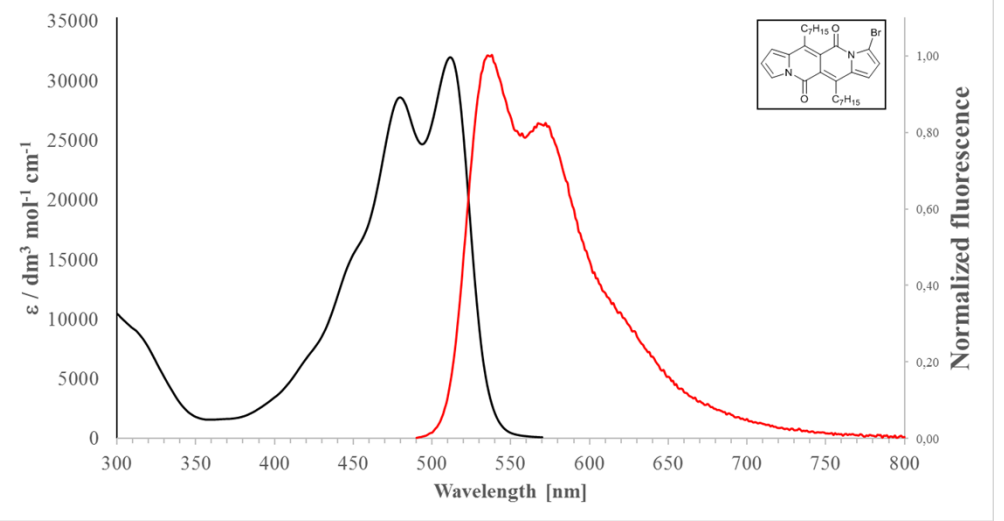
ε / dm³ mol⁻¹ cm⁻¹
Normalized fluorescence
Wavelength [nm]
Br

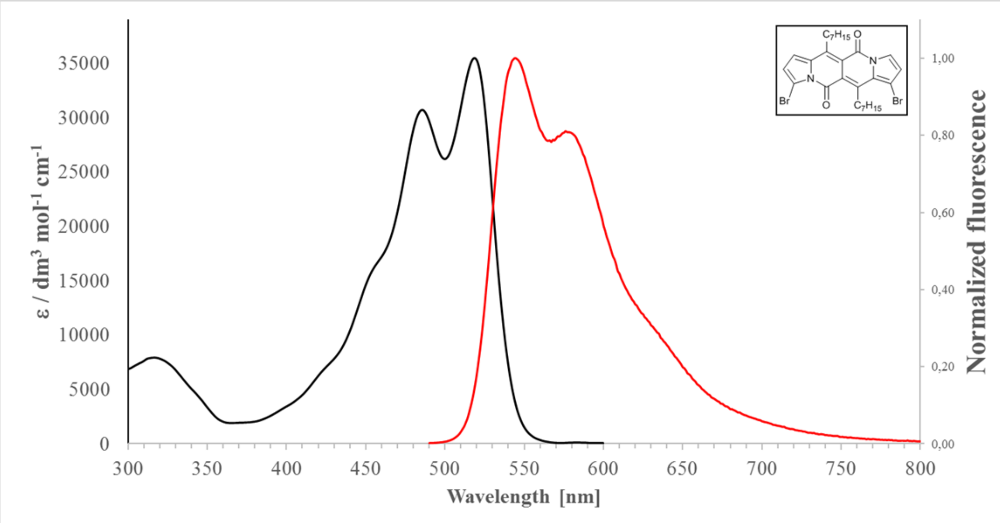
ε / dm3 mol-1 cm-1
Normalized fluorescence
Wavelength [nm]

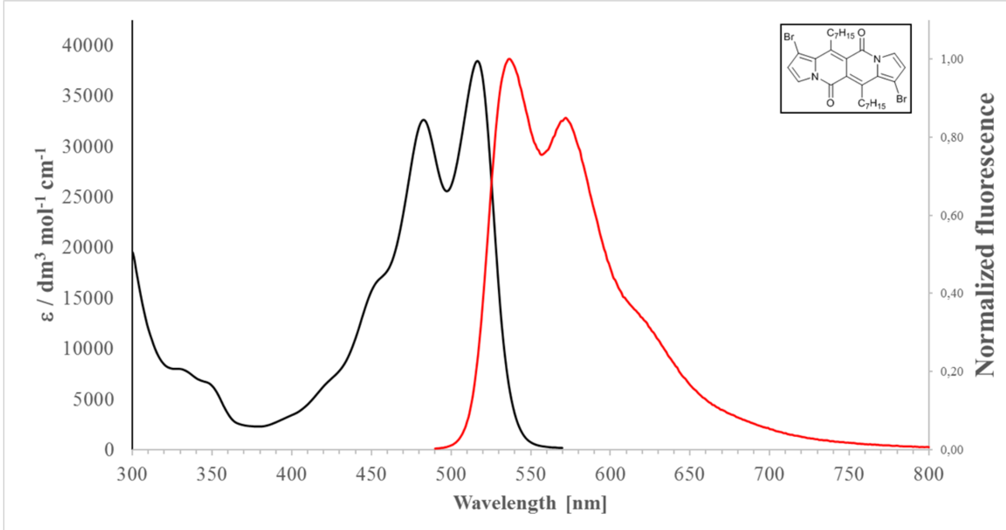
ε / dm3 mol-1 cm-1
Normalized fluorescence
Wavelength [nm]

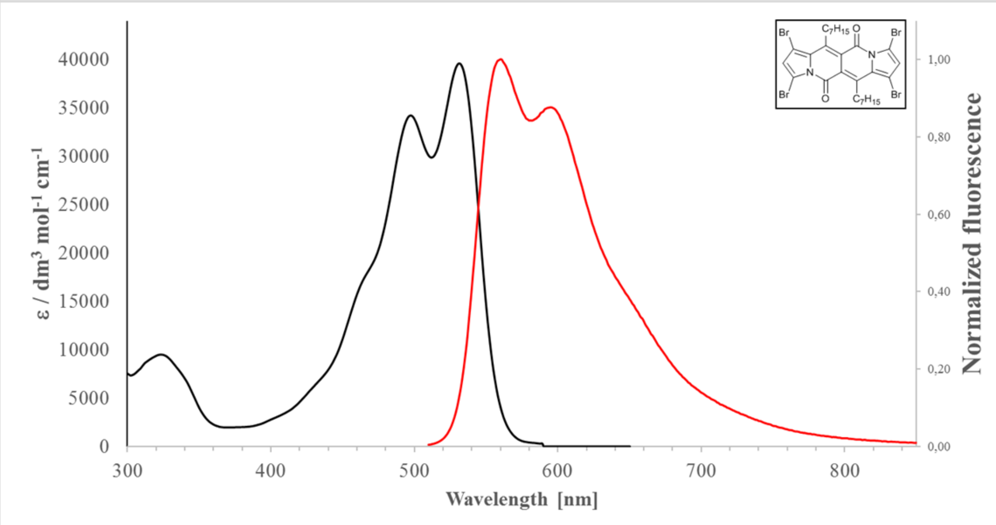
ε / dm3 mol-1 cm-1
Normalized fluorescence
Wavelength [nm]

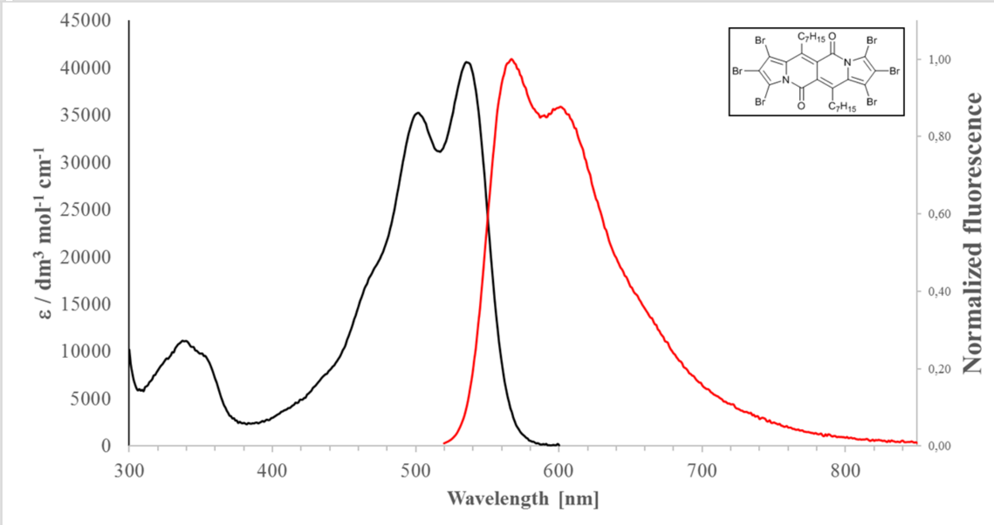
ε / dm3 mol-1 cm-1
Normalized fluorescence
Wavelength [nm]

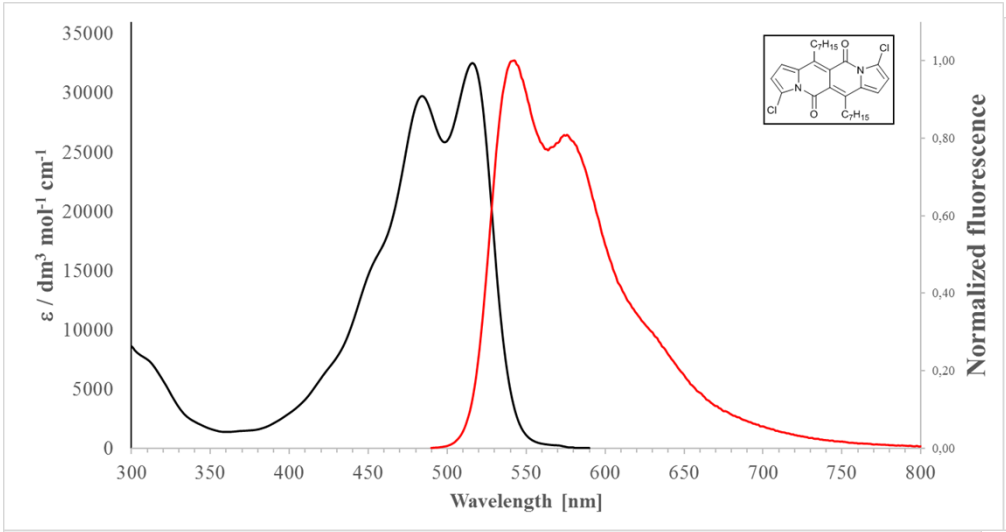
ε / dm³ mol⁻¹ cm⁻¹
Normalized fluorescence
Wavelength [nm]
35000
30000
25000
20000
15000
10000
5000
0
300
350
400
450
500
550
600
650
700
750
800
1,00
0,80
0,60
0,40
0,20
0,00
C7H15
O
N
Cl
Cl
O
C7H15

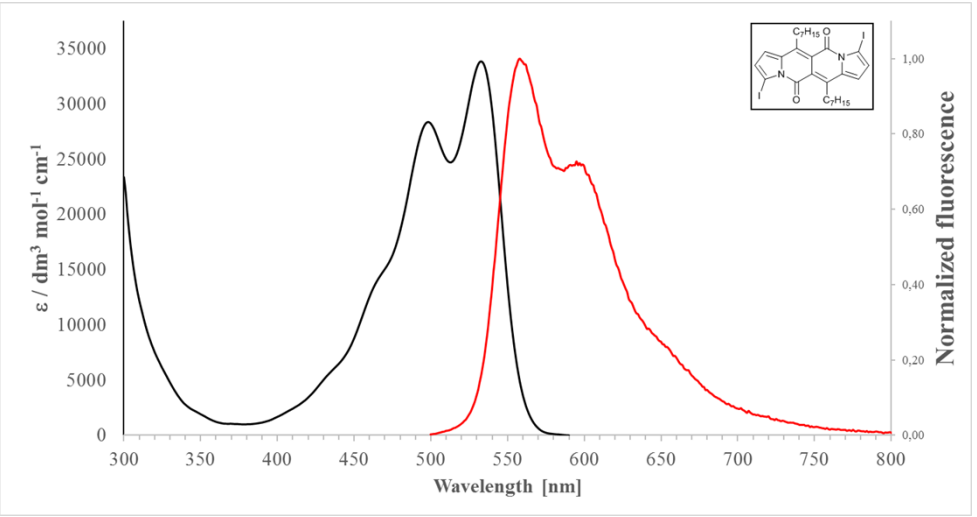
ε / dm³ mol⁻¹ cm⁻¹
Normalized fluorescence
Wavelength [nm]
35000
30000
25000
20000
15000
10000
5000
0
300
350
400
450
500
550
600
650
700
750
800
1,00
0,80
0,60
0,40
0,20
0,00
C7H15
O
N
I
I
O
C7H15

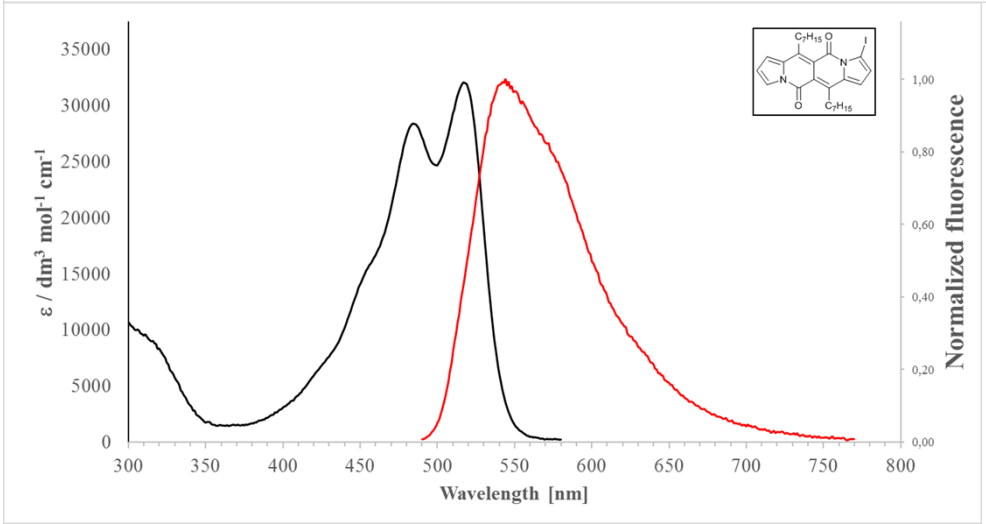
ε / dm³ mol⁻¹ cm⁻¹
Normalized fluorescence
Wavelength [nm]
35000
30000
25000
20000
15000
10000
5000
0
300
350
400
450
500
550
600
650
700
750
800
1,00
0,80
0,60
0,40
0,20
0,00
C7H15
O
N
I
O
C7H15

6. DFT calculations

Density functional theory (DFT) calculations were carried out in the gas phase using the M06-2X functional.[2] Geometry optimizations and frequency calculations were performed with the Def2-SVP basis set,[3] while orbital energies and time-dependent (TD-DFT) calculations employed the Def2-TZVPP basis set,[3] as implemented in the Gaussian 16 program.[4] Stationary points in the lowest singlet state (S_0) were optimized and characterized by frequency analysis (the number of imaginary frequencies: 0). TD-DFT calculations were performed on optimized geometries at the M06-2X/Def2-TZVPP level. The optimized structures and cartesian coordinates of the compounds are given below. Frontier orbitals were visualized with Jmol,[5] and the 3D models with Mercury software.[6] In all calculated molecules *n*-heptyl groups were replaced by methyl substituents to simplify calculations.

Nuclear-independent chemical shifts ($NICS(1)_{ZZ}$)[7] were calculated using the optimized geometries at the same level of theory (M06-2X/Def2-TZVPP). For the generation of 2D $NICS(1)_{ZZ}$ maps, pairs of dummy atoms (Bq) were placed in two hexagonal grids located 1.000 Å above and 1.000 Å below the plane of the DPND polycyclic system, with an average interpoint distance of approximately 0.2 Å. $NICS(1)_{ZZ}$ values from each pair (above and below the molecular plane) were averaged and mapped onto a 2D plane using a self-written Python script based on the Matplotlib library (matplotlib.pyplot).[8] The following RGB color space was used to visualize $NICS(1)_{ZZ}$ values in the range from −35 to +35 ppm:

```
[(0.12, 0.03, 0.39), (0.03, 0.04, 0.64), (0.05, 0.11, 0.98), (0.19, 0.68, 1), (0.73, 0.92, 1), (1, 1, 1), (1,
0.92, 0.73), (1, 0.68, 0.19), (0.98, 0.11, 0.05), (0.64, 0.04, 0.03), (0.39, 0.03, 0.12)]
```

[2] Y. Zhao, D.G. Truhlar, *Theor. Chem. Account.*, 2008, **120**, 215–241.
[3] a) F. Weigend, R. Ahlrichs, *Phys. Chem. Chem. Phys.*, 2005, **7**, 3297-3305; b) F. Weigend, *Phys. Chem. Chem. Phys.*, 2006, **8**, 1057-1065.
[4] Gaussian 16, Revision C.01, M. J. Frisch, G. W. Trucks, H. B. Schlegel, G. E. Scuseria, M. A. Robb, J. R. Cheeseman, G. Scalmani, V. Barone, G. A. Petersson, H. Nakatsuji, X. Li, M. Caricato, A. V. Marenich, J. Bloino, B. G. Janesko, R. Gomperts, B. Mennucci, H. P. Hratchian, J. V. Ortiz, A. F. Izmaylov, J. L. Sonnenberg, D. Williams-Young, F. Ding, F. Lipparini, F. Egidi, J. Goings, B. Peng, A. Petrone, T. Henderson, D. Ranasinghe, V. G. Zakrzewski, J. Gao, N. Rega, G. Zheng, W. Liang, M. Hada, M. Ehara, K. Toyota, R. Fukuda, J. Hasegawa, M. Ishida, T. Nakajima, Y. Honda, O. Kitao, H. Nakai, T. Vreven, K. Throssell, J. A. Montgomery, Jr., J. E. Peralta, F. Ogliaro, M. J. Bearpark, J. J. Heyd, E. N. Brothers, K. N. Kudin, V. N. Staroverov, T. A. Keith, R. Kobayashi, J. Normand, K. Raghavachari, A. P. Rendell, J. C. Burant, S. S. Iyengar, J. Tomasi, M. Cossi, J. M. Millam, M. Klene, C. Adamo, R. Cammi, J. W. Ochterski, R. L. Martin, K. Morokuma, O. Farkas, J. B. Foresman, and D. J. Fox, Gaussian, Inc., Wallingford CT, 2019.
[5] Jmol: an open-source Java viewer for chemical structures in 3D. http://www.jmol.org/
[6] C. F. Macrae, I. Sovago, S. J. Cottrell, P. T. A. Galek, P. McCabe, E. Pidcock, M. Platings, G. P. Shields, J. S. Stevens, M. Towler and P. A. Wood, *J. Appl. Crystallogr.*, 2020, **53**, 226–235.
[7] Z. Chen, C. S. Wannere, C. Corminboeuf, R. Puchta and P. von Ragué Schleyer, *Chem. Rev.*, 2005, **105**, 3842–3888.
[8] J. D. Hunter, *Computing in Science & Engineering*, 2007, **9**, 90–95.

Table S3. Thermodynamic data calculated for brominated isomers (M06-2X/Def2-SVP).

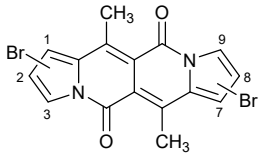

DPND	Br position(s)	Energy of formation [Hartree]			Relative energies* [kcal/mol]		
		ΔE_{SCF}	ΔH	ΔG	ΔE_{SCF}	ΔH	ΔG
2	3	-3449.1947117	-3448.936973	-3448.99983	2.51	2.43	2.85
9	1	-3449.1987104	-3448.940847	-3449.00437	0.00	0.00	0.00
3	3,9	-6022.4729470	-6022.224102	-6022.29337	5.04	4.68	4.04
11	1,9	-6022.4769042	-6022.227856	-6022.29604	2.55	2.32	2.36
10	1,7	-6022.4809753	-6022.231561	-6022.29980	0.00	0.00	0.00

* Energies relative to the most stable isomer.

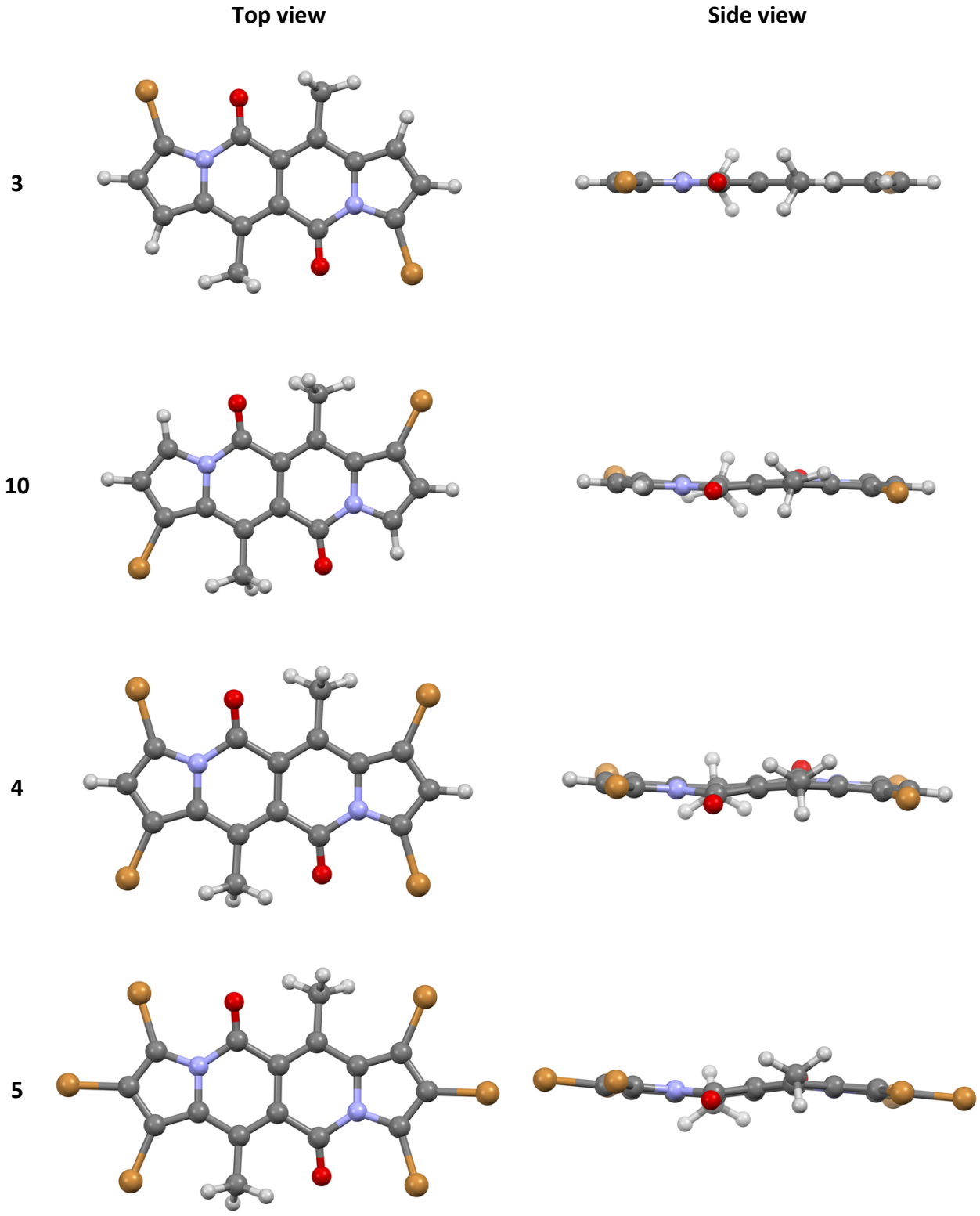

Figure S6. Optimized geometries of compounds **3**, **10**, **4** and **5** showing deviations from planarity in the latter three structures.

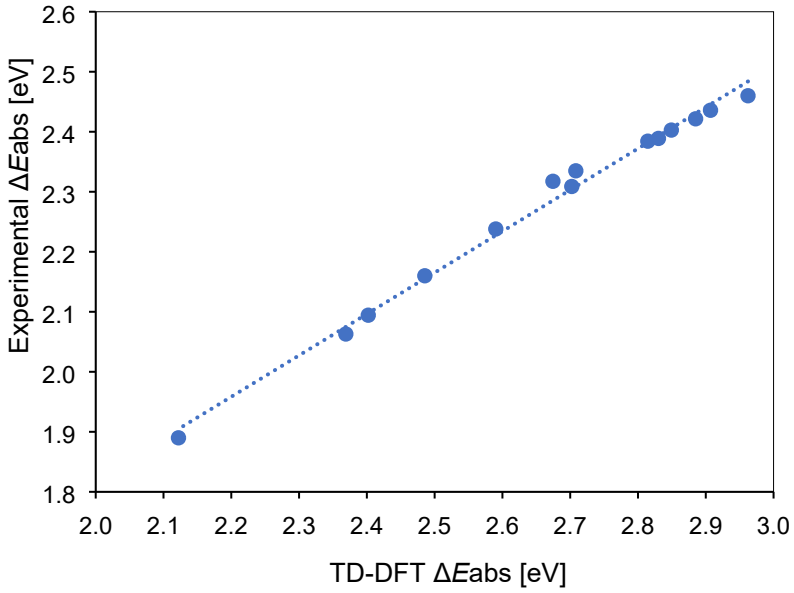

Figure S7. Correlation between calculated (TD-DFT: M06-2X/Def2-TZVPP) and experimental S_0-S_1 excitation energies. Experimental excitation energies were converted from maximum absorption wavelengths according to the following formula: $\Delta E_{abs} = 1239.842$ eV·nm / λ_{max}

Figure S8. Comparison of molecular orbital energies (DFT) and S_0-S_1 excitation characteristics (TD-DFT) calculated at M06-2X/Def2-TZVPP level for DPND **1** and its brominated derivatives **2-5** and **9-11**.

Table S4. Summary of the DFT and TD-DFT calculations (M06-2X/Def2-TZVPP).

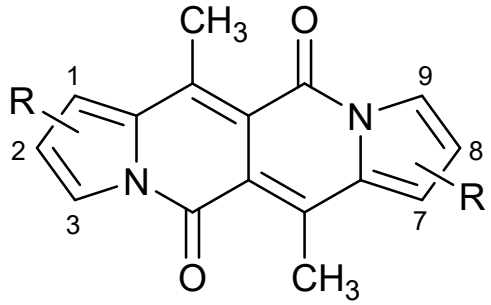

R	DPND	Substituents positions	HOMO [eV]	LUMO [eV]	TD-DFT results					
					Transition	$E(S_1)$ [eV]	λ_{abs} [nm]	osc. strength f	$E(T_1)$ [eV]	$E(T_1) / E(S_1)$
H	**1**	-	−6.83	−2.21	69 -> 70 (0.70441)	2.9623	418.5	0.5609	1.5606	0.527
Br	**2**	3	−6.80	−2.27	86 -> 87 (0.70476)	2.8850	429.8	0.6081	1.5281	0.530
	3	3,9	−6.77	−2.33	103 ->104 (0.70496)	2.8145	440.5	0.6647	1.4964	0.532
	4	1,3,7,9	−6.91	−2.58	137 ->138 (0.70515)	2.7083	457.8	0.7328	1.4325	0.529
	5	1,2,3,7,8,9	−7.09	−2.78	171 ->172 (0.70505)	2.6745	463.6	0.7635	1.4269	0.534
	9	1	−6.90	−2.35	86 -> 87 (0.70429)	2.9070	426.5	0.6251	1.5275	0.525
	10	1,7	−6.97	−2.50	103 ->104 (0.70477)	2.8492	435.2	0.7068	1.4885	0.522
	11	1,9	−6.87	−2.40	103 ->104 (0.70453)	2.8302	438.1	0.6582	1.5035	0.531
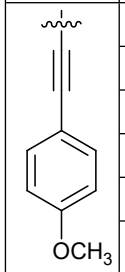	**12a**	3	−6.39	−2.26	103 -> 104 (0.69827)	2.5902	478.7	0.7934	1.4038	0.542
	12b	1	−6.53	−2.30	103 -> 104 (0.69646)	2.7023	458.8	0.9671	1.4324	0.530
	12c	3,9	−6.17	−2.31	137 -> 138 (0.69741)	2.3690	523.4	1.2066	1.2832	0.542
	12d	1,7	−6.35	−2.39	137 -> 138 (0.69700)	2.4855	498.8	1.4940	1.3220	0.532
	12e	1,9	−6.25	−2.35	137 -> 138 (0.69776)	2.4021	516.1	0.9330	1.2979	0.540
	12f	1,3,7,9	−5.97	−2.44	205 -> 206 (0.69886)	2.1221	584.3	1.1728	1.1159	0.526

Table S5. Diagrams of highest occupied (HOMO) and lowest unoccupied (LUMO) molecular orbitals calculated at the M06-2X/Def2-SVP level of theory.

Compound	HOMO	LUMO
1	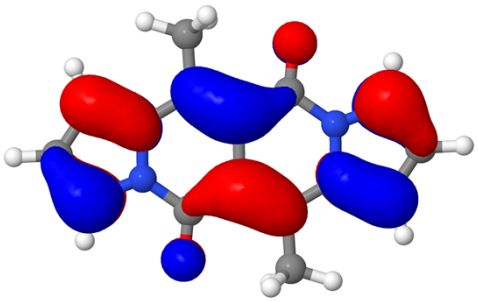	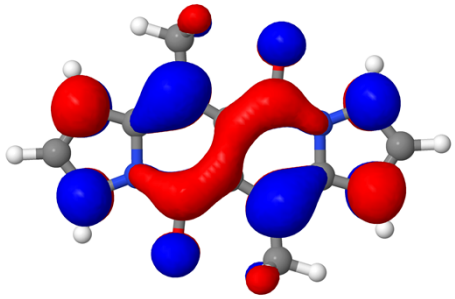
2	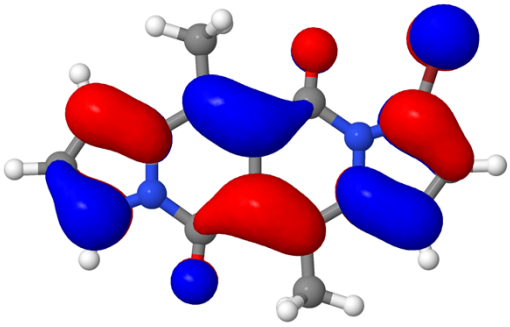	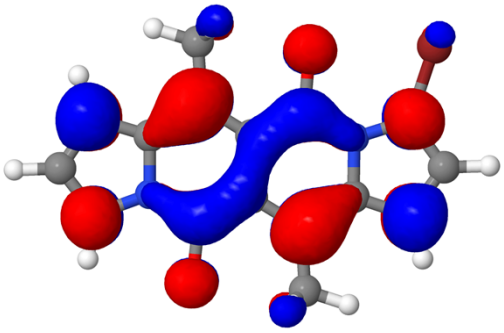
3	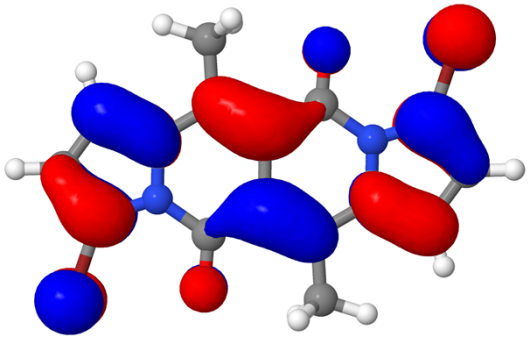	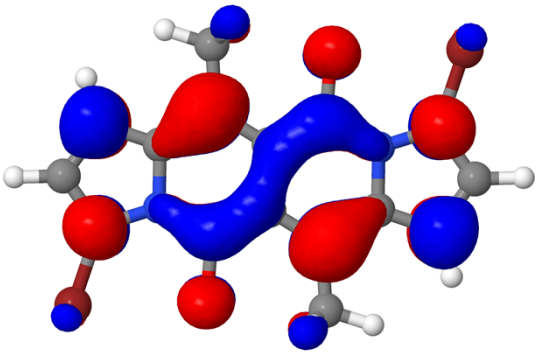
4	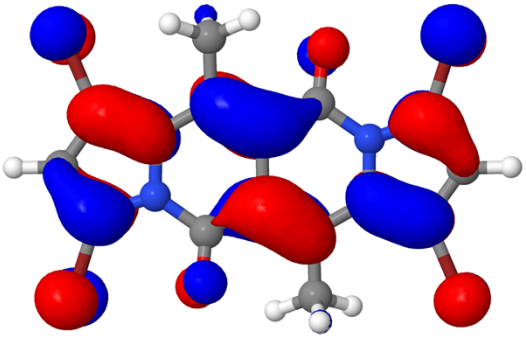	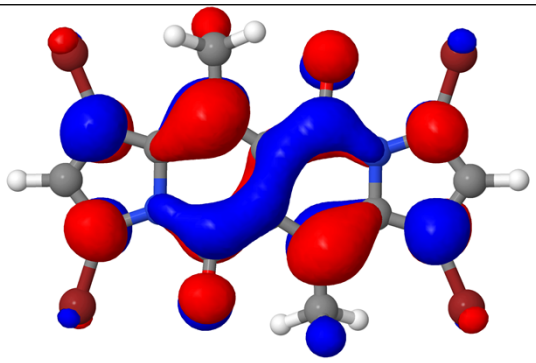
5	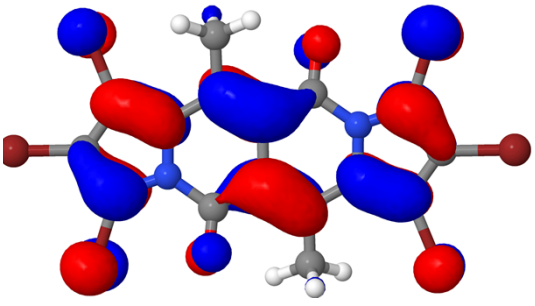	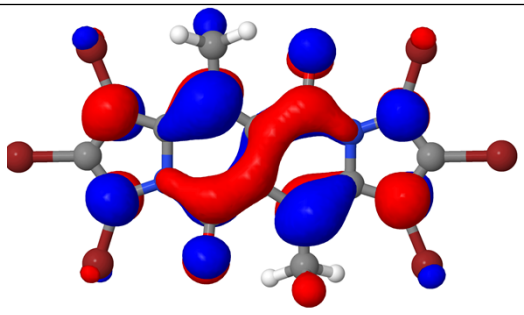

Table S5 - continued.

Compound	HOMO	LUMO
9	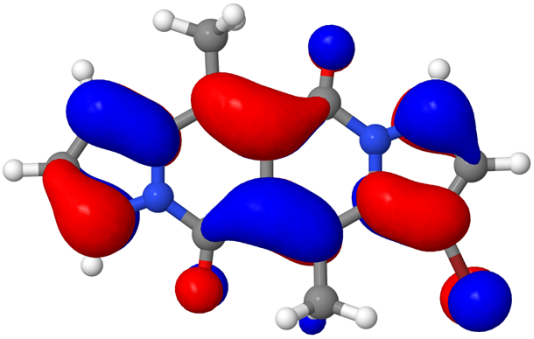	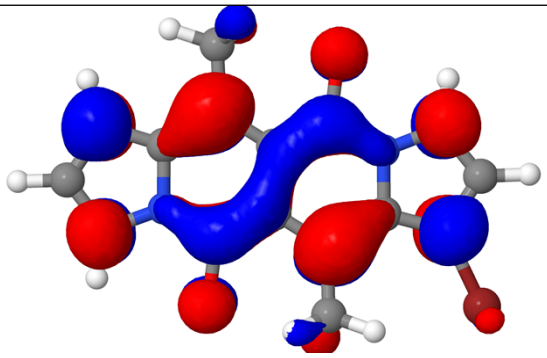
10	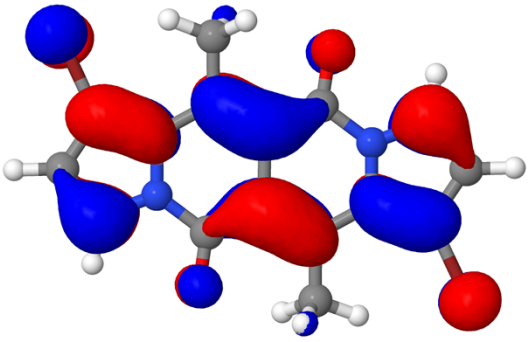	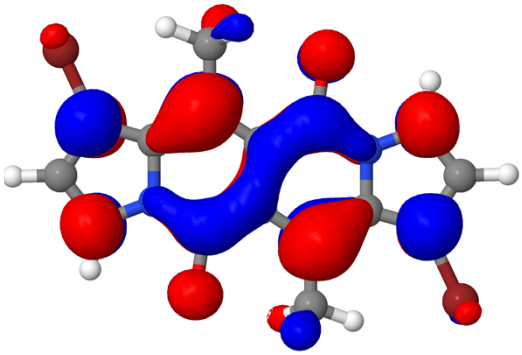
11	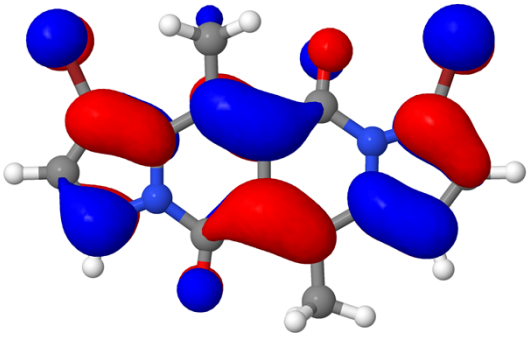	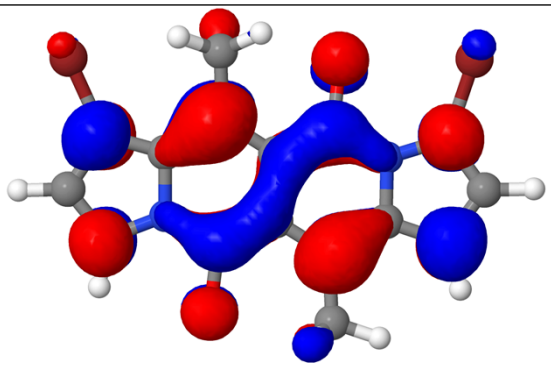
12a	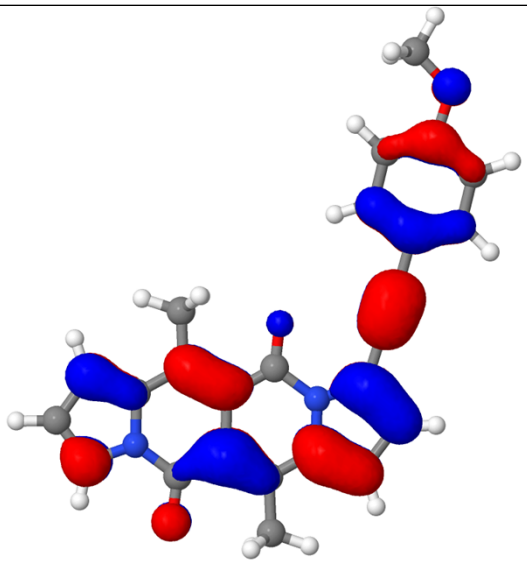	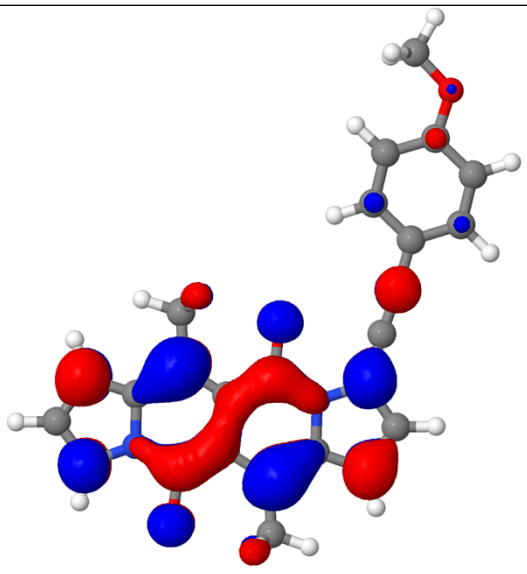

Table S5 - continued.

Compound	HOMO	LUMO
12b	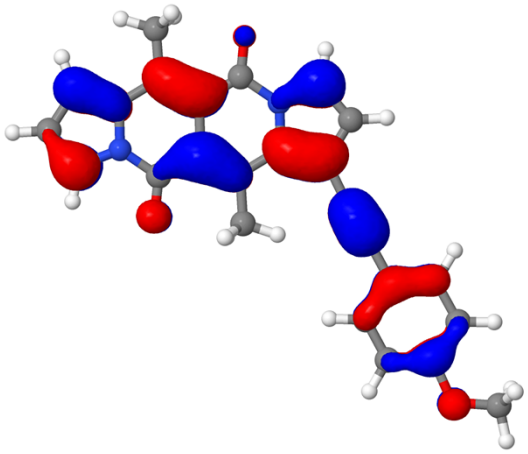	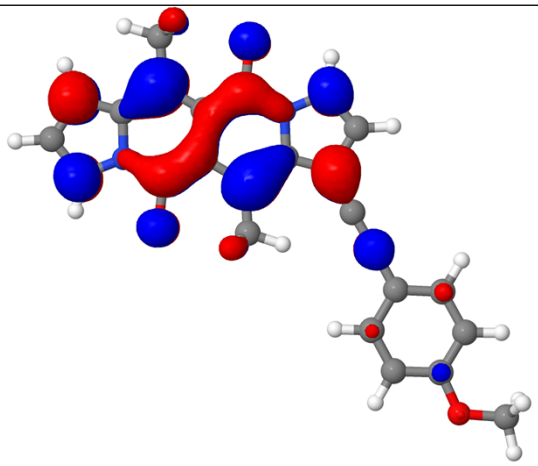
12c	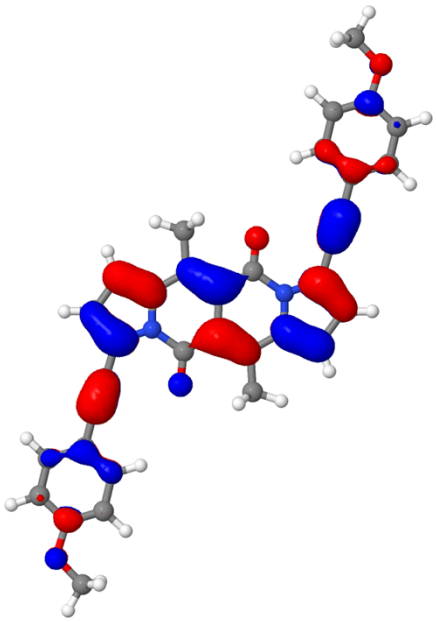	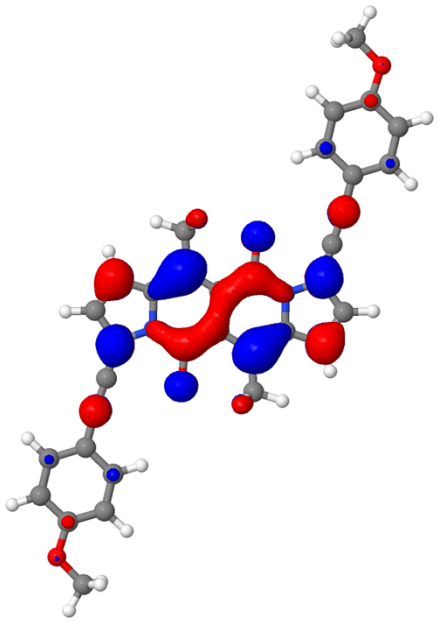
12d	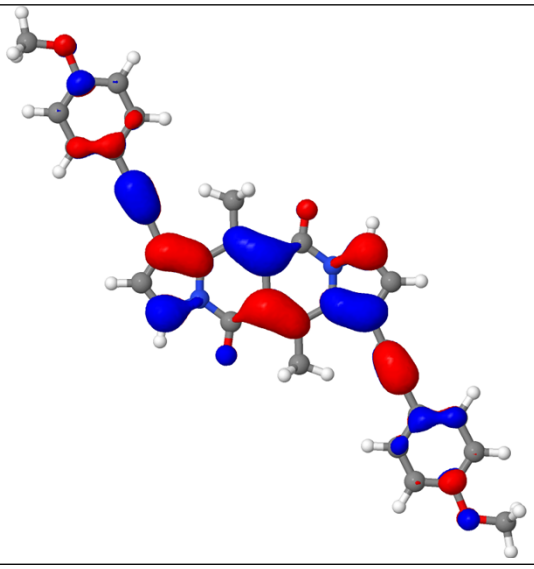	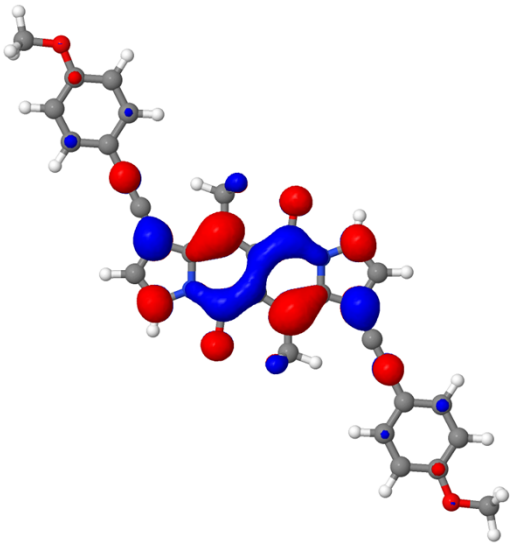

Table S5 - continued.

Compound	HOMO	LUMO
12e	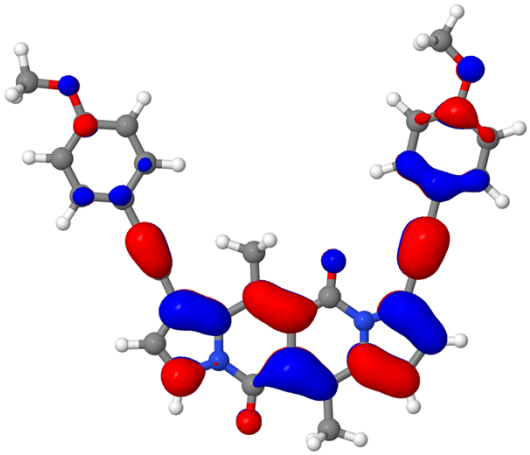	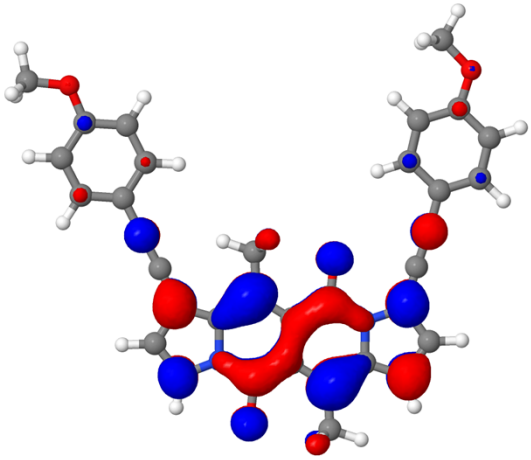
12f	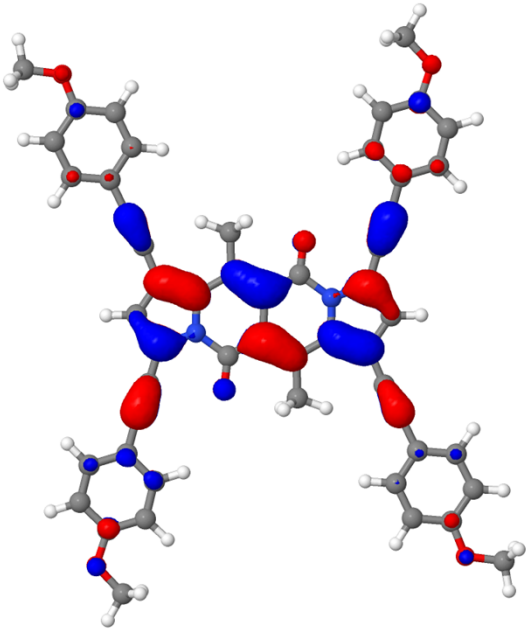	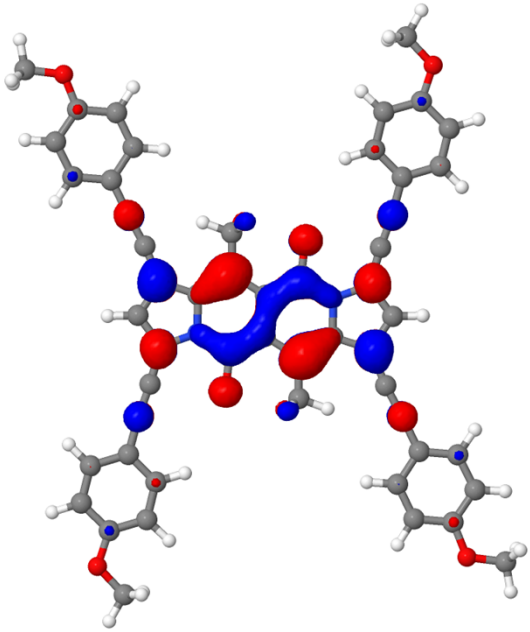

Table S6. NICS(1)$_{ZZ}$ values calculated at the ring centers of the DPND system using the GIAO method at the M06-2X/Def2-TZVPP level of theory.

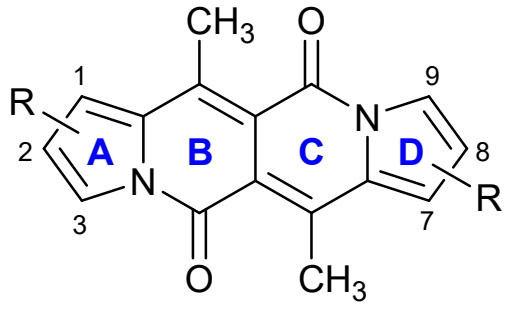

R	DPND	Substituents positions	NICS(1)$_{ZZ}$ [ppm]			
			A	B	C	D
H	**1**	-	-23.7	3.9	3.9	-23.7
Br	**2**	3	-21.9	4.4	3.4	-24.1
	3	3,9	-22.2	4.0	4.0	-22.2
	4	1,3,7,9	-19.8	4.3	4.3	-19.8
	5	1,2,3,7,8,9	-18.0	4.8	4.8	-18.0
	9	1	-21.7	3.8	4.0	-23.6
	10	1,7	-21.7	3.8	3.8	-21.7
	11	1,9	-21.5	4.6	3.4	-22.1
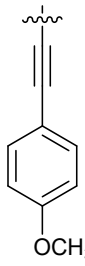	**12a**	3	-21.3	4.2	3.5	-24.0
	12b	1	-20.7	3.8	3.8	-23.8
	12c	3,9	-21.6	3.8	3.8	-21.6
	12d	1,7	-20.9	3.5	3.5	-20.9
	12e	1,9	-21.5	4.0	3.3	-21.0
	12f	1,3,7,9	-19.2	3.5	3.5	-19.2

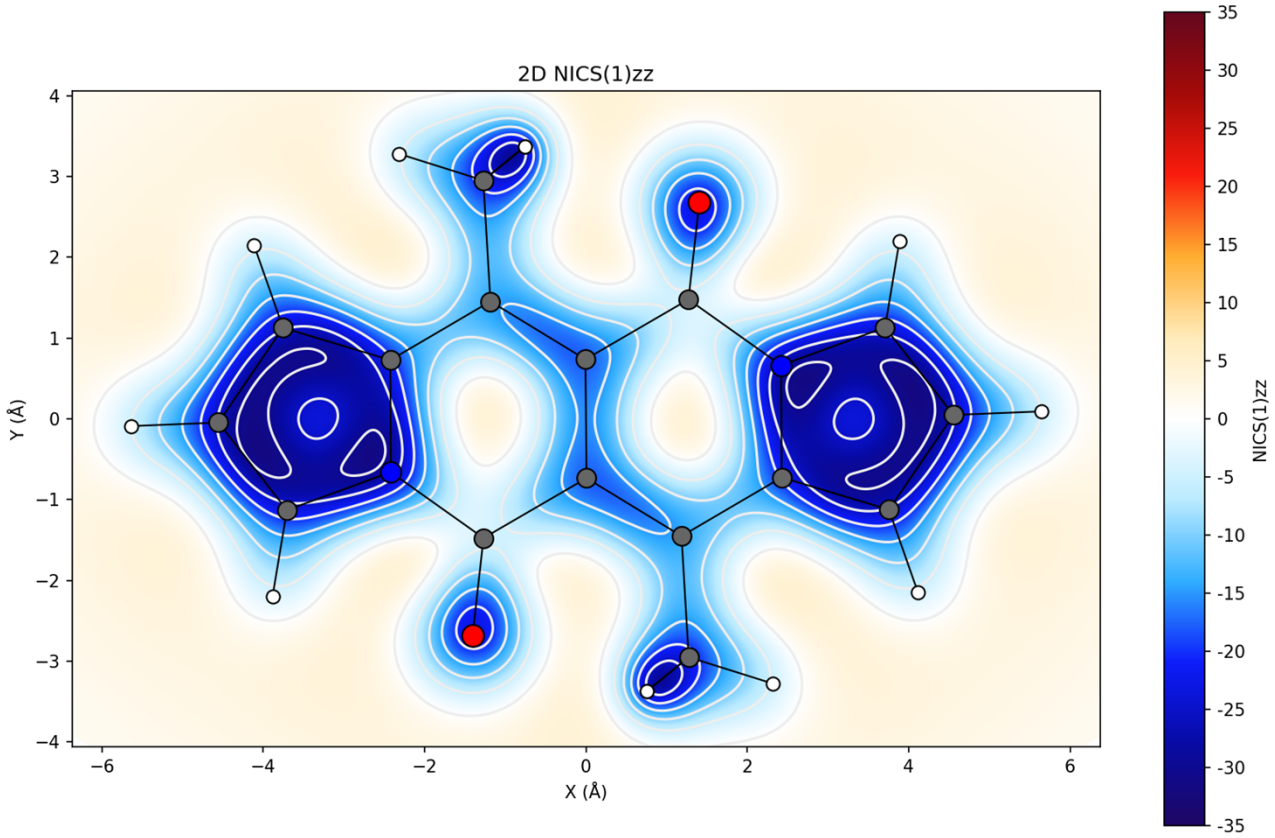

Figure S9. 2D NICS(1)$_{ZZ}$ map of compound **1**. Values given in ppm.

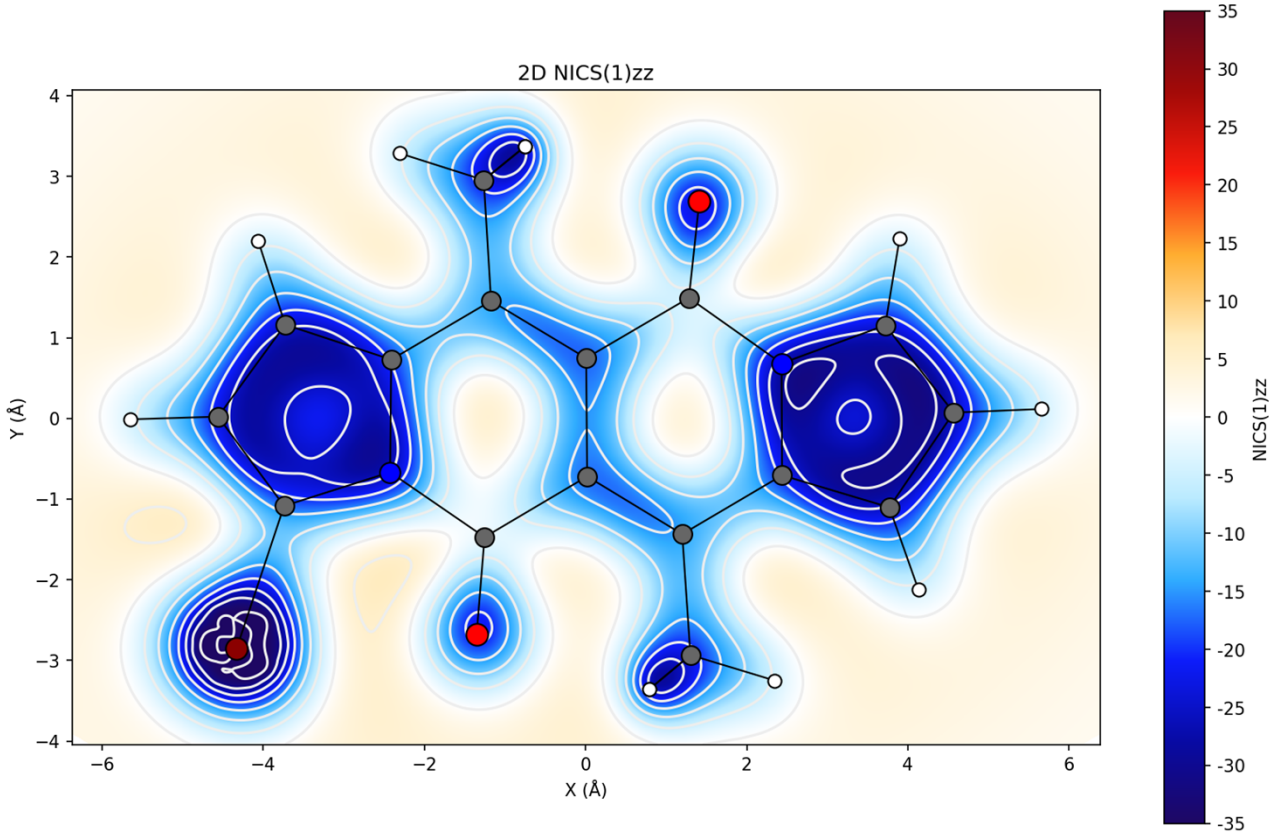

Figure S10. 2D NICS(1)$_{ZZ}$ map of compound **2**. Values given in ppm.

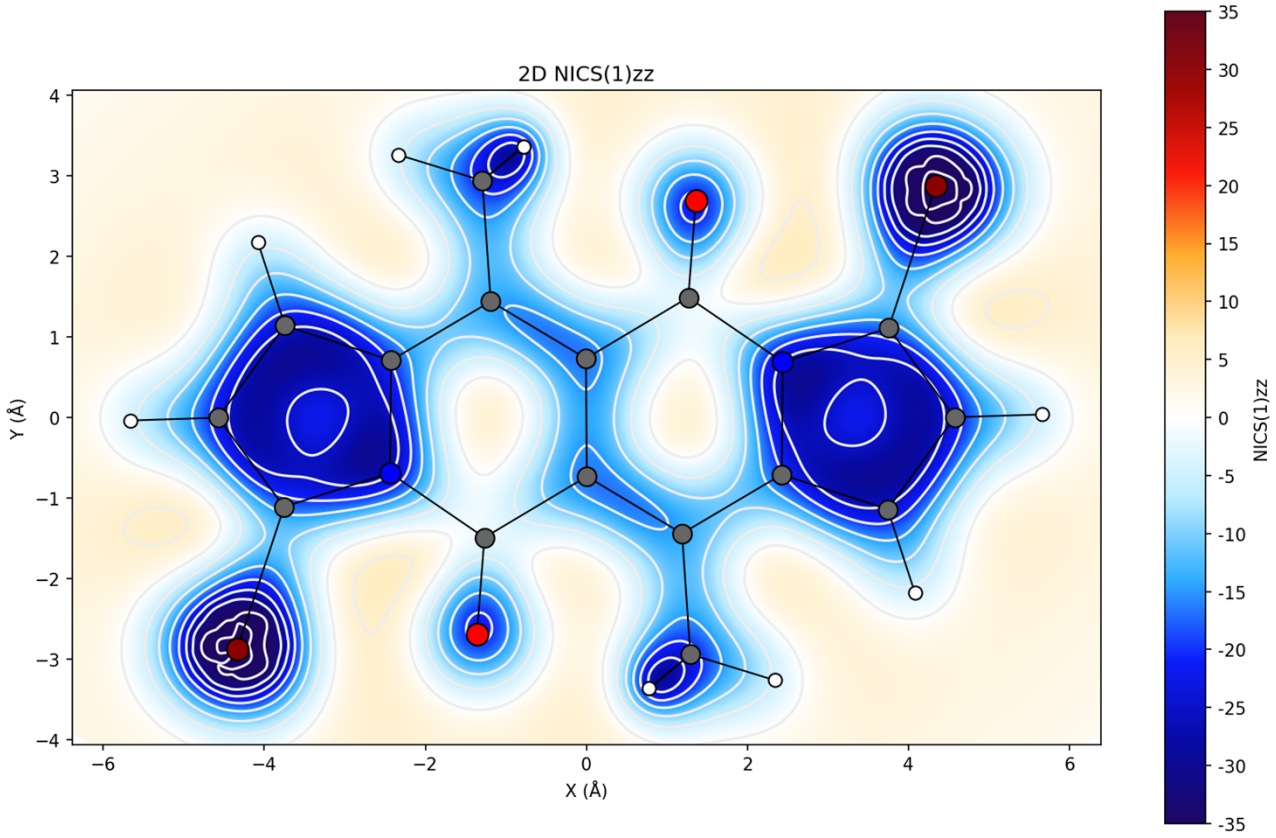

Figure S11. 2D NICS(1)$_{ZZ}$ map of compound **3**. Values given in ppm.

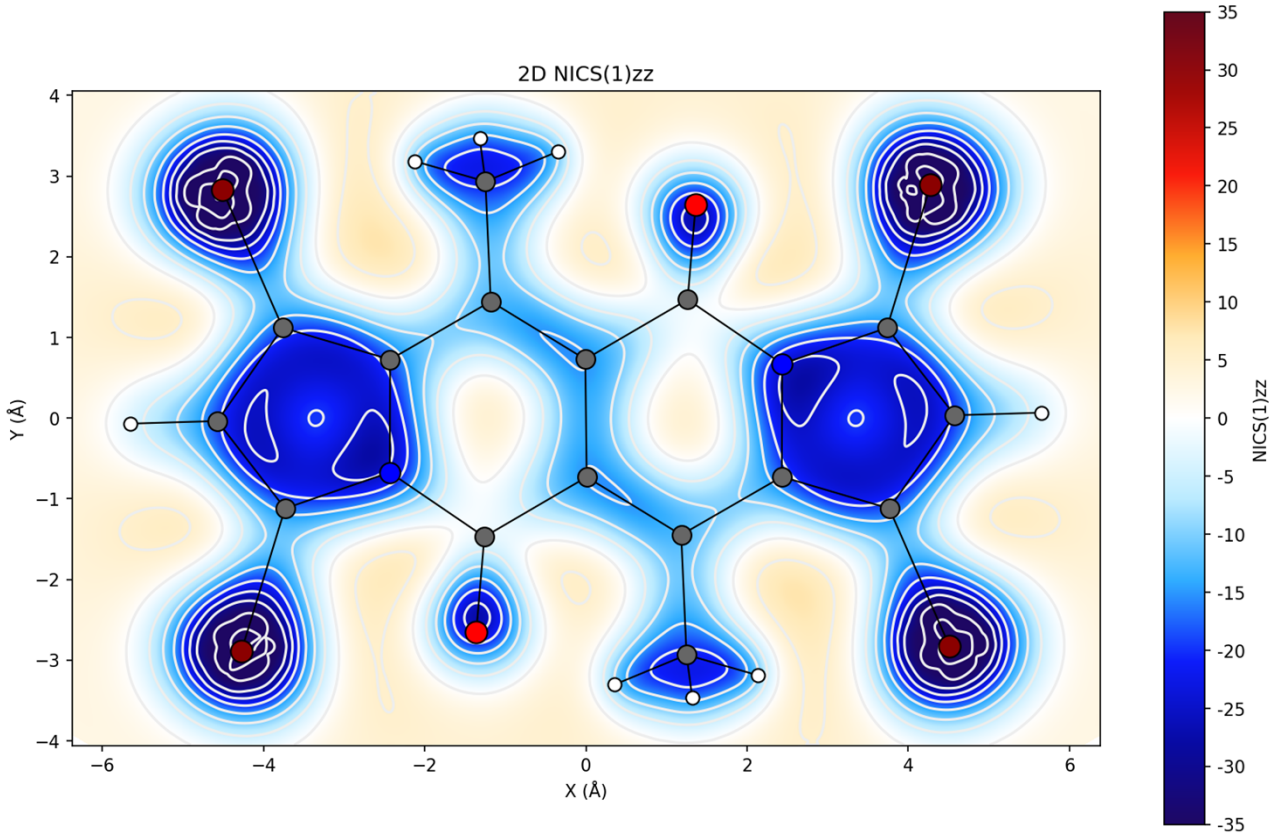

Figure S12. 2D NICS(1)$_{ZZ}$ map of compound **4**. Values given in ppm.

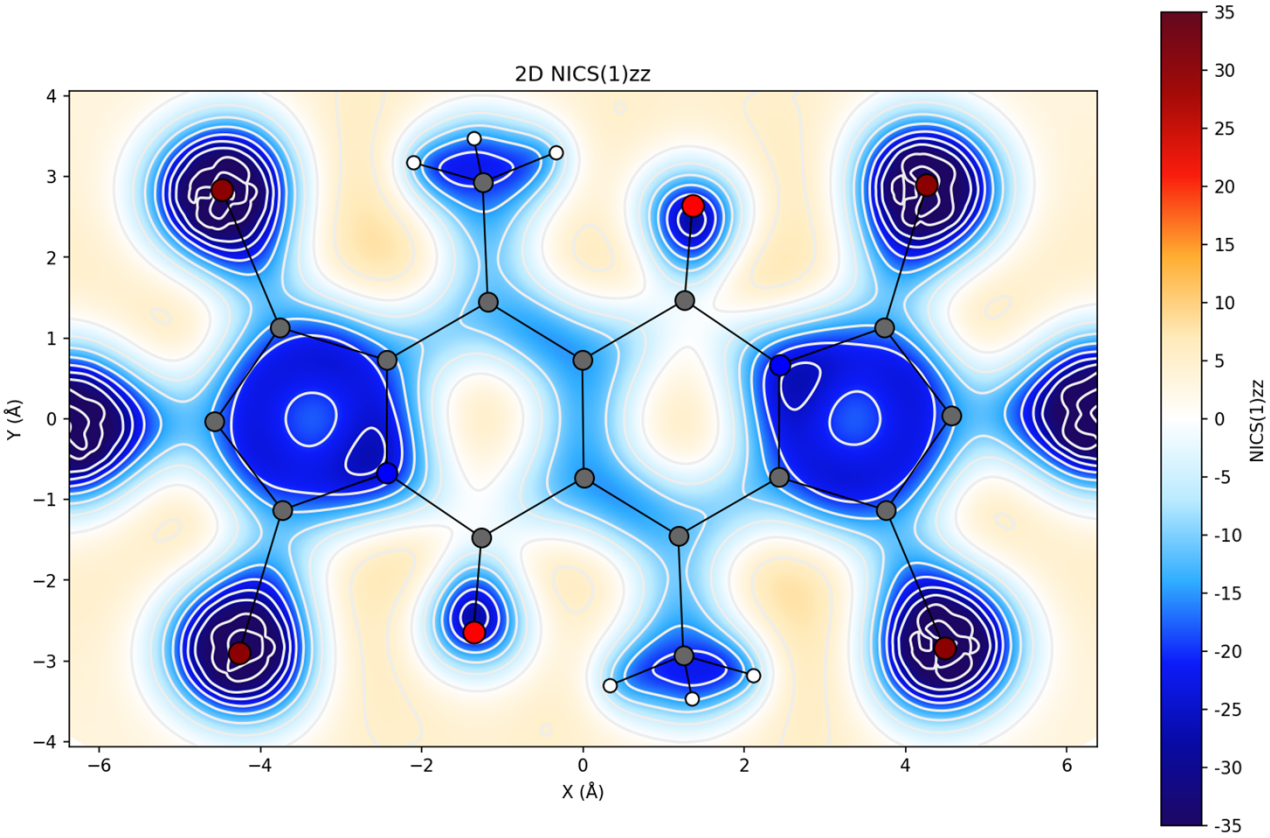

Figure S13. 2D NICS(1)$_{ZZ}$ map of compound **5**. Values given in ppm.

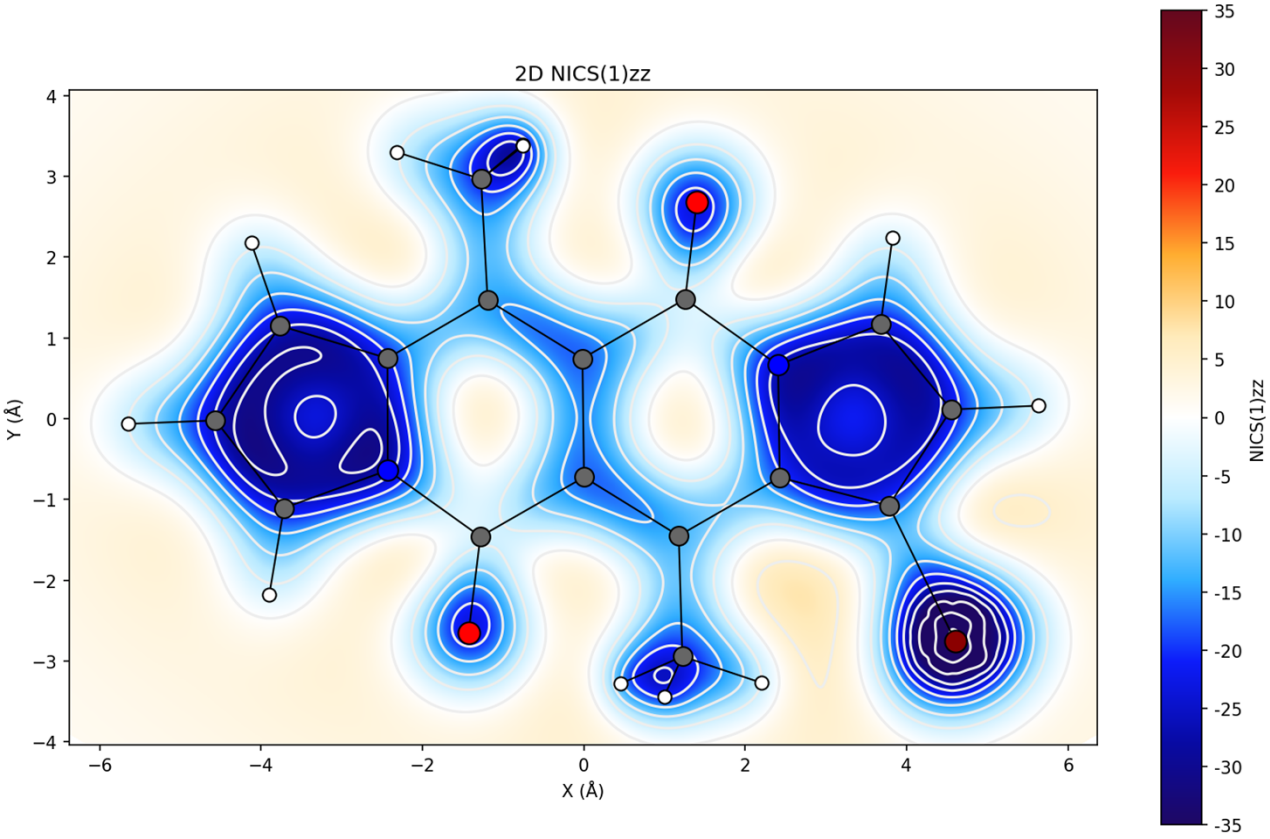

Figure S14. 2D NICS(1)$_{ZZ}$ map of compound **9**. Values given in ppm.

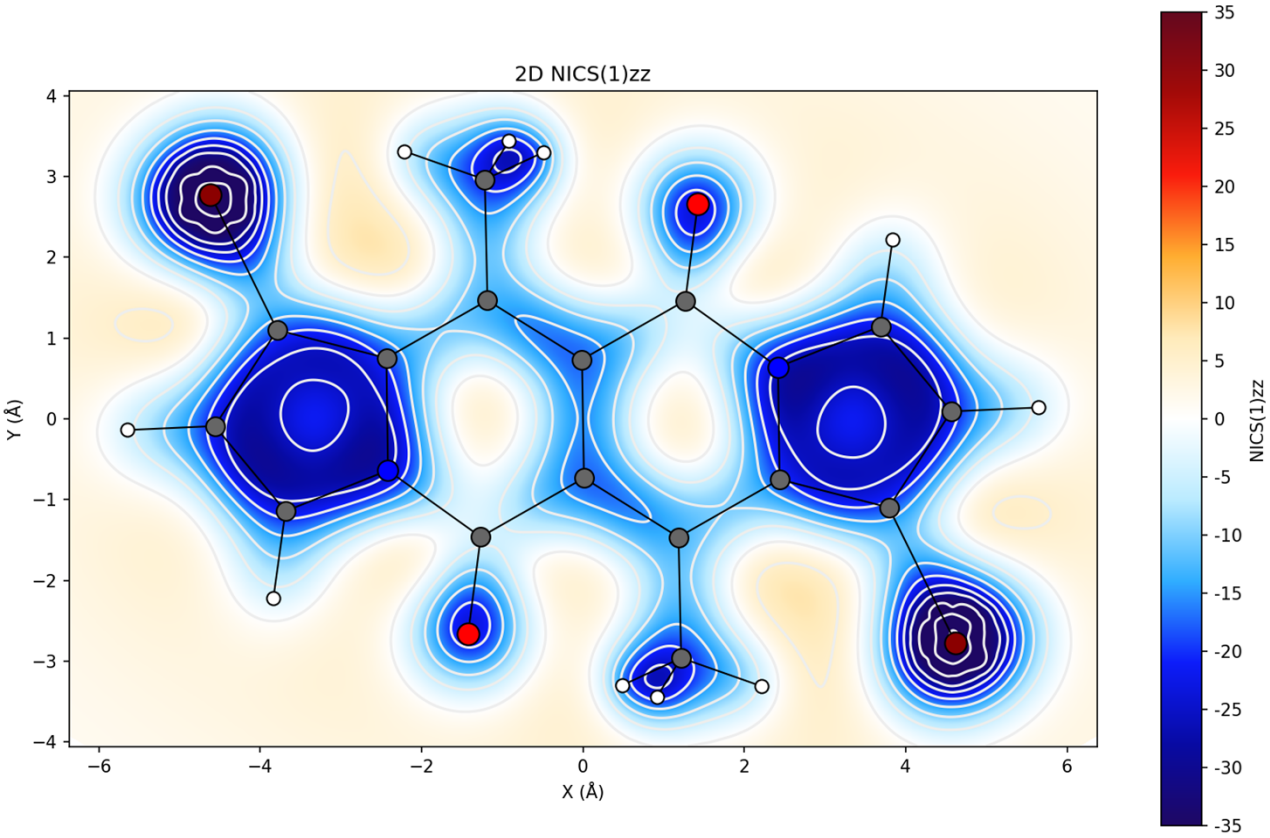

Figure S15. 2D NICS(1)$_{ZZ}$ map of compound **10**. Values given in ppm.

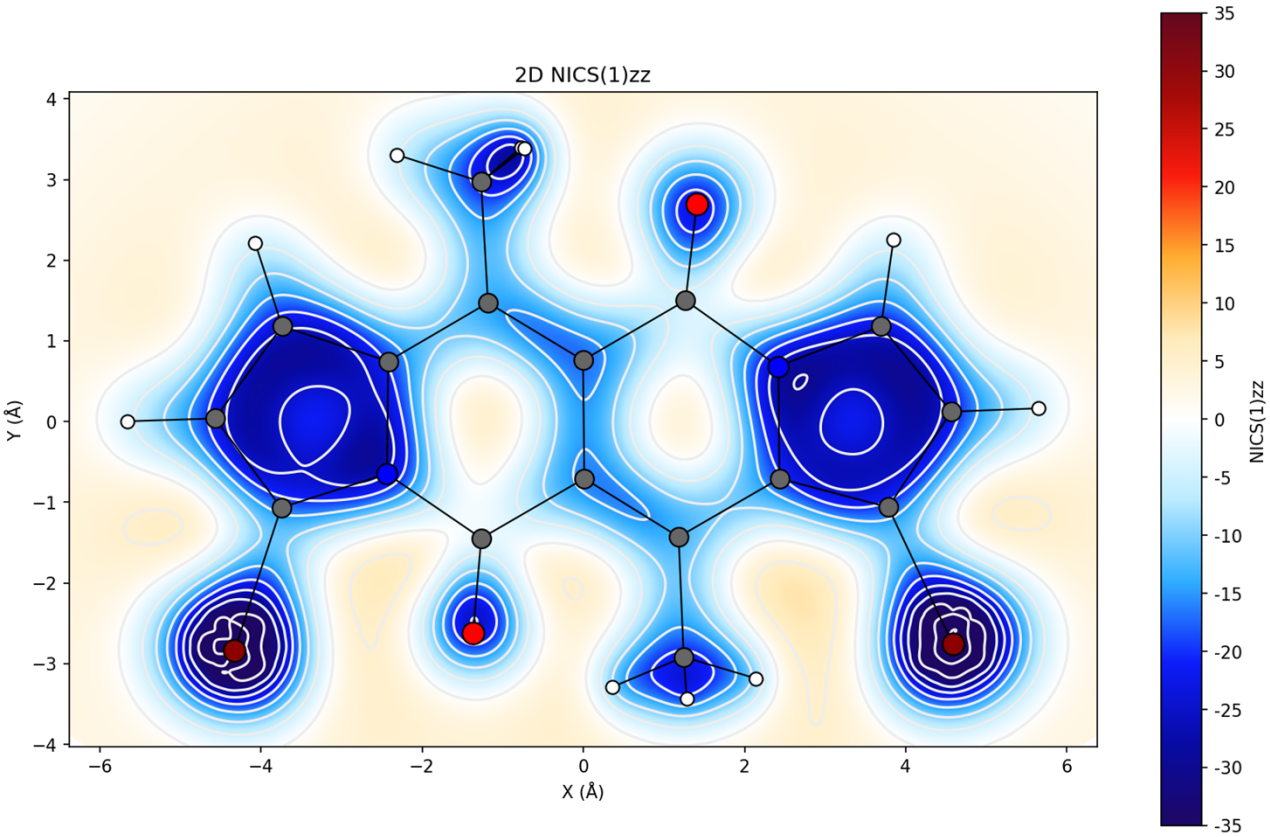

Figure S16. 2D NICS(1)$_{ZZ}$ map of compound **11**. Values given in ppm.

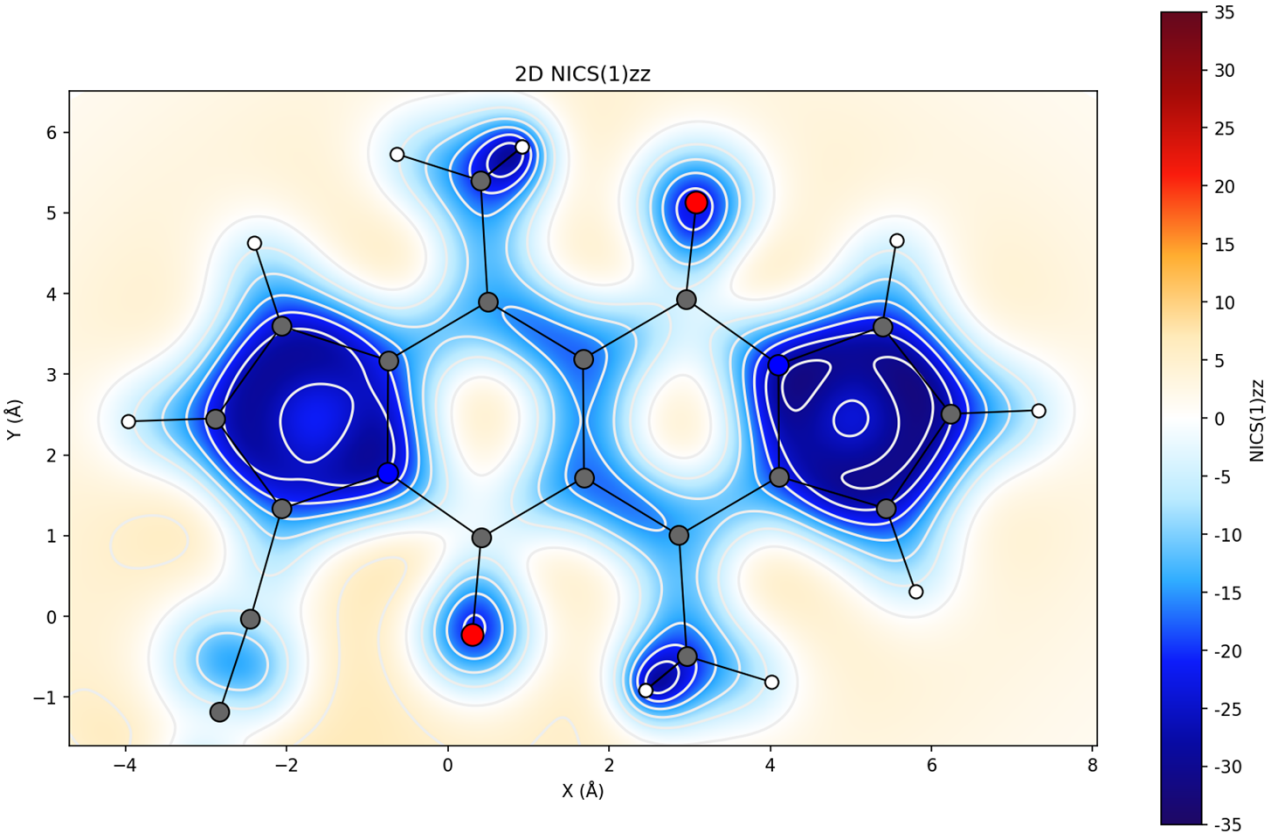

Figure S17. 2D NICS(1)$_{ZZ}$ map of compound **12a**. Values given in ppm.

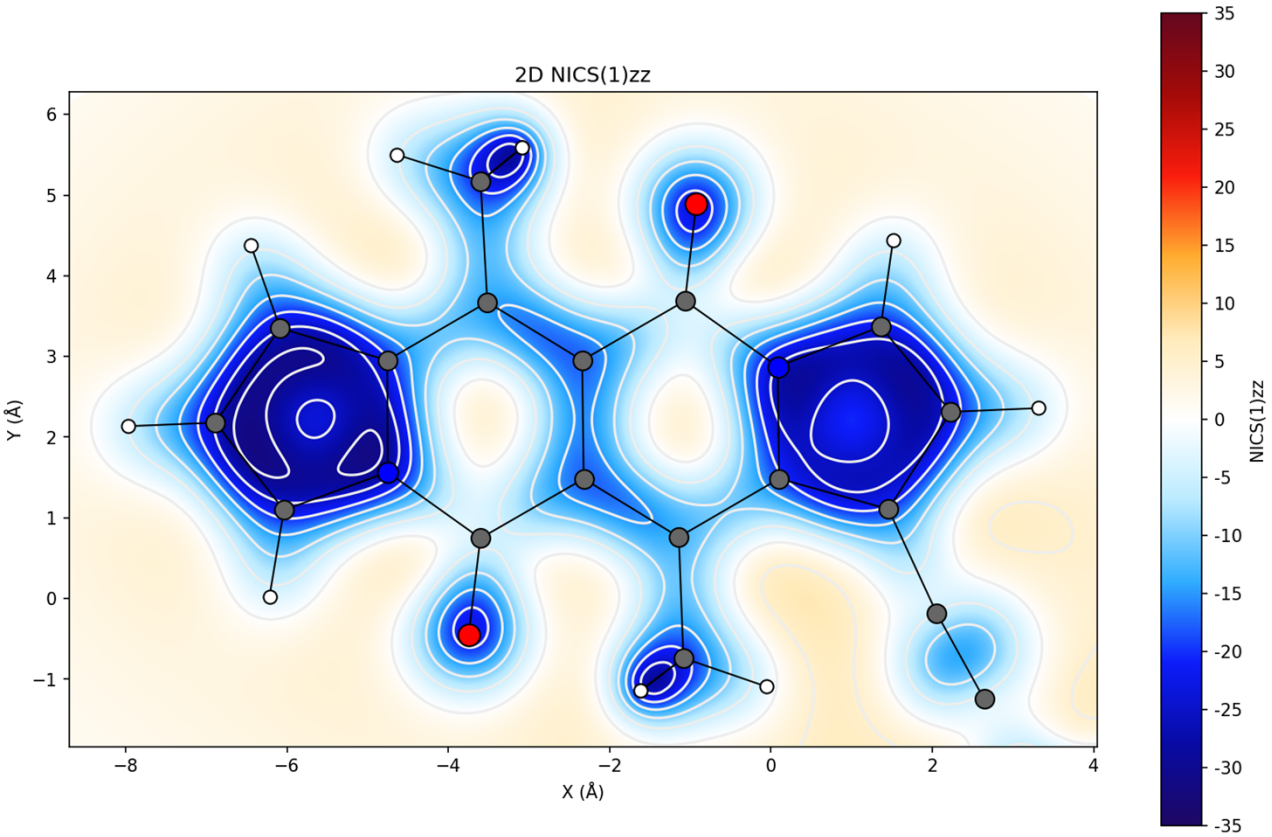

Figure S18. 2D NICS(1)$_{ZZ}$ map of compound **12b**. Values given in ppm.

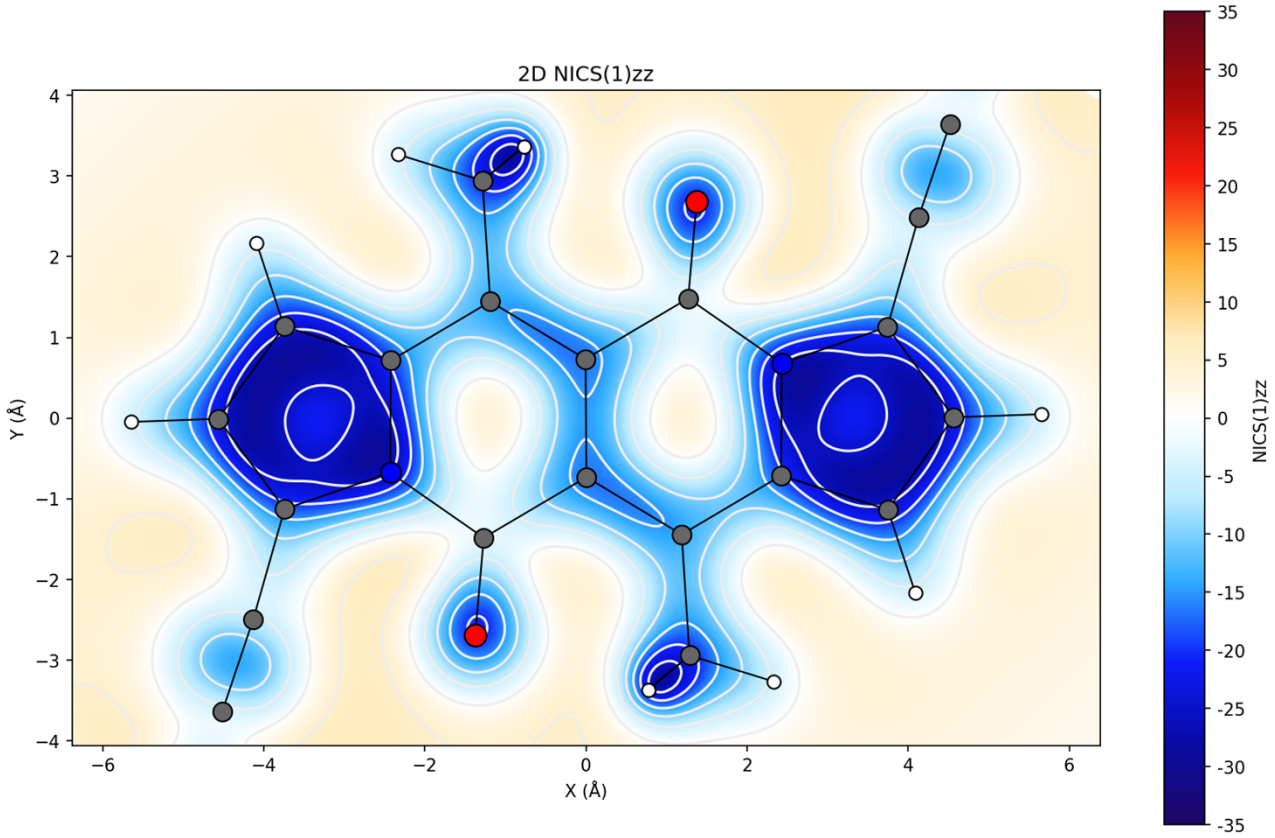

Figure S19. 2D NICS(1)$_{ZZ}$ map of compound **12c**. Values given in ppm.

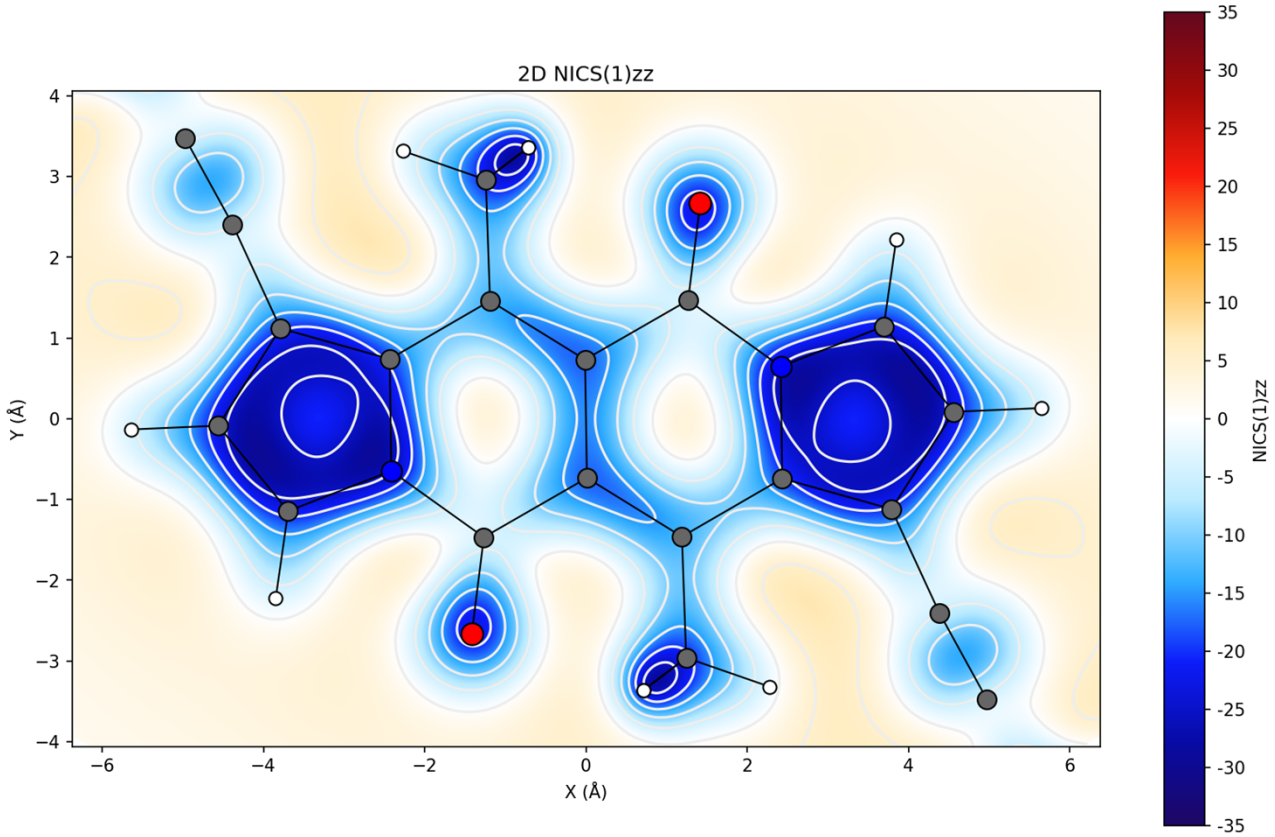

Figure S20. 2D NICS(1)$_{ZZ}$ map of compound **12d**. Values given in ppm.

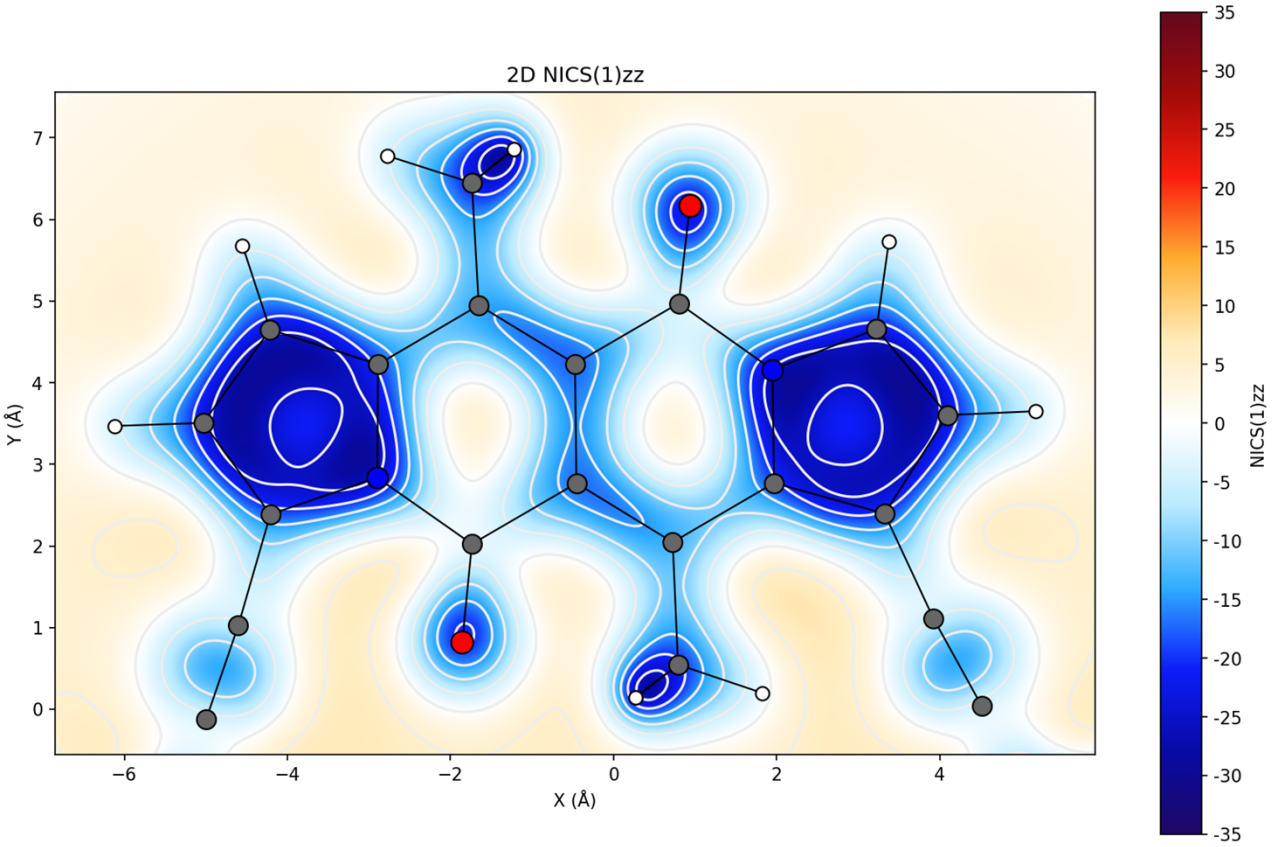

Figure S21. 2D NICS(1)$_{ZZ}$ map of compound **12e**. Values given in ppm.

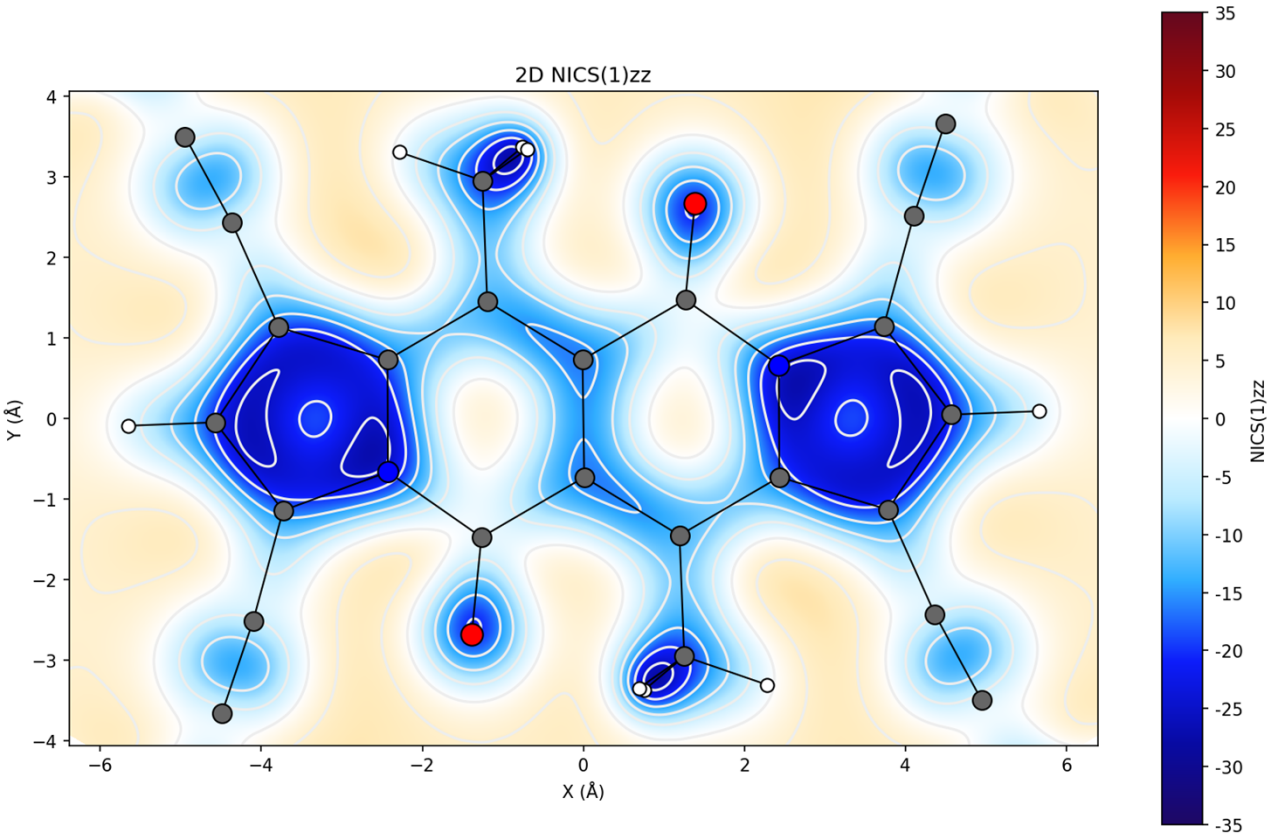

Figure S22. 2D NICS(1)$_{ZZ}$ map of compound **12f**. Values given in ppm.